Mapping the Metabolic Landscape of the Healthy Human Pancreas and the Pancreatic Tumor Microenvironment

by

Monica Bonilla

A dissertation submitted in partial fulfillment
of the requirements for the degree of
Doctor of Philosophy
(Cancer Biology)
in the University of Michigan
2024

Doctoral Committee:

Associate Professor Analisa Difeo, Chair
Assistant Professor Donnele Daley
Assistant Professor Mike Green
Associate Professor Costas Lyssiotis
Associate Professor Marina Pasca di Magliano
Lecturer Cristina Mitrea

Monica E. Bonilla

mebonill@umich.edu

ORCID iD: 0000-0002-1936-3712

Dedication

To Margeni Bonilla, who taught me the importance of authenticity.

Acknowledgements

Dr. Marina Pasca di Magliano I am forever grateful you took a chance on me and allowed me the freedom to pursue the questions I found interesting with full autonomy. Dr. Costas Lyssiotis thank you for your unwavering support, enthusiasm, and guidance throughout my PhD training. Dr. Cristina Mitrea "thank you" falls short in expressing my gratitude for you throughout the entirety of my doctoral training. Cristina, you have been my biggest supporter, loudest advocate, and a role model for the kind of educator and computational biologist I'd like to be. Dr. Fil Bednar, you are a brilliant scientist who has taught me the power of effective story telling. A lesson I will always keep with me. Dr. Donnele Daley I have always admired your solution-oriented mindset and the way you make people feel seen and heard. Donnele, you remind to me live in my truth, because you so fully live in yours. Dr. Analisa Difeo thank you for being such a grounding force throughout my training and having my best interest at heart. I would not have pursued research, or a PhD had it not been for Dr. Margaret Saha, Dr. Mark Forsyth, and Dr. Paul Heideman. Going to the College of William and Mary changed the trajectory of my life. Dr. Saha you were my first research advisor and went to bat for me throughout my undergraduate career. If it were not for you, I doubt I'd be a scientist today. Dr. Mark Forsyth you are such a dear friend in my life, and I am eternally grateful you didn't allow me to lose hope. Dr. Forsyth I am better person for knowing you, thank you for giving me space to be unapologetically myself. Dr. Heideman you have always seen the best in me, at times even before I recognized it. Dr. Heideman thank you for giving me space to figure out what you already knew to be true. Dr.

Hinton thank you for always being honest, authentic, and straight forward about your scientific journey, it has brought me great clarity in my own.

The power high school teachers possess to change the lives of students is never lost on me. Christopher Wode, you taught me math could be something I excelled at, but you also taught me that I am more than my background, upbringing, and worst days. Mr. Wode thank you for believing I too deserved a seat at the table. As a first generation citizen, first generation college student, and the first in my family to pursue a graduate degree – you were of one of the first people in my life who gave me permission to dream big. Emma Boyle, you brighten up every room you come into, and have been such a comforting presence in my life. You greet adversity with a smile, not reluctance, a quality few possess.

I would like to thank Rackham Merit Fellowship program for funding and creating a vibrant, supportive, and diverse community for me to be a part of during my time in Michigan. To the Department of Computational Medicine and Bioinformatics thank you for the continued support and funding on the Proteogenomics of Caner Training Program (T32 CA140044). To Sam Wilhemi, thank you for being the best Cancer Biology program manager, and helping me in every way possible! To Dr. Ashwini Mallappa, thank you for being the best mentor I could've asked for, at every stage in my scientific journey. To Megan Radyk, thank you for guiding me through the PhD process and being a safe space.

To my closest, dearest friends over the past half decade plus… thank you for being my support system. Ben Hauk, you push me to be the best version of myself in every aspect possible. Ben, you have stayed up thinking through specific aims for grant applications with me, poked holes in my experimental design, and have pushed me to be better than I believed I could be. To Anthony Jones, our friendship has stood the test of time and I'm lucky to know you. Ashley

Mello, becoming friends with you is one of the best things to come out of my PhD experience. Julia and Widmar, thank you for always welcoming me with open arms... and reminding me that my mom left with the best role models possible. Lastly, I would like to thank my mom and little cousin who have parted from this world due to cancer. My mom was fiercely herself, in every aspect… and she raised me to pave a path that felt completely authentic to me. My little cousin taught me we should all strive to be helpers in this world, and I am hoping I never lose sight of that.

Table of Contents

List of Tables

List of Figures

List of Abbreviations

PDA- Pancreatic Ductal Adenocarcinoma

TME - Tumor microenvironment

DGE- Differential Gene Expression

GSEA - Gene Set Enrichment Analysis

TAMs- Tumor associated macrophages

IHC- Immunohistochemistry

PanINs- Pancreatic intraepithelial lesions

GTP- Guanosine- 5'- triphosphate

GDP- Guanosine-5'- diphosphate

GAP- GTPase activating proteins

UMAP- Uniform Manifold Approximation and Projection

SCENIC- Single cell regulatory network inference and clustering program

PPP- Pentose Phosphate Pathway

BCAA- Branch chain Amino Acid

BMDM- Bone marrow derived macrophage

iCAFs- inflammatory cancer associated fibroblasts

Abstract

Pancreatic ductal adenocarcinoma (PDA) is a lethal disease with a current 5-year survival rate of 13% (1). PDA accounts for ~90% of pancreatic cancer cases and arises from the exocrine tissue – responsible for digestive functions in the pancreas. The pancreas also has endocrine functions primarily responsible for blood/sugar homeostasis, composed of acinar, islet, and ductal cells (4). Most patients present with locally advanced or metastatic disease at diagnosis, which is refractory to chemotherapy, radiotherapy, and immunotherapy (1,2). Even when surgical resection is possible, relapse is frequent (3). Thus, there is a critical need to identify new treatment strategies, increase the efficacy of standard of care, and overcome therapeutic resistance. Pancreatic cancer cells are encapsulated by a dense, fibrotic, heterogenous stroma consisting of the extracellular matrix, immune cells, and fibroblasts (4). Metabolic reprogramming due to tumorigenesis engenders metabolic co-adaptations in malignant, non-malignant, and immune cells in the tumor microenvironment (TME) (5–18). The advent of single cell RNA-seq has aided in assessing immune infiltration, identifying novel cellular subtypes, and inferring putative cellular interactions in the pancreatic cancer microenvironment (19–26,26–30). Still, access to healthy pancreas tissue for sequencing is difficult as there isn't clinical indication to biopsy. Further, adjacent normal tissue has been found to display signs of inflammation, thus not an appropriate control to compare to tumor tissue (30).

Through a unique partnership with Gift of Life Michigan (tissue and organ procurement program), we were able to obtain healthy pancreata for single cell RNA-Seq – a true

experimental “control”. Our lab previously published findings characterizing the immune landscape of pancreatic cancer via the sequencing of human pancreatic tumor samples (29). Taken together, these data sets presented the opportunity to investigate metabolic alterations across cellular compartments engendered by malignancy. To map metabolic alterations engendered by malignancy I developed a robust computational pipeline employing various computational approaches; pseudo bulk analysis, differential gene expression (DGE) analysis, gene set enrichment analysis (GSEA), and transcription factor inference analysis. In addition, I assessed cellular crosstalk activity between cancer cells and immune cells. To validate computational findings, in vitro experiments were performed as well as co-immunofluorescent staining on healthy human pancreata and patient cancer tumor tissue. In summary, I identified downregulation of mitochondrial programs in several immune populations, relative to their normal counterparts in healthy pancreas. While granulocytes, B cells, and CD8+ T cells all downregulated oxidative phosphorylation, the mechanisms by which this occurred was cell-type specific. In fact, the expression pattern of the electron transport chain complexes was sufficient to identify immune cell types without the use of lineage markers. I also observed changes in tumor associated macrophage (TAM) lipid metabolism, with increased expression of enzymes mediating unsaturated fatty acid synthesis and upregulation in cholesterol export. Concurrently, cancer cells exhibit upregulation of lipid/cholesterol receptor import. Thus, I identified a potential crosstalk whereby TAMs provide cholesterol to cancer cells. I suggest that this may be a new mechanism boosting cancer cell growth and therapeutic target in the future.

In this body of work, I present the first metabolic atlas of co-adaptations engendered by malignant and non-malignant cells in human pancreatic cancer. Further, I define novel metabolic

alterations that may aid our understanding of the role of metabolic rewiring in immune cell dysfunction and subsequent therapeutic resistance in pancreatic cancer.

Unpublished work characterizing immune landscape changes following genetic inactivation or pharmacological inhibition of oncogenic Kras in a late stage murine model of PDA will also be presented. Initial studies performed include analysis of single cell sequencing data, flow cytometry results, multiplex immunofluorescent staining, and immunohistochemistry (IHC) on orthoptic tumors harvested from murine models of PDA . Future directions arising from these studies are also detailed in this section. Overall, this chapter will provide an overview of pancreatic cancer metabolism, the composition of the pancreatic tumor microenvironment, and the immune landscape of PDA to provide context for the following chapters in this dissertation.

Chapter 1 Introduction

1.1 Pancreatic Cancer

Pancreatic ductal adenocarcinoma is a deadly malignancy, with a dismal 5 year survival rate of 13% (1). New therapeutic approaches are desperately needed to increase the efficacy of current standard of care, overcome therapeutic resistance, and increase life expectancy for patients. Detecting pancreatic cancer is difficult, as symptom presentation is rare and generalizable to a variety of diseases, thus detection and diagnosis occurs when a patient already presents with locally advanced or metastatic disease (31,32). The most common form of pancreatic cancer is pancreatic ductal adenocarcinoma (PDA), responsible for ~90% of cases. Even for 15-20% of cases in which surgical resection is possible ~80% of patients go on to develop resistance to chemotherapy (4,33) . Often drugs targeting pancreatic cancer cells fail due to resistance mechanisms engendered in neighboring stromal cells (31,34–40). In this manner, the tumor milieu aids in creating a microenvironment apt at immune suppression.

Oncogenic KRAS is the driving mutation in PDA, with ~ 95% of tumors carrying a mutant form. This genetic alteration is typically accompanied by loss of function or deletion of the following tumor suppressors ; TP53, SMAD4, and CDKN2A (32). Pancreatic cancer arises from the exocrine pancreas, responsible for digestive functions - composed of acinar and ductal cells (32,41,42). The progression of PDA is a multi-step process in which early precursor lesions, pancreatic intraepithelial lesions (PanINs) become progressively higher grade lesions over time,

ultimately leading to metastasis (4). Currently, there is a still a need to develop biomarkers for early detection of PDA. Though, the advent of small molecule inhibitors targeting mutant KRAS variants have recently become available, and new combinatorial treatment strategies are currently underway (43,44).

1.2 Oncogenic Kras

$KRAS^{G12D}$ is most frequent amino acid substitution in PDA, consisting of a single base substitution, glycine to aspartic acid at position 12, KRASG12D. About 90% of PDA tumors carry this mutant form of KRAS (33). KRAS is a GTPase from the Ras G protein family responsible for signaling involved in cell proliferation, survival, and invasion (45,46). More specifically, KRAS is a membrane bound G protein and functions as a molecular switch; either in an active state when bound to guanosine- 5'-triphospahte (GTP) or inactive when bound to guanosine- 5'- diphosphate (GDP). The oscillation between states is modulated by GTPase activating proteins (GAPs), which hydrolyze GTP, rendering KRAS inactive. KRAS mutations typically occur close to the binding pocket, consequently decreasing GAP binding affinity, leading to a constitutively active state (47). Consequently, the increased GTP binding affinity leads to increased levels of GTP bound oncogenic KRAS, driving cell growth and survival via the downstream effector pathways mitogen activated protein kinase (MAPK) and phosphatidylinositol 3 kinase (PI3K).

1.2.1 Targeting Mutant KRAS

Previously, oncogenic KRAS was thought to be "undruggable" due to inaccessible binding sites for small molecule inhibitors, and its high affinity for GTP binding. Attempts at manufacturing drugs targeting mutant KRAS were largely unsuccessful due to low binding affinity and poor

selectivity, rendering them ineffective (47). For the first time in decades targeting $KRAS^{G12C}$ became possible with the small molecule inhibitor (Sotarasib), which binds covalently to the cysteine 12 residue. Sotarasib is a highly specific, irreversible inhibitor of $KRAS^{G12C}$ (glycine to cysteine), with shown anti-tumor activity and minimal safety concerns in a phase 2 trial. Importantly, this trial administered Sotarasib (AMG510) as a monotherapy, in a cohort of patients who had been previously treated for colorectal cancer (31,36). Response rate was a mere 9.7% overall, but as previously mentioned most patients had been heavily pretreated with a variety of chemotherapy and immunotherapy regimens. Adagrasib (MRTX849), another selective inhibitor of KRASG12C irreversibly binds at the switch II pocket, locking it in its inactive state (43,48,49) . In a phase 1B clinical trial, in a cohort of patients with non-small cell lung cancer (NSCLC), with previous treatment status (chemotherapy and immunotherapy) 42.9% had a response to monotherapy. Unfortunately, the median duration of response to treatment was 8.5 months, with a median progression free survival of 6.5 months. Again, treatment intervention with this inhibitor was in a cohort of patients with refractory or metastatic cancer whom previously received treatment (49).

Although the clinical trials with Sotarasib and Adagrasib monotherapies showed promising results, mechanisms of acquired resistance were investigated shortly after. Genomic analysis was performed on a cohort of patients treated with Adagrasib, utilizing paired patient samples before and after treatment with Adagrasib. The cohort consisted of patients with colorectal, NSCLC, or appendiceal cancer, and detected putative resistance mechanisms in 17/38 patients (45%) (50). Multiple KRAS alterations were found to be highly amplified, to name a few (G12D/R/V). In addition, $KRAS^{G12C}$ was amplified and downstream mediators of RAS signaling such as MET, BRAF, RAF1 demonstrated amplification and activating mutations, all acquired bypass

mechanisms in response to targeting mutant KRASG12C. Collectively, these results show acquired resistance to single agent therapy through binding pocket mutations, mutant KRAS amplification, loss of function mutations in tumor suppressors, and acquired bypass mechanisms (amplification of downstream RAS signaling mediators) (51).

KRASG12D (glycine to aspartic acid) is the prominent mutation in pancreatic cancer and recently became an actionable target with the small molecule inhibitor MRTX1133, which binds noncovalently and irreversibly to the switch 2 pocket of mutant $KRAS^{G12D}$ (51,52). In PDA murine implantation models, MRTX1133 inhibited tumor growth, and altered macrophage polarization in the TME (51). Currently, there is a phase 1b clinical trial utilizing the MRTX1133 inhibitor in a cohort of patients with advanced solid tumors; with the genetic $KRAS^{G12D}$ alteration. As previously demonstrated with targeting $KRAS^{G12C}$, acquired resistance mechanisms are likely to arise (53). Nonetheless, targeting $KRAS^{G12D}$ in combination with current standard of care may be provide a promising new treatment strategy.

1.3 Pancreatic Tumor Microenvironment

The pancreatic tumor microenvironment is composed of various fibroblast sub types, cancer cells, extracellular matrix components, and immune cells (4). Oncogenic KRAS alters pancreatic cancer cell signaling and reprograms neighboring immune cells towards an immunosuppressive phenotype, aiding in immune evasion (14). PDA is characterized by a fibroinflammatory stroma, in which cancer cells orchestrate cellular crosstalk with immune cells and fibroblasts to gain access to bio intermediates to survive the harsh conditions of the TME (12). Consequently, competition for resources engenders T cell exhaustion/dysfunction due to unmeet energetic demands, unable to execute an anti-tumor response (54,55).

Myeloid cells are the most abundant immune compartment present in the pancreatic TME and play a critical role in immune suppression as most are myeloid derived suppressor cells. Tumor associated macrophages are involved in a myriad in metabolic process that can be either pro or anti-tumor, and secrete cytokines and metabolites which drive tumor survival and therapeutic resistance (8,38,56–59). The complex interplay between cancer cells, the immune milieu, fibroblasts, and the extracellular matrix make targeting one specific metabolic pathway, signaling axis, or cell type difficult in PDA. As compensatory and resistance mechanisms arise in response, due to the complex nature of the TME. Combinatorial targeting of multiple components of the TME are underway and may be a promising approach in advancing treatment strategies in PDA (60,61). Of note, studies have recently identified "sub TMEs" in patients that differ based on spatial location within the tumor, further highlighting the complexity of the PDA tumor landscape (62,63). Here, the focus will be on cancer cell autonomous metabolic reprogramming and extrinsic metabolic rewiring in the pancreatic tumor microenvironment.

1.4 Metabolic Reprogramming

Metabolic reprogramming is a consequence of cancer cells adjusting to meet metabolic requirements necessary to continue proliferation, survival, and metastasis in a resource limited microenvironment (13,64–68). Oncogenic signaling shifts metabolic dependencies in cancer cells, and in response non-malignant and immune cells must also acquire metabolic co-adaptations to compete for fuel sources (69–73). Symbiotic interactions between cancer cells and immune cells restructure the metabolic landscape in the microenvironment by modulating levels of nutrients, increasing byproducts due uptick in catabolism, and metabolite signaling (12,32). Cancer cell intrinsic metabolic rewiring promotes cancer cell intrinsic changes as well as reciprocal changes in immune and non-malignant cells as an adaptive response.

1.5 Cancer cell autonomous metabolic reprogramming

Oncogenic KRAS alters various metabolic processes in pancreatic cancer cells such as upregulation of glycolysis, the hexosamine biosynthesis pathway, and glutamine metabolism (7,13,14,67,74,75). Due to the reversibility of enzymatic reactions and overlap in enzymes driving multiple pathways, metabolic mutations are rare. Typically, metabolic enzyme expression is up/down regulated transcriptionally.

1.5.1 Glycolysis

Glucose reprogramming driven by mutant KRAS alters glucose availability in the TME and increases lactate production in parallel. The increase in glycolytic flux is mediated through augmented expression of key enzymes driving glycolysis such as hexokinase (HK1/2), phosphofructokinase (PFK1), and lactate dehydrogenase (LDHA). Further, glycolytic intermediates may be funneled into the non-oxidative arm of the pentose phosphate pathway, to be utilized for nucleotide biosynthesis and ribose production (15,76). A byproduct of lactate uptake is NADPH production, which can be shunted to the mitochondria to participate in the ETC, ultimately replenishing NAD+ levels (15).

RAS signaling initiates a downstream signaling cascade which activates the PI3K-Akt signaling axis, which in turn upregulates the expression of glucose transporter 1 (GLUT1), which is then translocated to the outer membrane to participate in glucose uptake. Downstream intermediates in glycolysis can also be shunted into the serine biosynthesis pathway, creating an alternative source of phospholipids and carbon backbones for cancer cells (15). Since, cancer cells can divert to serine thesis for a variety of bio intermediates, even including electrons to fuel the ETC, enzymes in this pathway are often upregulated (12). One such example is the amplification of

phosphoglycerate dehydrogenase (PHGDH), a key rate limiting enzyme in the serine synthesis pathway (77,78).

Hypoxia is a hallmark of pancreatic cancer, which drives metabolic reprogramming, epigenetic modifications, and gene expression in malignant and non-malignant cells in hypoxic niches. Limited oxygen supply pressures cancer cells to shift dependency to anaerobic glycolysis and decrease reliance on oxidative phosphorylation (39,79). Since oxygen is the last electron acceptor in the ETC, hypoxia may lead to stalling, resulting in inability to carry out oxidative phosphorylation. Hence, pancreatic cancer cells metabolically adapt and obtain energy through other metabolic pathways.

1.5.2 Amino acids

Amino acid metabolism is co-opted by cancer cells to acquire biomass, sustain proliferation demands, and promote survival. Glutamine metabolism is typically increased in cancer cells as glutathione (GSH) biosynthesis requires glutamine derived glutamate, which is then converted to alpha- ketoglutarate by glutamate dehydrogenase 1 (GLUD1) to fuel the TCA cycle(13,67,75,80). But in pancreatic cancer cells, glutamine derived glutamate is used to obtain aspartate, which is then converted to oxaloacetate by glutamic oxaloacetate transaminase 1 (GOT1) (81). This process is catalyzed by the mitochondrial uncoupling protein 2 (UCP2), which is deregulated in various cancer settings (74). Oxaloacetate can be further processed into pyruvate, which increases NAD+/NADPH ratios in the mitochondria, aiding in redox balance, cholesterol biosynthesis, and fatty acid synthesis, (15,81). KRAS mutations drive glutaminolysis in tumors as well, this metabolic co-adaptation leads to increased gene expression of the glutamine transporter in the amino acid transport family; ASCT2 (76). Pancreatic cancer cells also gain access to carbon sources and nitrogen via branch chain amino acid (BCAA)

metabolism. BCAA metabolism plays a role in fatty acid biosynthesis, lipogenesis, and contribution towards metabolites that may feed into the TCA cycle (34,82). This is mediated in part by the increased uptake of BCAAs in pancreatic cancer tissue, via carrier transporters, which are significantly upregulated as well.

1.5.3 Mitochondria

Redox homeostasis is often disrupted in cancer, as reactive oxygen species (ROS) levels increase due to increased electron flow through the electron transport chain (ETC) (10,65,83,84). The NAD+/NADH cofactors drive multiple anabolic processes; oxidative phosphorylation, glycolysis, and the tricarboxylic acid (TCA) cycle, all processes necessary for cancer cells to sustain an increased bioenergetic state. Increased demand for NADH production can overload the ETC capacity to regenerate NAD+, especially in oxygen limited environments such as hypoxic regions in pancreatic cancer tumors. To offset this, carbon units from the TCA cycle can be diverted to be used as precursors to produce amino acids. For example, α-ketoglutarate can be converted to glutamate, which may be further processed to make proline (76). Oxaloacetate, a TCA cycle intermediate can be funneled into aspartate biosynthesis, which in turn produces asparagine – a pyrimidine building block (85). The mitochondria is a signaling hub that drives multiple metabolic processes, fine tunes redox homeostasis to protect against free radical damage, and plays a role a role in tumor initiation and progression (84,86–89).

1.5.4 Nutrient Scavenging

Oncogenic KRAS triggers pro-survival and pro-proliferation signaling through downstream mediators, and due the constitutively active state of mutant KRAS, these signals are in essence

always “on”. Cancer cells consume copious amounts of nutrients and metabolites in the already resource scare tumor milieu, exacerbating poor vascularization and oxygen availability in the TME (39,90). Due the limited availability of bio intermediates cancer cells may rely on scavenging and recycling pathways for alternative fuel sources. Autophagy is a highly evolutionarily conserved process triggered during cell stress and nutrient deprivation, through which organelles, proteins, and other macromolecules are degraded and byproducts are recycled. Cellular components are degraded by lysosomes, turnover of biomaterial then allows cancer cells to access metabolic precursors (91). Thus, autophagy plays a critical role in regulating cell proliferation and energy homeostasis. In several pancreatic cancer cell lines, inhibition of autophagy with pharmacological agents or siRNA resulted in decreased proliferation (92).

Autophagy also plays a role in immune evasion (92,93). Yamamoto et al. demonstrated increased lysosomal degradation of MHC- I molecules in pancreatic cancer ,via an autophagy mediated mechanism, involving the NBR1 cargo receptor (93). KRAS alters dependency on macropinocytosis as well, an endocytic pathway responsible for the digestion/internalization of plasma membrane proteins, and immune cells (93). In a murine model of pancreatic adenocarcinoma, loss of function in the PTEN tumor suppressor led to increased mTOR and macropinocytosis. Combined inhibition of mTOR signaling and lysosomal processes reversed resistance mediated through macropinocytosis in this model, demonstrating combined inhibition to be synergistic in this model (94). Overall, KRAS alters scavenging and recycling pathways so that cancer cells can divert intracellular energy sources to acquire more biomass and sustain bioenergetic process while protecting against reactive oxygen species damage.

1.5.5 Lipid metabolism

Lipids play a critical role as signaling molecules, providing substrates for membranes, and contributing nutrients in the form of; fatty acids, cholesterol, glycerolipids, sphingolipids, phospholipids, etc. Lipid composition, metabolism, and availability is directly impacted by changes metabolic alterations engendered in non-malignant and malignant cells present in the tumor microenvironment (95,96). Lipids are composed of a hydrophilic head group and hydrophobic tail which dictate the curvature of the lipid bilayer and transmembrane composition. This is crucial as many growth factor receptors inhabit the transmembrane, and lipid rafts serve as docking sites for signaling complexes (16). Oncogenic KRAS signal transduction leads the activation of downstream pathways such as the PI3K- AKT- mammalian target of rapamycin(mTORC1) axis, as well as MYC (64). Activation of this signaling cascade triggers de novo synthesis of fatty acids, mediated by the transcription factor sterol regulatory binding element protein 1 SREBP1 (97–99). Augmented levels of monounsaturated and saturated fatty acids have been linked to combatting ROS damage but have also been shown to contribute to tumor progression.

1.6 Metabolic Rewiring in the Tumor Microenvironment

Oncogenic signaling and nutrient dysregulation in the tumor microenvironment leads to metabolic rewiring of immune cells and non-malignant cells in proximity. As competition for scarce resources engenders immune dysfunction due to unmeet energetic demands necessary to execute an immune response (15). PDA is characterized a complex, fibro-inflammatory microenvironment rich in extracellular matrix components, myeloid cells, and fibroblast (4). CD8+ T cells have been shown to be sparce and show signs of "exhaustion" which can in part be attributed to insufficient nutrients ([54,100,101]). Macrophages, the most prominent immune cell type present, engage in cooperative metabolic exchange with cancer cells which aids in tumor growth

and survival ([40,58,59,102–105]). Recent work has also shown that fibroblasts participate in metabolic exchange with cancer cells, specifically by increasing expression of branch chain amino transferase BCAT1.

1.6.1 T cells

When naïve T cells are stimulated by costimulatory molecules and TCR ligation, metabolic rewiring ensues marked by a shift towards aerobic glycolysis and increase in oxidative phosphorylation (69,106–108). Glycolysis and oxidative phosphorylation provide T cells with glucose necessary to fuel nucleotide biosynthesis, DNA replication, and serine synthesis. These metabolic alterations are mediated by cytokine growth factors such as IL-2 and IL-17, mTOR signaling, transcription factors, and increased expression of nutrient transporters. Together mTOR and Akt regulate T cell differentiation through the activation of downstream signaling cascades which stimulate transcription factors such as SREBF2, which regulates cholesterol and lipid synthesis (71,108). T cell proliferation is also promoted by the upregulation of nutrient transporters such as GLUT1, the enzyme responsible for glucose transport (76).

Transcription factors play a critical role in T cell reprogramming, hypoxia inducible factor-1α (HIF1α) and c-Myc promote metabolic processes necessary to satisfy energetic demands associated with T cell differentiation and effector T cell clonal expansion (108,109). More specifically, c-MYC drives aerobic glycolysis and glutamine synthesis during T cell expansion, which provides bio intermediates that can be utilized for nucleotide and lipid biosynthesis (109). HIF1α promotes upregulation of GLUT1 and other key enzymes which drive glycolysis, a process critical for T cell effector activity (79,110).

Mitochondrial programs are also employed in T cell metabolic rewiring, as ROS signaling plays a critical role in T cell response to viral infections and tumor encounters (65,89). Importantly,

different T cell subsets have distinct metabolic profiles based on function, developmental stage, and external stimuli. For example, TH17 CD4+ T cells have recently been reported to largely depend on oxidative phosphorylation to execute anti tumoral response, without an accompanied shift of augmented glycolytic activity (72). Murine derived naïve CD4+ T cells were cultured and polarized towards TH17 activation, under conditions optimized to promote oxidative phosphorylation. Oxidative phosphorylation enabled TH17 cells to resist apoptosis via a mitophagy mediated mechanism (72), subsequently allowing the cells to mount an immune response upon tumor challenge. Methionine import is also augmented in T cell for S-adenosylmethionine (SAM) synthesize, a substrate involved in DNA histone methylation. In this manner, metabolic programs dictate epigenetic programming and promote T cell engagement with a myriad of metabolic processes to sustain activation, proliferation, and differentiation (111). T cells strategically engage metabolic processes such as glycine and serine synthesis, the TCA cycle, fatty acid synthesis, as well as one carbon anabolism to gain access to energetic substrates and co-factors to fuel a epigenetic programs needed for proliferation and survival (69). Extracellular metabolites, nutrient availability, and intrinsic and extrinsic signaling in the tumor microenvironment inform T cell metabolic reprogramming . For example, lactate, the end product of glycolysis has been shown to be involved in immune modulation of T cells. Nutrient availability and metabolite levels are altered in cancer settings and lead t exhausted/dysfunctional phenotypes in CD8+ T cells. Competition for fuel sources limits the T cell engagement with metabolic programs, leading to inability to mount an anti-tumor response, sustain proliferation, and undergo differentiation (112). As previously mentioned, CD8+ T cells upregulate glycolysis to meet metabolic demands imposed by effector functions, but glucose levels are depleted in the tumor microenvironment – suppressing cytotoxic T cells activity. Transcriptional analysis of T

cells has revealed heterogenous profiles amongst CD8+ T cells subsets, as naïve and memory CD8+ T cells shift towards fatty acid metabolism in glucose deprivation- but effector CD8+ T cells do not (71). Overall, T cells up/down regulate various metabolic process based on extrinsic cues in the microenvironment, nutrient availability, and inflammatory signaling and adjust metabolic dependencies in response.

1.6.2 Macrophages

Macrophages are the largest immune component in the pancreatic tumor microenvironment. Tumor associated macrophages (TAMs) participate in immune crosstalk, extracellular matrix remodeling, immunosuppressive signaling, and aid in tumor maintenance and progression (28,113–115). Thus, TAMs carry out a myriad of metabolic processes that may be either pro-tumor or anti-tumor. Macrophages present in the pancreatic cancer tumor environment are largely derived from myeloid derive suppressor cells (MDSCs) , a majority of which are pro tumori-genic. When activated in a cancer setting, macrophages can phagocytosis cancer cells, engage in metabolic crosstalk with innate and adaptive immune cells, and execute metabolic programs in response to extrinsic cues in the microenvironment (11,34,35,56,116–118). M1- like macrophages metabolically shift towards increased dependence on glycolysis, resulting in increased levels of reactive oxygen species (119,120). M2- like macrophages increase oxidative phosphorylation and fatty acid synthesis and oxidation, thus this subset of macrophages is more resistant to hypoxia in the tumor microenvironment (90). Still, TAMs are diverse and metabolic transcriptional programs can't be ascribed in a binary fashion, where a metabolic process is either antitumorigenic or inflammatory.

In pancreatic cancer, TAMs have been shown to be largely immunosuppressive, participating in cooperative metabolic crosstalk with cancer cells, augmenting expression of

immune checkpoint glands, immune suppressive cytokine signaling - enabling tumor cell growth and survival (63,119,121). TAMs undergo metabolic reprogramming in response to altered metabolite levels, crosstalk with malignant cells and immune cells, and in response adjust cytokine and growth factor signaling. Primary pancreatic tumor samples in PDA, demonstrated that a bulk of TAMs present were alternatively activated towards and M2-like phenotype. Myeloid cells drive therapeutic resistance, TAMs have been shown to expel pyrimidines which can be taken up by cancer cells, making pyrimidine nucleoside analogs such as gemcitabine, a chemotherapeutic for pancreatic less effective (115).

1.6.3 Innate immune cell metabolism

Neutrophils are innate immune cells that undertake different metabolic phenotypes depending on environmental stimuli during their lifespan. At basal state neutrophils rely largely on glycolysis, but in setting of tissue inflammation or cancer neutrophils shift to oxidative phosphorylation to facilitate bursting. Respiratory bursting is activated by chemokines, chemo attractants, or other environmental stimuli, causing neutrophils to release reactive oxygen species, degrading foreign pathogens and nearby tissue in the process (9). Neutrophils migrate to sites of inflammation in a multistep process consisting of; selectin mediated rolling, chemokine stimulated activation, integrin mediated adhesion, and ultimately migration (9,18,122).

B cells are a part of the innate immune system and contribute towards mounting an anti-tumor response. The role of B cell immune-metabolism modulation in the context of the tumor microenvironment remains to be fully investigated, though it has been established that B cells metabolism influences efficacy of immunotherapy in solid tumors (123). The lifespan of B cells entails multiple transitional stages from an immature to mature B cell, ultimately to a memory B cell. At each stage metabolic dependencies shift to fulfill demands of the functional phenotype

imposed on B cells due to environmental stimuli. Glycolysis and oxidative phosphorylation mediate are the prime metabolic processes altered by B cells to transition through development though (118,123). Overall, there is a need to understand how environmental cues and extrinsic signaling influence B cell immune metabolism activity, as B cells may also dampen the immune response.

1.6.4 Fibroblasts

The tumor milieu in pancreatic cancer is characterized by a fibroinflammatory stroma, abundant with a heterogenous mixture of cancer associated fibroblasts (CAFs) and extra cellular matrix components (4,119,124). CAFs are key immune modulators that dictate an immunosuppressive program in PDA by secreting paracrine signals, inhibiting cytotoxic functions of CD8+ T cells, and increasing vascularization of the tumor microenvironment (26). Further, a recent report has demonstrated CAFs provide branch chain ketoacid derivatives to pancreatic cancer cells, as a result of cancer mediated stromal reprogramming (34). CAFs also participate in ECM remodeling which contributes to tumor progression, invasion, and metastasis (125–127).

1.7 Single cell RNA- Seq

The advent of next generation sequencing (NGS) has enabled the characterization of tumor microenvironment landscapes, novel cellular subtypes, and putative cellular interactions at an unprecedented rate (19–25,27,29,126,128). More specifically, single cell -RNA sequencing has enabled the identification of new cancer associated fibroblast subtypes in a murine model of PDA (129). Single cell RNA -Seq data has also been utilized to query metabolic programs utilized by diverse subsets of TAMs derived from murine models with liver metastasis, revealing purine metabolism as a metabolic co-adaptation that promotes tumor growth (11). To decipher if

this metabolic reliance on purine metabolism translated to human data, publicly available single cell sequencing data from patients was mined. Indeed, human derived TAMs with increased expression of genes driving purine metabolism correlated with poor response to immunotherapy (11).

The immune landscape has also been profiled in pancreatic cancer by utilizing single cell RN-Seq on human pancreatic cancer samples (29). This study reported a heterogenous profile of cytotoxic T cells across patients samples, but strikingly a large proportion of cytotoxic T cells were found to have exhausted/dysfunctional transcriptomic profiles with high expression of TIGIT (29).

1.8 PDA Murine Models

To investigate pancreatic cancer, murine models have been genetically engineered to closely recapitulate human PDA, via expression of mutant KRAS and loss of expression in tumor suppressor genes (45). Murine PDA models demonstrate a similar genetic landscape, mirror disease progression, and the immune profile mimics that seen in human PDA (33).

To understand the role of mutant KRAS in pancreatic cancer initiation and progression am inducible and reversible murine model of pancreatic tumorigenesis was genetically engineered by the Pasca Lab (45). The iKras* mouse model enables the activation and inactivation of KRASG12D in the pancreas epithelium, enabling the investigation of the role of oncogenic KRAS during early and late stage PDA. To develop the model, three genetically altered mouse stains were utilized to create triple transgenic p48-Cre;R26-rtTa-IRES-EGFP;TetO-KrasG12D mice. Expression of Cre is driven by the p48-Cre allele which is specific to the pancreas, and rtTA activation through doxycycline administration or removal dictates mutant Kras* expression – hence the process is organ specific and reversible. In addition, to more closely mimic disease

progression the iKras model was crossed with mice in which there inactivation of one allele of tumor suppressor gene tp53 – iKras *-p53+/- (45). Overall, the iKras* model is an organ specific, reversible, and inducible system that serves as a powerful tool to study immune cell interactions, genetic alterations, and immunosuppressive signaling in pancreatic cancer.

References

1. Siegel RL, Giaquinto AN, Jemal A. Cancer statistics, 2024. CA Cancer J Clin. 2024;74(1):12-49. doi:10.3322/caac.21820

2. Sia, J. et al. Regulatory T Cells Shape the Differential Impact of Radiation Dose-Fractionation Schedules on Host Innate and Adaptive Antitumor Immune Defenses. Int. J. Radiat. Oncol. Biol. Phys. 111, 502–514 (2021).

3. Quiñonero F, Mesas C, Doello K, et al. The challenge of drug resistance in pancreatic ductal adenocarcinoma: a current overview. Cancer Biol Med. 2019;16(4):688-699. doi:10.20892/j.issn.2095-3941.2019.0252

4. Ying H, Dey P, Yao W, et al. Genetics and biology of pancreatic ductal adenocarcinoma. Genes Dev. 2016;30(4):355-385. doi:10.1101/gad.275776.115

5. Friedrich M, Sankowski R, Bunse L, et al. Tryptophan metabolism drives dynamic immunosuppressive myeloid states in IDH-mutant gliomas. Nat Cancer. 2021;2(7):723-740. doi:10.1038/s43018-021-00201-z

6. Rosa Neto JC, Calder PC, Curi R, Newsholme P, Sethi JK, Silveira LS. The Immunometabolic Roles of Various Fatty Acids in Macrophages and Lymphocytes. Int J Mol Sci. 2021;22(16):8460. doi:10.3390/ijms22168460

7. Bechard ME, Word AE, Tran AV, Liu X, Locasale JW, McDonald OG. Pentose conversions support the tumorigenesis of pancreatic cancer distant metastases. Oncogene. 2018;37(38):5248-5256. doi:10.1038/s41388-018-0346-5

8. Apiz Saab JJ, Dzierozynski LN, Jonker PB, et al. Pancreatic tumors exhibit myeloid-driven amino acid stress and upregulate arginine biosynthesis. DeNicola GM, El-Deiry WS, DeNicola GM, Gomes A, eds. eLife. 2023;12:e81289. doi:10.7554/eLife.81289

9. Injarabian L, Devin A, Ransac S, Marteyn BS. Neutrophil Metabolic Shift during Their Lifecycle: Impact on Their Survival and Activation. Int J Mol Sci. 2019;21(1):287. doi:10.3390/ijms21010287

10. Reyes-Castellanos G, Masoud R, Carrier A. Mitochondrial Metabolism in PDAC: From Better Knowledge to New Targeting Strategies. Biomedicines. 2020;8(8):270. doi:10.3390/biomedicines8080270

11 .Li S, Yu J, Huber A, et al. Metabolism drives macrophage heterogeneity in the tumor microenvironment. Cell Rep. 2022;39(1):110609. doi:10.1016/j.celrep.2022.110609
12. Lyssiotis CA, Kimmelman AC. Metabolic Interactions in the Tumor Microenvironment. Trends Cell Biol. 2017;27(11):863-875. doi:10.1016/j.tcb.2017.06.003
13. Biancur DE, Paulo JA, Małachowska B, et al. Compensatory metabolic networks in pancreatic cancers upon perturbation of glutamine metabolism. Nat Commun. 2017;8:15965. doi:10.1038/ncomms15965
14. Kerk SA, Papagiannakopoulos T, Shah YM, Lyssiotis CA. Metabolic networks in mutant KRAS-driven tumours: tissue specificities and the microenvironment. Nat Rev Cancer. 2021;21(8):510-525. doi:10.1038/s41568-021-00375-9
15. Dey P, Kimmelman AC, DePinho RA. Metabolic Codependencies in the Tumor Microenvironment. Cancer Discov. 2021;11(5):1067-1081. doi:10.1158/2159-8290.CD-20-1211
16. Vogel FCE, Chaves-Filho AB, Schulze A. Lipids as mediators of cancer progression and metastasis. Nat Cancer. 2024;5(1):16-29. doi:10.1038/s43018-023-00702-z
17. Nwosu ZC, Ward MH, Sajjakulnukit P, et al. Uridine-derived ribose fuels glucose-restricted pancreatic cancer. Nature. 2023;618(7963):151-158. doi:10.1038/s41586-023-06073-w
18. Abdalla HB, Napimoga MH, Lopes AH, et al. Activation of PPAR-γ induces macrophage polarization and reduces neutrophil migration mediated by heme oxygenase 1. Int Immunopharmacol. 2020;84:106565. doi:10.1016/j.intimp.2020.106565
19. Burclaff J, Bliton RJ, Breau KA, et al. A Proximal-to-Distal Survey of Healthy Adult Human Small Intestine and Colon Epithelium by Single-Cell Transcriptomics. Cell Mol Gastroenterol Hepatol. 2022;13(5):1554-1589. doi:10.1016/j.jcmgh.2022.02.007
20. Huang Y, Mohanty V, Dede M, et al. Characterizing cancer metabolism from bulk and single-cell RNA-seq data using METAFlux. Nat Commun. 2023;14(1):4883. doi:10.1038/s41467-023-40457-w
21. Oh K, Yoo YJ, Torre-Healy LA, et al. Coordinated single-cell tumor microenvironment dynamics reinforce pancreatic cancer subtype. Nat Commun. 2023;14(1):5226. doi:10.1038/s41467-023-40895-6
22. Hosein AN, Huang H, Wang Z, et al. Cellular heterogeneity during mouse pancreatic ductal adenocarcinoma progression at single-cell resolution. JCI Insight. 2019;4(16). doi:10.1172/jci.insight.129212

23. Loke P, Lin JD. Redefining inflammatory macrophage phenotypes across stages and tissues by single-cell transcriptomics. Sci Immunol. 2022;7(70):eabo4652. doi:10.1126/sciimmunol.abo4652

24. Qian J, Olbrecht S, Boeckx B, et al. A pan-cancer blueprint of the heterogeneous tumor microenvironment revealed by single-cell profiling. Cell Res. 2020;30(9):745-762. doi:10.1038/s41422-020-0355-0

25. Ma RY, Black A, Qian BZ. Macrophage diversity in cancer revisited in the era of single-cell omics. Trends Immunol. 2022;43(7):546-563. doi:10.1016/j.it.2022.04.008

26. Velez-Delgado A, Donahue KL, Brown KL, et al. Extrinsic KRAS Signaling Shapes the Pancreatic Microenvironment Through Fibroblast Reprogramming. Cell Mol Gastroenterol Hepatol. 2022;13(6):1673-1699. doi:10.1016/j.jcmgh.2022.02.016

27. Eze UC, Bhaduri A, Haeussler M, Nowakowski TJ, Kriegstein AR. Single-cell atlas of early human brain development highlights heterogeneity of human neuroepithelial cells and early radial glia. Nat Neurosci. 2021;24(4):584-594. doi:10.1038/s41593-020-00794-1

28. Menjivar RE, Nwosu ZC, Du W, et al. Arginase 1 is a key driver of immune suppression in pancreatic cancer. eLife. 2023;12:e80721. doi:10.7554/eLife.80721

29. Steele NG, Carpenter ES, Kemp SB, et al. Multimodal Mapping of the Tumor and Peripheral Blood Immune Landscape in Human Pancreatic Cancer. Nat Cancer. 2020;1(11):1097-1112. doi:10.1038/s43018-020-00121-4

30. Carpenter ES, Elhossiny AM, Kadiyala P, et al. Analysis of Donor Pancreata Defines the Transcriptomic Signature and Microenvironment of Early Neoplastic Lesions. Cancer Discov. 2023;13(6):1324-1345. doi:10.1158/2159-8290.CD-23-0013

31. Sarantis P, Koustas E, Papadimitropoulou A, Papavassiliou AG, Karamouzis MV. Pancreatic ductal adenocarcinoma: Treatment hurdles, tumor microenvironment and immunotherapy. World J Gastrointest Oncol. 2020;12(2):173. doi:10.4251/wjgo.v12.i2.173

32. Halbrook CJ, Lyssiotis CA, Pasca di Magliano M, Maitra A. Pancreatic cancer: Advances and challenges. Cell. 2023;186(8):1729-1754. doi:10.1016/j.cell.2023.02.014

33. Martínez-Jiménez F, Muiños F, Sentís I, et al. A compendium of mutational cancer driver genes. Nat Rev Cancer. 2020;20(10):555-572. doi:10.1038/s41568-020-0290-x

34. Zhu Z, Achreja A, Meurs N, et al. Tumour-reprogrammed stromal BCAT1 fuels branched-chain ketoacid dependency in stromal-rich PDAC tumours. Nat Metab. 2020;2(8):775-792. doi:10.1038/s42255-020-0226-5

35. Mitchem JB, Brennan DJ, Knolhoff BL, et al. Targeting Tumor-Infiltrating Macrophages Decreases Tumor-Initiating Cells, Relieves Immunosuppression, and Improves Chemotherapeutic Responses. Cancer Res. 2013;73(3):1128-1141. doi:10.1158/0008-5472.CAN-12-2731

36. Miret JJ, Kirschmeier P, Koyama S, et al. Suppression of Myeloid Cell Arginase Activity leads to Therapeutic Response in a NSCLC Mouse Model by Activating Anti-Tumor Immunity. J Immunother Cancer. 2019;7(1):32. doi:10.1186/s40425-019-0504-5

37. Zhang Y, Lazarus J, Steele NG, et al. Regulatory T-cell Depletion Alters the Tumor Microenvironment and Accelerates Pancreatic Carcinogenesis. Cancer Discov. 2020;10(3):422-439. doi:10.1158/2159-8290.CD-19-0958

38. Kemp SB, Pasca di Magliano M, Crawford HC. Myeloid Cell Mediated Ilmmune Suppression in Pancreatic Cancer. Cell Mol Gastroenterol Hepatol. 2021;12(5):1531-1542. doi:10.1016/j.jcmgh.2021.07.006

39. Hao X, Ren Y, Feng M, Wang Q, Wang Y. Metabolic reprogramming due to hypoxia in pancreatic cancer: Implications for tumor formation, immunity, and more. Biomed Pharmacother. 2021;141:111798. doi:10.1016/j.biopha.2021.111798

40. Netea-Maier RT, Smit JWA, Netea MG. Metabolic changes in tumor cells and tumor-associated macrophages: A mutual relationship. Cancer Lett. 2018;413:102-109. doi:10.1016/j.canlet.2017.10.037

41. Wang L, Xie D, Wei D. Pancreatic Acinar-to-Ductal Metaplasia and Pancreatic Cancer. Methods Mol Biol Clifton NJ. 2019;1882:299-308. doi:10.1007/978-1-4939-8879-2_26

42. Zhang Y, Yan W, Mathew E, et al. Epithelial-Myeloid cell crosstalk regulates acinar cell plasticity and pancreatic remodeling in mice. Rath S, ed. eLife. 2017;6:e27388. doi:10.7554/eLife.27388

43. Hallin J, Engstrom LD, Hargis L, et al. The KRASG12C Inhibitor MRTX849 Provides Insight toward Therapeutic Susceptibility of KRAS-Mutant Cancers in Mouse Models and Patients. Cancer Discov. 2020;10(1):54-71. doi:10.1158/2159-8290.CD-19-1167

44. Combining immunotherapy with KRAS inhibitor eliminates advanced KRAS-mutant pancreatic cancer in preclinical models | MD Anderson Cancer Center. Accessed January 27, 2024.

https://www.mdanderson.org/newsroom/combining-immunotherapy-kras-inhibitor-eliminates-advanced-kras-mutant-pancreatic-cancer-preclinical-models.h00-159621012.html
45. Collins MA, Bednar F, Zhang Y, et al. Oncogenic Kras is required for both the initiation and maintenance of pancreatic cancer in mice. J Clin Invest. 2012;122(2):639-653. doi:10.1172/JCI59227
46. Cowzer D, Zameer M, Conroy M, Kolch W, Duffy AG. Targeting KRAS in Pancreatic Cancer. J Pers Med. 2022;12(11):1870. doi:10.3390/jpm12111870
47. Huang L, Guo Z, Wang F, Fu L. KRAS mutation: from undruggable to druggable in cancer. Signal Transduct Target Ther. 2021;6(1):1-20. doi:10.1038/s41392-021-00780-4
48. Skoulidis F, Li BT, Dy GK, et al. Sotorasib for Lung Cancers with KRAS p.G12C Mutation. N Engl J Med. 2021;384(25):2371-2381. doi:10.1056/NEJMoa2103695
49. Fakih MG, Kopetz S, Kuboki Y, et al. Sotorasib for previously treated colorectal cancers with KRASG12C mutation (CodeBreaK100): a prespecified analysis of a single-arm, phase 2 trial. Lancet Oncol. 2022;23(1):115-124. doi:10.1016/S1470-2045(21)00605-7
50. Jänne PA, Riely GJ, Gadgeel SM, et al. Adagrasib in Non–Small-Cell Lung Cancer Harboring a KRASG12C Mutation. N Engl J Med. 2022;387(2):120-131. doi:10.1056/NEJMoa2204619
51. Kemp SB, Cheng N, Markosyan N, et al. Efficacy of a Small-Molecule Inhibitor of KrasG12D in Immunocompetent Models of Pancreatic Cancer. Cancer Discov. 2023;13(2):298-311. doi:10.1158/2159-8290.CD-22-1066
52. Wei D, Wang L, Zuo X, Maitra A, Bresalier RS. A Small Molecule with Big Impact: MRTX1133 Targets the KRASG12D Mutation in Pancreatic Cancer. Clin Cancer Res. 2024;30(4):655-662. doi:10.1158/1078-0432.CCR-23-2098
53. Mirati Therapeutics Inc. A Phase 1/2 Multiple Expansion Cohort Trial of MRTX1133 in Patients With Advanced Solid Tumors Harboring a KRAS G12D Mutation. clinicaltrials.gov; 2023. Accessed December 31, 2023. https://clinicaltrials.gov/study/NCT05737706
54. Jiang Y, Li Y, Zhu B. T-cell exhaustion in the tumor microenvironment. Cell Death Dis. 2015;6(6):e1792-e1792. doi:10.1038/cddis.2015.162
55. Li J, He Y, Hao J, Ni L, Dong C. High Levels of Eomes Promote Exhaustion of Anti-tumor CD8+ T Cells. Front Immunol. 2018;9. Accessed October 2, 2023. https://www.frontiersin.org/articles/10.3389/fimmu.2018.02981

56. Fletcher M, Ramirez ME, Sierra RA, et al. l-Arginine depletion blunts antitumor T-cell responses by inducing myeloid-derived suppressor cells. Cancer Res. 2015;75(2):275-283. doi:10.1158/0008-5472.CAN-14-1491

57. Gionfriddo G, Plastina P, Augimeri G, et al. Modulating Tumor-Associated Macrophage Polarization by Synthetic and Natural PPARγ Ligands as a Potential Target in Breast Cancer. Cells. 2020;9(1):174. doi:10.3390/cells9010174

58. Goossens P, Rodriguez-Vita J, Etzerodt A, et al. Membrane Cholesterol Efflux Drives Tumor-Associated Macrophage Reprogramming and Tumor Progression. Cell Metab. 2019;29(6):1376-1389.e4. doi:10.1016/j.cmet.2019.02.016

59. Puthenveetil A, Dubey S. Metabolic reprograming of tumor-associated macrophages. Ann Transl Med. 2020;8(16):1030. doi:10.21037/atm-20-2037

60. Nywening TM, Wang-Gillam A, Sanford DE, et al. Targeting tumour-associated macrophages with CCR2 inhibition in combination with FOLFIRINOX in patients with borderline resectable and locally advanced pancreatic cancer: a single-centre, open-label, dose-finding, non-randomised, phase 1b trial. Lancet Oncol. 2016;17(5):651-662. doi:10.1016/S1470-2045(16)00078-4

61. Hosein AN, Dougan SK, Aguirre AJ, Maitra A. Translational advances in pancreatic ductal adenocarcinoma therapy. Nat Cancer. 2022;3(3):272-286. doi:10.1038/s43018-022-00349-2

62. Grünwald BT, Devisme A, Andrieux G, et al. Spatially confined sub-tumor microenvironments in pancreatic cancer. Cell. 2021;184(22):5577-5592.e18. doi:10.1016/j.cell.2021.09.022

63. Cui Zhou D, Jayasinghe RG, Chen S, et al. Spatially restricted drivers and transitional cell populations cooperate with the microenvironment in untreated and chemo-resistant pancreatic cancer. Nat Genet. 2022;54(9):1390-1405. doi:10.1038/s41588-022-01157-1

64. Dong Y, Tu R, Liu H, Qing G. Regulation of cancer cell metabolism: oncogenic MYC in the driver's seat. Signal Transduct Target Ther. 2020;5(1):1-11. doi:10.1038/s41392-020-00235-2

65. Purohit V, Simeone DM, Lyssiotis CA. Metabolic Regulation of Redox Balance in Cancer. Cancers. 2019;11(7):955. doi:10.3390/cancers11070955

66. Ying H, Kimmelman AC, Lyssiotis CA, et al. Oncogenic Kras maintains pancreatic tumors through regulation of anabolic glucose metabolism. Cell. 2012;149(3):656-670. doi:10.1016/j.cell.2012.01.058

67. Son J, Lyssiotis CA, Ying H, et al. Glutamine supports pancreatic cancer growth through a KRAS-regulated metabolic pathway. Nature. 2013;496(7443):101-105. doi:10.1038/nature12040
68. Halbrook CJ, Lyssiotis CA. Employing Metabolism to Improve the Diagnosis and Treatment of Pancreatic Cancer. Cancer Cell. 2017;31(1):5-19. doi:10.1016/j.ccell.2016.12.006
69. Reina-Campos M, Scharping NE, Goldrath AW. CD8+ T cell metabolism in infection and cancer. Nat Rev Immunol. 2021;21(11):718-738. doi:10.1038/s41577-021-00537-8
70. Rodríguez-Enríquez S, Marín-Hernández Á, Gallardo-Pérez JC, et al. Transcriptional Regulation of Energy Metabolism in Cancer Cells. Cells. 2019;8(10):1225. doi:10.3390/cells8101225
71. Pearce EL, Walsh MC, Cejas PJ, et al. Enhancing CD8 T-cell memory by modulating fatty acid metabolism. Nature. 2009;460(7251):103-107. doi:10.1038/nature08097
72. Hong HS, Mbah NE, Shan M, et al. OXPHOS promotes apoptotic resistance and cellular persistence in TH17 cells in the periphery and tumor microenvironment. Sci Immunol. 2022;7(77):eabm8182. doi:10.1126/sciimmunol.abm8182
73. Caronni N, La Terza F, Vittoria FM, et al. IL-1β+ macrophages fuel pathogenic inflammation in pancreatic cancer. Nature. 2023;623(7986):415-422. doi:10.1038/s41586-023-06685-2
74. Xu R, Yang J, Ren B, et al. Reprogramming of Amino Acid Metabolism in Pancreatic Cancer: Recent Advances and Therapeutic Strategies. Front Oncol. 2020;10. Accessed August 21, 2023. https://www.frontiersin.org/articles/10.3389/fonc.2020.572722
75. Kerk SA, Lin L, Myers AL, et al. Metabolic requirement for GOT2 in pancreatic cancer depends on environmental context. Finley LW, White RM, eds. eLife. 2022;11:e73245. doi:10.7554/eLife.73245
76. Pavlova NN, Zhu J, Thompson CB. The hallmarks of cancer metabolism: Still emerging. Cell Metab. 2022;34(3):355-377. doi:10.1016/j.cmet.2022.01.007
77. Banh RS, Biancur DE, Yamamoto K, et al. Neurons Release Serine to Support mRNA Translation in Pancreatic Cancer. Cell. 2020;183(5):1202-1218.e25. doi:10.1016/j.cell.2020.10.016
78. Yang M, Vousden KH. Serine and one-carbon metabolism in cancer. Nat Rev Cancer. 2016;16(10):650-662. doi:10.1038/nrc.2016.81
79. Daniel SK, Sullivan KM, Labadie KP, Pillarisetty VG. Hypoxia as a barrier to immunotherapy in pancreatic adenocarcinoma. Clin Transl Med. 2019;8(1):e10. doi:10.1186/s40169-019-0226-9

80. Bott AJ, Shen J, Tonelli C, et al. Glutamine Anabolism Plays a Critical Role in Pancreatic Cancer by Coupling Carbon and Nitrogen Metabolism. Cell Rep. 2019;29(5):1287-1298.e6. doi:10.1016/j.celrep.2019.09.056

81. Liu YH, Hu CM, Hsu YS, Lee WH. Interplays of glucose metabolism and KRAS mutation in pancreatic ductal adenocarcinoma. Cell Death Dis. 2022;13(9):1-10. doi:10.1038/s41419-022-05259-w

82. Lee JH, Cho Y ra, Kim JH, et al. Branched-chain amino acids sustain pancreatic cancer growth by regulating lipid metabolism. Exp Mol Med. 2019;51(11):1-11. doi:10.1038/s12276-019-0350-z

83. Mangalhara KC, Varanasi SK, Johnson MA, et al. Manipulating mitochondrial electron flow enhances tumor immunogenicity. Science. 2023;381(6664):1316-1323. doi:10.1126/science.abq1053

84. Yu J, Shi L, Lin W, Lu B, Zhao Y. UCP2 promotes proliferation and chemoresistance through regulating the NF-κB/β-catenin axis and mitochondrial ROS in gallbladder cancer. Biochem Pharmacol. 2020;172:113745. doi:10.1016/j.bcp.2019.113745

85. Halbrook CJ, Thurston G, Boyer S, et al. Differential integrated stress response and asparagine production drive symbiosis and therapy resistance of pancreatic adenocarcinoma cells. Nat Cancer. 2022;3(11):1386-1403. doi:10.1038/s43018-022-00463-1

86. Kiritsy MC, McCann K, Mott D, et al. Mitochondrial respiration contributes to the interferon gamma response in antigen-presenting cells. Horng T, Garrett WS, Zanoni I, eds. eLife. 2021;10:e65109. doi:10.7554/eLife.65109

87. Gobelli D, Serrano-Lorenzo P, Esteban-Amo MJ, et al. The mitochondrial succinate dehydrogenase complex controls the STAT3-IL-10 pathway in inflammatory macrophages. iScience. 2023;26(8):107473. doi:10.1016/j.isci.2023.107473

88. Vasan K, Werner M, Chandel NS. Mitochondrial Metabolism as a Target for Cancer Therapy. Cell Metab. 2020;32(3):341-352. doi:10.1016/j.cmet.2020.06.019

89. Zhang L, Zhang W, Li Z, et al. Mitochondria dysfunction in CD8+ T cells as an important contributing factor for cancer development and a potential target for cancer treatment: a review. J Exp Clin Cancer Res. 2022;41(1):227. doi:10.1186/s13046-022-02439-6

90. Pietrobon V, Marincola FM. Hypoxia and the phenomenon of immune exclusion. J Transl Med. 2021;19(1):9. doi:10.1186/s12967-020-02667-4

91. Mulcahy Levy JM, Thorburn A. Autophagy in cancer: moving from understanding mechanism to improving therapy responses in patients. Cell Death Differ. 2020;27(3):843-857. doi:10.1038/s41418-019-0474-7

92. Piffoux M, Eriau E, Cassier PA. Autophagy as a therapeutic target in pancreatic cancer. Br J Cancer. 2021;124(2):333-344. doi:10.1038/s41416-020-01039-5

93. Yamamoto K, Venida A, Yano J, et al. Autophagy promotes immune evasion of pancreatic cancer by degrading MHC-I. Nature. 2020;581(7806):100-105. doi:10.1038/s41586-020-2229-5

94. Michalopoulou E, Auciello FR, Bulusu V, et al. Macropinocytosis Renders a Subset of Pancreatic Tumor Cells Resistant to mTOR Inhibition. Cell Rep. 2020;30(8):2729-2742.e4. doi:10.1016/j.celrep.2020.01.080

95. Auciello FR, Bulusu V, Oon C, et al. A Stromal Lysolipid–Autotaxin Signaling Axis Promotes Pancreatic Tumor Progression. Cancer Discov. 2019;9(5):617-627. doi:10.1158/2159-8290.CD-18-1212

96. Cheng H, Wang M, Su J, et al. Lipid Metabolism and Cancer. Life. 2022;12(6):784. doi:10.3390/life12060784

97. Guo C, Chi Z, Jiang D, et al. Cholesterol Homeostatic Regulator SCAP-SREBP2 Integrates NLRP3 Inflammasome Activation and Cholesterol Biosynthetic Signaling in Macrophages. Immunity. 2018;49(5):842-856.e7. doi:10.1016/j.immuni.2018.08.021

98. Kusnadi A, Park SH, Yuan R, et al. The cytokine TNF promotes transcription factor SREBP activity and binding to inflammatory genes to activate macrophages and limit tissue repair. Immunity. 2019;51(2):241-257.e9. doi:10.1016/j.immuni.2019.06.005

99. Gu X, Zhu Q, Tian G, et al. KIF11 manipulates SREBP2-dependent mevalonate cross talk to promote tumor progression in pancreatic ductal adenocarcinoma. Cancer Med. 2022;11(17):3282-3295. doi:10.1002/cam4.4683

100. Huang Y, Si X, Shao M, Teng X, Xiao G, Huang H. Rewiring mitochondrial metabolism to counteract exhaustion of CAR-T cells. J Hematol OncolJ Hematol Oncol. 2022;15(1):38. doi:10.1186/s13045-022-01255-x

101. Li J, He Y, Hao J, Ni L, Dong C. High Levels of Eomes Promote Exhaustion of Anti-tumor CD8+ T Cells. Front Immunol. 2018;9. Accessed October 2, 2023. https://www.frontiersin.org/articles/10.3389/fimmu.2018.02981

102. El-Kenawi A, Dominguez-Viqueira W, Liu M, et al. Macrophage-Derived Cholesterol Contributes to Therapeutic Resistance in Prostate Cancer. Cancer Res. 2021;81(21):5477-5490. doi:10.1158/0008-5472.CAN-20-4028
103. Rosa Neto JC, Calder PC, Curi R, Newsholme P, Sethi JK, Silveira LS. The Immunometabolic Roles of Various Fatty Acids in Macrophages and Lymphocytes. Int J Mol Sci. 2021;22(16):8460. doi:10.3390/ijms22168460
104. Wu H, Han Y, Rodriguez Sillke Y, et al. Lipid droplet-dependent fatty acid metabolism controls the immune suppressive phenotype of tumor-associated macrophages. EMBO Mol Med. 2019;11(11):e10698. doi:10.15252/emmm.201910698
105. Tekin C, Aberson HL, Bijlsma MF, Spek CA. Early macrophage infiltrates impair pancreatic cancer cell growth by TNF-α secretion. BMC Cancer. 2020;20(1):1183. doi:10.1186/s12885-020-07697-1
106. Buck MD, O'Sullivan D, Klein Geltink RI, et al. Mitochondrial Dynamics Controls T Cell Fate through Metabolic Programming. Cell. 2016;166(1):63-76. doi:10.1016/j.cell.2016.05.035
107. Cao J, Liao S, Zeng F, Liao Q, Luo G, Zhou Y. Effects of altered glycolysis levels on CD8+ T cell activation and function. Cell Death Dis. 2023;14(7):1-13. doi:10.1038/s41419-023-05937-3
108. Chang CH, Curtis JD, Maggi LB, et al. Posttranscriptional Control of T Cell Effector Function by Aerobic Glycolysis. Cell. 2013;153(6):1239-1251. doi:10.1016/j.cell.2013.05.016
109. Man K, Kallies A. Synchronizing transcriptional control of T cell metabolism and function. Nat Rev Immunol. 2015;15(9):574-584. doi:10.1038/nri3874
110. Heiduk M, Klimova A, Reiche C, et al. TIGIT Expression Delineates T-cell Populations with Distinct Functional and Prognostic Impact in Pancreatic Cancer. Clin Cancer Res. 2023;29(14):2638-2650. doi:10.1158/1078-0432.CCR-23-0258
111. Shyh-Chang N, Locasale JW, Lyssiotis CA, et al. Influence of Threonine Metabolism on S-adenosyl-methionine and Histone Methylation. Science. 2013;339(6116):222-226. doi:10.1126/science.1226603
112. Hanahan D, Weinberg RA. Hallmarks of cancer: the next generation. Cell. 2011;144(5):646-674. doi:10.1016/j.cell.2011.02.013
113. Rodriguez PC, Quiceno DG, Zabaleta J, et al. Arginase I Production in the Tumor Microenvironment by Mature Myeloid Cells Inhibits T-Cell Receptor Expression and Antigen-

Specific T-Cell Responses. Cancer Res. 2004;64(16):5839-5849. doi:10.1158/0008-5472.CAN-04-0465

114. Eisinger S, Sarhan D, Boura VF, et al. Targeting a scavenger receptor on tumor-associated macrophages activates tumor cell killing by natural killer cells. Proc Natl Acad Sci U S A. 2020;117(50):32005-32016. doi:10.1073/pnas.2015343117

115. Halbrook CJ, Pontious C, Kovalenko I, et al. Macrophage-Released Pyrimidines Inhibit Gemcitabine Therapy in Pancreatic Cancer. Cell Metab. 2019;29(6):1390-1399.e6. doi:10.1016/j.cmet.2019.02.001

116. Laviron M, Petit M, Weber-Delacroix E, et al. Tumor-associated macrophage heterogeneity is driven by tissue territories in breast cancer. Cell Rep. 2022;39(8). doi:10.1016/j.celrep.2022.110865

117. Mantovani A, Allavena P, Marchesi F, Garlanda C. Macrophages as tools and targets in cancer therapy. Nat Rev Drug Discov. 2022;21(11):799-820. doi:10.1038/s41573-022-00520-5

118. Zuo C, Baer JM, Knolhoff BL, et al. Stromal and therapy-induced macrophage proliferation promotes PDAC progression and susceptibility to innate immunotherapy. J Exp Med. 2023;220(6):e20212062. doi:10.1084/jem.20212062

119. DeNardo DG, Ruffell B. Macrophages as regulators of tumour immunity and immunotherapy. Nat Rev Immunol. 2019;19(6):369-382. doi:10.1038/s41577-019-0127-6

120. Boyer S, Lee HJ, Steele N, et al. Multiomic characterization of pancreatic cancer-associated macrophage polarization reveals deregulated metabolic programs driven by the GM-CSF–PI3K pathway. Fertig EJ, Zaidi M, DeNardo D, eds. eLife. 2022;11:e73796. doi:10.7554/eLife.73796

121. Arlauckas SP, Garren SB, Garris CS, et al. Arg1 expression defines immunosuppressive subsets of tumor-associated macrophages. Theranostics. 2018;8(21):5842-5854. doi:10.7150/thno.26888

122. Cao Z, Zhao M, Sun H, Hu L, Chen Y, Fan Z. Roles of mitochondria in neutrophils. Front Immunol. 2022;13:934444. doi:10.3389/fimmu.2022.934444

123. Jiang S, Feng R, Tian Z, Zhou J, Zhang W. Metabolic dialogs between B cells and the tumor microenvironment: Implications for anticancer immunity. Cancer Lett. 2023;556:216076. doi:10.1016/j.canlet.2023.216076

124. Angius F, Spolitu S, Uda S, et al. High-density lipoprotein contribute to G0-G1/S transition in Swiss NIH/3T3 fibroblasts. Sci Rep. 2015;5(1):17812. doi:10.1038/srep17812

125. Raghavan KS, Francescone R, Franco-Barraza J, et al. NetrinG1+ Cancer-Associated Fibroblasts Generate Unique Extracellular Vesicles that Support the Survival of Pancreatic Cancer Cells Under Nutritional Stress. Cancer Res Commun. 2022;2(9):1017-1036. doi:10.1158/2767-9764.CRC-21-0147

126. Steele NG, Biffi G, Kemp SB, et al. Inhibition of Hedgehog Signaling Alters Fibroblast Composition in Pancreatic Cancer. Clin Cancer Res Off J Am Assoc Cancer Res. 2021;27(7):2023-2037. doi:10.1158/1078-0432.CCR-20-3715

127. Zhang T, Ren Y, Yang P, Wang J, Zhou H. Cancer-associated fibroblasts in pancreatic ductal adenocarcinoma. Cell Death Dis. 2022;13(10):1-11. doi:10.1038/s41419-022-05351-1

128. Hanley CJ, Waise S, Ellis MJ, et al. Single-cell analysis reveals prognostic fibroblast subpopulations linked to molecular and immunological subtypes of lung cancer. Nat Commun. 2023;14(1):387. doi:10.1038/s41467-023-35832-6

129. Sahai E, Astsaturov I, Cukierman E, et al. A framework for advancing our understanding of cancer-associated fibroblasts. Nat Rev Cancer. 2020;20(3):174-186. doi:10.1038/s41568-019-0238-1

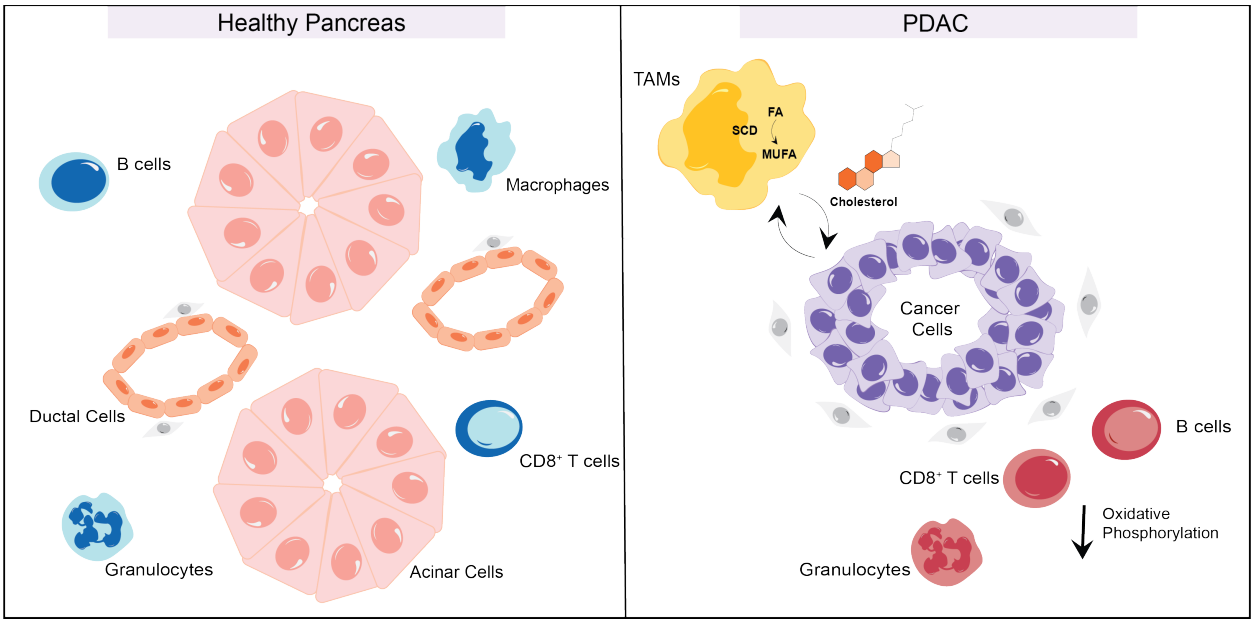
Healthy Pancreas
B cells
Macrophages
Ductal Cells
CD8⁺ T cells
Granulocytes
Acinar Cells
PDAC
TAMs
FA
SCD
MUFA
Cholesterol
Cancer Cells
B cells
CD8⁺ T cells
Oxidative Phosphorylation
Granulocytes

Figure 1.1 Schematic for metabolic alterations engendered by the pancreatic tumor microenvironment.

The healthy pancreas is composed of islet, acinar, and ductal cells as well as extracellular matrix and immune components. The endocrine system is responsible for blood/sugar homeostasis levels and the exocrine system is concerned with digestive functions – pancreatic ductal adenocarcinoma arises through the exocrine tissue. To investigate metabolic alterations across cellular compartments engendered by malignancy, a unique single cell data set compromised of healthy pancreata, and patient pancreatic cancer samples was leveraged. Tumor associated macrophages displayed an upregulation of lipid/cholesterol production, while cancer cancers cells differentially increased expression of the cognate receptor for lipid/cholesterol import. Tumor associated immune compartments significantly decreased oxidative phosphorylation in an electron transport chain (ETC) complex and cell type dependent manner. Overall, cancer cell underwent autonomous metabolic reprogramming , immune cells underwent metabolic alterations, and TAMs participated in cellular crosstalk with cancer cells.

Chapter 2 Mapping the Metabolic Landscape of the Healthy Human and Pancreatic Tumor Microenvironment

2.1 Abstract

Pancreatic cancer, one of the deadliest human malignancies, is characterized by a fibro-inflammatory tumor microenvironment and wide array of metabolic alterations. To comprehensively map metabolism in a cell type specific manner, we harnessed a unique single cell RNA sequencing dataset of normal human pancreata. This was compared with human pancreatic cancer samples using a computational pipeline optimized for this study. In the cancer cells we observed enhanced biosynthetic programs. We identified downregulation of mitochondrial programs in several immune populations, relative to their normal counterparts in healthy pancreas. While granulocytes, B cells, and CD8+ T cells all downregulated oxidative phosphorylation, the mechanisms by which this occurred was cell-type specific. In fact, the expression pattern of the electron transport chain complexes was sufficient to identify immune cell types without the use of lineage markers. We also observed changes in tumor associated macrophage (TAM) lipid metabolism, with increased expression of enzymes mediating unsaturated fatty acid synthesis and upregulation in cholesterol export. Concurrently, cancer cells exhibit upregulation of lipid/cholesterol receptor import. We thus identified a potential crosstalk whereby TAMs provide cholesterol to cancer cells. We suggest that this may be a new mechanism boosting cancer cell growth and therapeutic target in the future.

[1] Chapter 2 has been submitted for publication to JCI Insight as a resource article.

[2] Author List: Monica E. Bonilla[1,4], Megan D. Radyk[2], Matthew D.Perricone[3], Ahmed M. Elhossiny[4], Alexis C. Harold[1], Paola I. Medina-Cabrera[1], Padma Kadiyala[3], Jiaqi Shi[5,6], Timothy L. Frankel[5,7], Eileen S. Carpenter[5,8], Michael D. Green[1,5,10,11,12] , Cristina Mitrea[4,†], Costas A. Lyssiotis[2,5,8,†], Marina Pasca di Magliano[5,7,9,†]

[†]Corresponding authors

2.2 Introduction

Pancreatic ductal adenocarcinoma (PDA) is a lethal disease with a current 5-year survival rate of 13% (1). Its poor prognosis can be attributed to a lack of early detection methods and a paucity of effective therapeutic options. Indeed, at diagnosis, most patients present with locally advanced or metastatic disease that is refractory to chemotherapy, radiotherapy, and immunotherapy (2). At the genetic level, pancreatic cancer is almost invariably associated with mutations in Kras, together with common loss of tumor suppressor genes such as TP53, the INK4A locus and SMAD4 (3). A hallmark of pancreatic cancer is the extensive tumor microenvironment (TME), an agglomerate of fibroblasts, immune cells, and non-cellular components of the extracellular matrix, that is hypovascularized and extremely nutrient deprived (3,4). Within the TME, fibroblasts and immune cells actively support cancer cells, allowing them to persist and grow even in the absence of adequate vascularization (5). PDA cells scavenge nutrients to circumvent limited supply, sourcing non-classical nutrients from their environment through expression of high avidity nutrient transporters, bulk engulfment, and crosstalk with other cell types (6–11).

Competition for nutrients promotes immune cell dysfunction (12). Metabolic restrictions imposed on T cells have been shown to decrease proliferation and cytotoxic effector functions which dampen anti-tumor responses (13). Tumor associated macrophages (TAMs), the most prevalent immune cell type in pancreatic cancer, exert tumor-promoting and immunosuppressive functions through multiple parallel mechanisms, including expression of immune checkpoint ligands, production of tumor-supporting growth factors, and production of immune suppressive cytokines (14). Among the mechanisms through which TAMs promote immunosuppression is depletion of nutrients that are essential for T cell proliferation/activation, such as arginine,

through expression of the enzyme Arginase (15–17); arginine is one of the most depleted nutrients in the pancreatic TME (18). In addition to dampening immune responses, arginine depletion directly benefits cancer cells (19). In another role, TAMs can also provide cancer cells with pyrimidines, a building block for DNA required for proliferation; in the process also conferring resistance to pyrimidine nucleoside analog chemotherapeutics such as gemcitabine (20). However, a comprehensive map of metabolic co-adaptations across cell types in human pancreatic cancer has so far been missing.

Until recently, one of the challenges with generating data from normal pancreas was the lack of single cell level gene expression data. The latter is explained by the absence of clinical indications for sampling normal pancreas in healthy individuals, and by the rapid degradation of pancreas tissue through autodigestion after death. As a result, most studies have used adjacent normal samples as controls; this approach has significant limitations, as the adjacent normal pancreas presents with morphologic and inflammatory changes that lead to gene expression alterations (21). Through a unique partnership with Gift of Life Michigan, an organ donation organization, we have obtained pancreata from healthy individuals of varied age group, sex, and race, and performed single cell RNA sequencing (21). The availability of "true normal" pancreas has given us a unique opportunity to define metabolic alterations, at the transcriptional level, between the normal pancreas and pancreatic cancer on a cell type by cell type basis.

To investigate both (i) cell type specific metabolic changes and (ii) coordinated changes between cell types that promote cooperative metabolism in the pancreatic microenvironment, we leveraged single cell RNA sequencing data from normal human pancreata and human pancreatic tumors (21,22). To this data, we performed differential gene expression (DGE) analysis, gene set enrichment analysis (GSEA), and transcription factor activity analysis. In addition, we also

assessed for cooperative metabolic crosstalk pathways that were differentially regulated in cancer relative to normal. This collective analysis revealed prominent changes in amino acid and vitamin metabolism in the epithelial compartment that recapitulated previous findings (11,23,24). We also discovered alterations that were not previously described. In the immune compartments, multiple tumor associated immune cell subtypes had decreased expression of the oxidative phosphorylation signature compared to their counterparts in the healthy pancreas. Intriguingly, the specific gene expression signatures were cell-type specific.

We then investigated reciprocal metabolic interactions between cancer cells and components of the microenvironment. Notably, TAMs were found to upregulate the cholesterol exporter ABCG1, while pancreatic cancer cells significantly increased expression of the cognate receptor LDLR. This interaction was validated through immunofluorescent staining of human tissue, suggesting a novel metabolic interaction in pancreatic cancer that allows cancer cells to prioritize cholesterol scavenging relative to biosynthesis. Overall, our study provides an atlas of metabolic alterations engendered in pancreatic cancer across multiple cellular compartments, which may promote cancer cell growth and the maintenance of an immunosuppressive microenvironment resistant to existing therapeutic strategies.

2.3 Results

2.3.1 Single cell atlas from healthy human pancreata and pancreatic cancer samples reveals metabolic alterations in several compartments of the tumor microenvironment.

To query metabolic reprogramming across the pancreatic tumor microenvironment, we leveraged datasets previously published by our laboratory, including pancreatic cancer (n=16, across disease stages) and normal pancreas (n= 6) (21,22). Using DGE analysis, GSEA, and

transcription factor inference analysis, we sought to understand metabolic alterations in malignant and non-malignant cells in the pancreas (Figure 2.1A). The data, visualized using Uniform Manifold Approximation and Projection (UMAP), included 44,019 cells from healthy pancreata and 43,997 cells from pancreatic cancer samples (Figure 2.1B and Figure 2.1C). Healthy and tumor samples readily segregated based on gene expression profiles (Figure 2.1D).

In the healthy exocrine pancreas, the epithelial compartment is composed of acinar, ductal, and endocrine cells. While both acinar and ductal cells can give rise to pancreatic cancer in mouse models, cancer cells are more transcriptionally similar to ductal cells. Conversely, acinar cells have a specific transcriptional profile characterized by a prevalence of genes encoding for digestive enzymes (25,26). To compare tumor and healthy tissue, we excluded acinar cells from our analysis and focused primarily on ductal and malignant cells, hereafter referred to as non-acinar epithelial cells. As expected, acinar cells were mostly detected in healthy tissue, while non-acinar epithelial cells, fibroblasts, and multiple immune compartments were present in both healthy and malignant tissue, although immune cells were more abundant in tumors (Figure 2.2A). A few populations, namely endocrine, dendritic, and neural cells, had limited representation with only hundreds of cells. Due to low statistical power, these cell types were interrogated only in a subset of our analyses (Figure 2.2B-H).

DGE analysis allows for the investigation of differentially regulated genes that drive multiple biological processes, including metabolism, on a per cell type basis. Application of DGE analysis on tumor samples relative to normal revealed differential upregulation of 4,977 genes and downregulation of 4,104 genes in non-acinar epithelial cells, which includes normal ductal cells and cancer cells (Figure 2.1E). Granulocytes from tumors exhibited differential upregulation of 18 genes and downregulation of 812 genes (Figure 2.1F). Among lymphocyte

populations, CD8+ T cells from pancreatic tumors exhibited significant differential upregulation of 287 genes and downregulation of 89 genes; in CD4+ T cells, we observed 121 upregulated and 6,530 downregulated genes, respectively (Figure 2.1G and Figure 2.1H). Macrophages upregulated 993 genes and downregulated 881 genes (Figure 2.1I). We also analyzed several less abundant types of cells; however, due to limited cell number, the DGE were less informative (Figure 2.2C-H).

We next performed transcription factor inference analysis to ascertain master regulatory networks in the healthy human pancreas and PDA samples (Table 1 and Table 2**).** Further, we performed analysis to distinguish transcription factors that had the highest log fold change in PDA samples compared to healthy tissue (Table 3). We used the single-cell regulatory network inference and clustering (SCENIC) package in R to infer putative regulon activity. Transcription factor motif enrichment analysis enables the identification of gene targets regulated by a transcription factor – these comprise a "regulon", and AUCell assigns a corresponding regulon activity score to cells (27). Collectively, these analyses revealed changes in regulon activity for corresponding transcription factors by cell type and disease status.

In epithelial cells, we observed increased activity for transcription factors that positively regulate cell proliferation (GRHL1, NR2F6, FOXC2) and immunosuppression (KLF3, IRF6, TBX21) in tumor samples as compared to normal pancreata (28–33). In addition, regulon activity corresponding to ONECUT2 increased in epithelial cells from tumor tissue. ONECUT2 has been implicated in driving neuroendocrine prostate cancer and promoting metastasis in ovarian cancer (34,35). Tumor infiltrating T cells expressed higher regulon activity scores for FOXO family transcription factors, which mediate induction of renewal capacity in memory T cells and effector function in cytotoxic T cells (36–38). In addition, NFKB2, STAT4, and

STAT1 regulon activity were increased in T cells from tumor tissue. These transcription factors are critical regulators of innate and adaptive immune responses, T cell effector and memory function, and helper T cell differentiation (39,40). Tumor associated macrophages exhibited enrichment for SREBF2 and PPARG, regulators of cholesterol and lipid homeostasis, respectively (31,41). Recent studies have shown that PPARG plays a critical role in TAM polarization in the tumor microenvironment, and may be an actionable therapeutic target (42,43).

Finally, to compare metabolic gene expression programs, we performed GSEA with a curated list of pathways containing all metabolic gene sets available from the KEGG database (44). GSEA relies on gene sets to computationally determine statistical significance between two states. It is therefore more stringent than DGE analysis and may capture processes not readily apparent with DGE analysis. We focused this analysis on epithelial cells, macrophages, granulocytes, T cells (both $CD4^+$, and $CD8^+$), and B cells, based on the abundance of cells available for this analysis (Figure 2.1C). As noted above, some cell populations could not be compared as they had limited representation in both healthy and tumor samples. Epithelial cancer cells exhibited higher vitamin A and biosynthetic machinery (Figure 2.3B-E), while many immune cell types in the tumor downregulated mitochondrial respiration (Figure 2.5B-D), and $CD8^+$ T cells in the tumor demonstrated unique metabolic deregulation associated with exhaustion (Figure 2.7G-H). These observations are divided on a cell type-specific basis in the sections that follow.

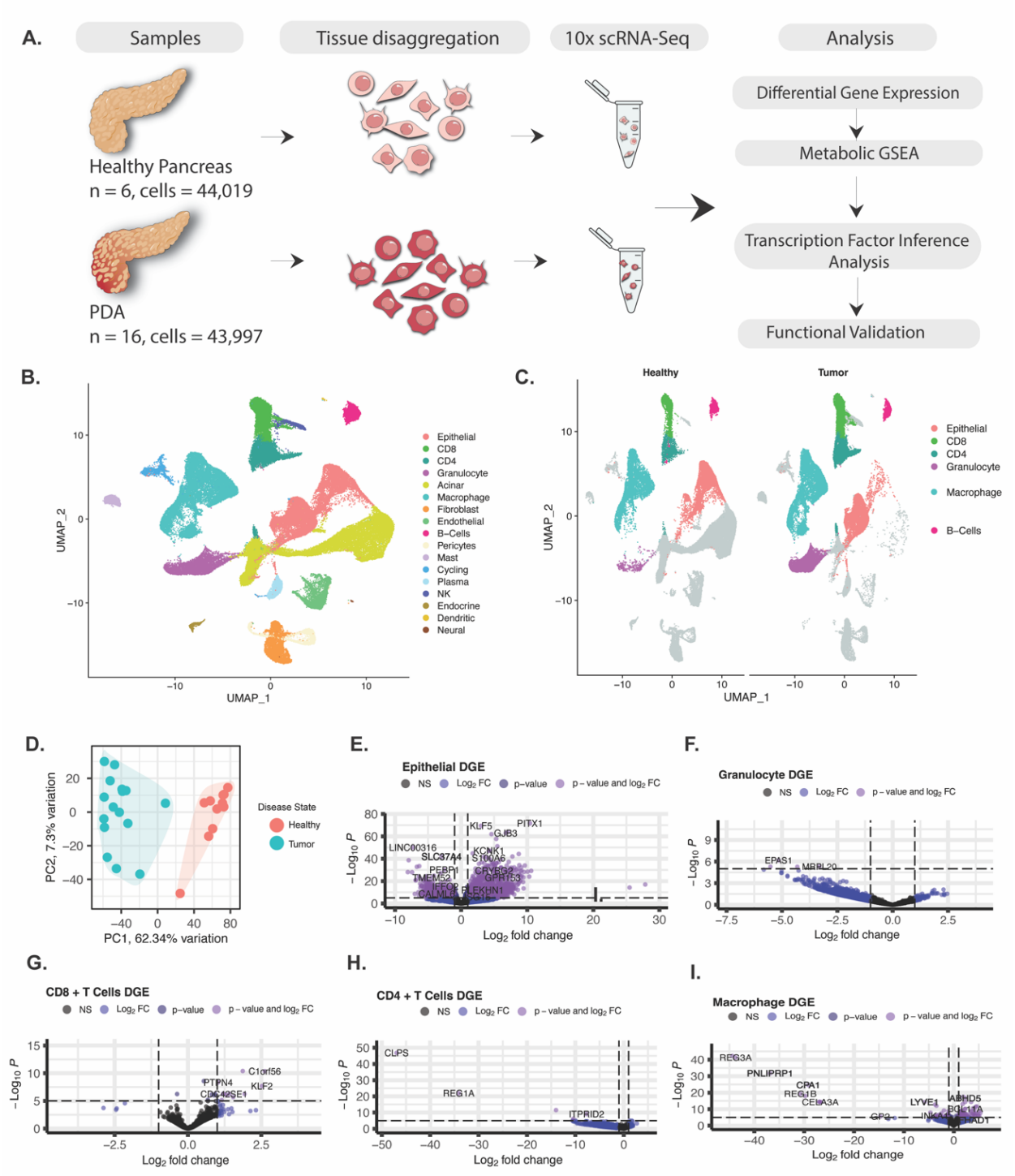
A.
Samples
Tissue disaggregation
10x scRNA-Seq
Analysis
Healthy Pancreas
n = 6, cells = 44,019
PDA
n = 16, cells = 43,997
Differential Gene Expression
Metabolic GSEA
Transcription Factor Inference Analysis
Functional Validation
B.
Epithelial
CD8
CD4
Granulocyte
Acinar
Macrophage
Fibroblast
Endothelial
B–Cells
Pericytes
Mast
Cycling
Plasma
NK
Endocrine
Dendritic
Neural
UMAP_1
UMAP_2
C.
Healthy
Tumor
D.
PC2, 7.3% variation
PC1, 62.34% variation
Disease State
Healthy
Tumor
E.
Epithelial DGE
NS
Log2 FC
p–value
p – value and log2 FC
Log2 fold change
F.
Granulocyte DGE
G.
CD8 + T Cells DGE
H.
CD4 + T Cells DGE
I.
Macrophage DGE

Figure 2.1 Data composition and workflow.

(A) Schematic of single cell sequencing performed on 6 healthy pancreatas procured from a collaboration with the Gift of Life Michigan, a center for organ and tissue procurement and 16 pancreatic cancer samples; 10 from surgical resections and 6 from fine needle biopsies at the University of Michigan. Followed by analysis workflow.

(B) Uniform manifold approximation and projection (UMAP) visualization of all identified cell types present in the pancreatic microenvironment.

(C) UMAP visualization of cell types which demonstrated significant metabolic alterations in the pancreatic cancer samples compared to healthy human pancreas tissue when GSEA is performed with metabolic gene sets.
(D)Principal component analysis (PCA) plot of healthy human pancreata samples and PDA samples.

(E-I) Volcano plots of differential gene expression by cell type. Genes that are significantly up- (top-right) and down- regulated (top-left) in tumor versus heathy and the gene symbols are included for representative differentially expressed genes.

A

Healthy	
Cell Type	Cell Number
Epithelial	7060
CD8	1335
CD4	1244
Granulocyte	349
Acinar	17450
Macrophage	5844
Fibroblast	2405
Endothelial	3911
B-Cells	1715
Pericytes	1165
Mast	159
Cycling	639
Plasma	90
NK	89
Endocrine	529
Dendritic	0
Neural	35

Tumor	
Cell Type	Cell Number
Epithelial	9584
CD8	3813
CD4	5074
Granulocyte	4859
Acinar	1290
Macrophage	9085
Fibroblast	2434
Endothelial	396
B-Cells	1209
Pericytes	813
Mast	1682
Cycling	1005
Plasma	1476
NK	1089
Endocrine	18
Dendritic	127
Neural	43

B

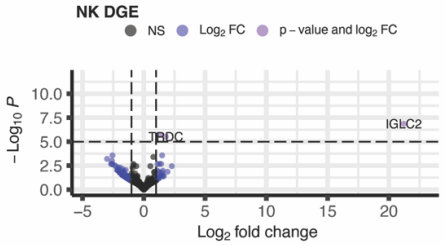

C

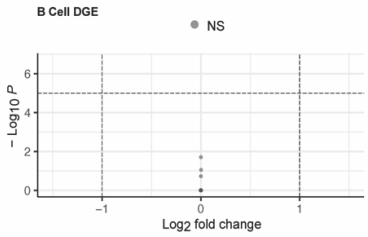

D.

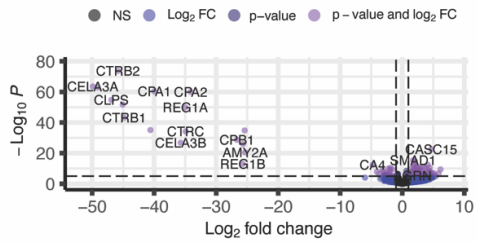

E.

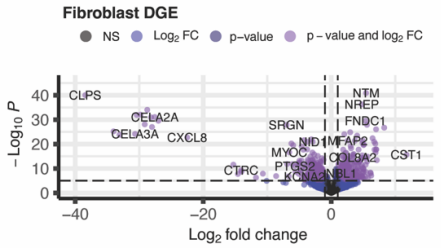

F.

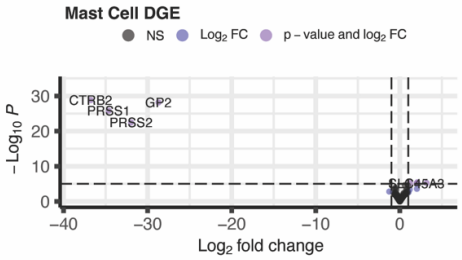

G.

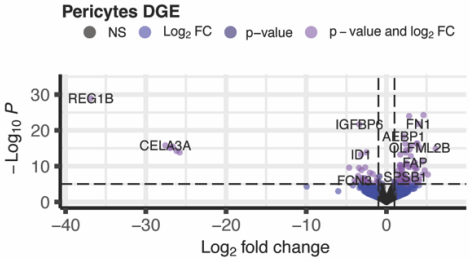

H.

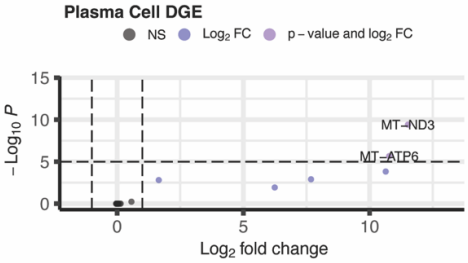

Figure 2.2 Cell numbers across cell types in healthy and pancreatic tissue and DGE analysis.

(A) Table with number of cells per population in the healthy and tumor samples.

(**B-H)** Volcano plots of differential gene expression by cell type. Genes that are significantly up- (top-right) and down- regulated (top-left) in tumor versus heathy and the gene symbols are included for representative differentially expressed genes.

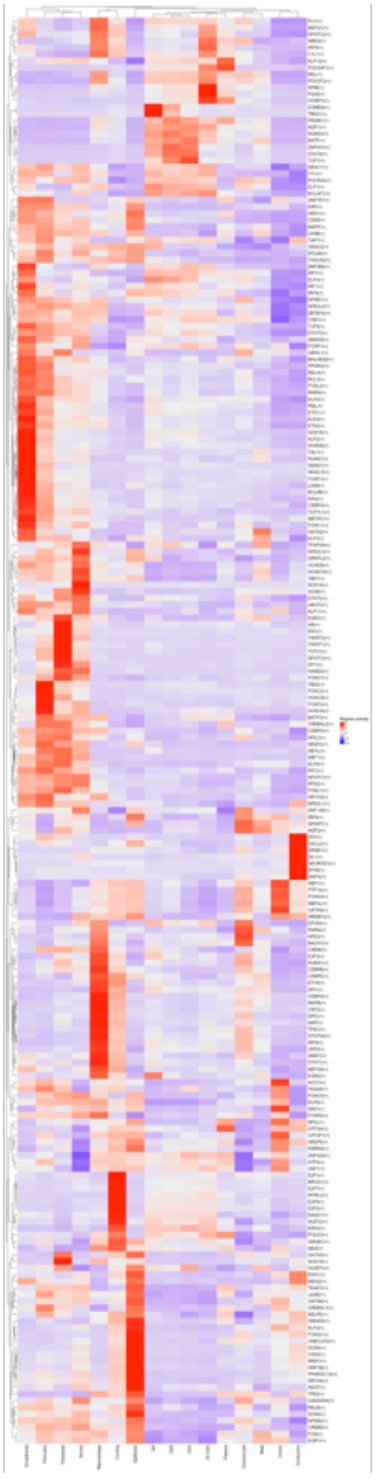

Table 1 Transcription Factor Analysis for the Healthy Pancreas

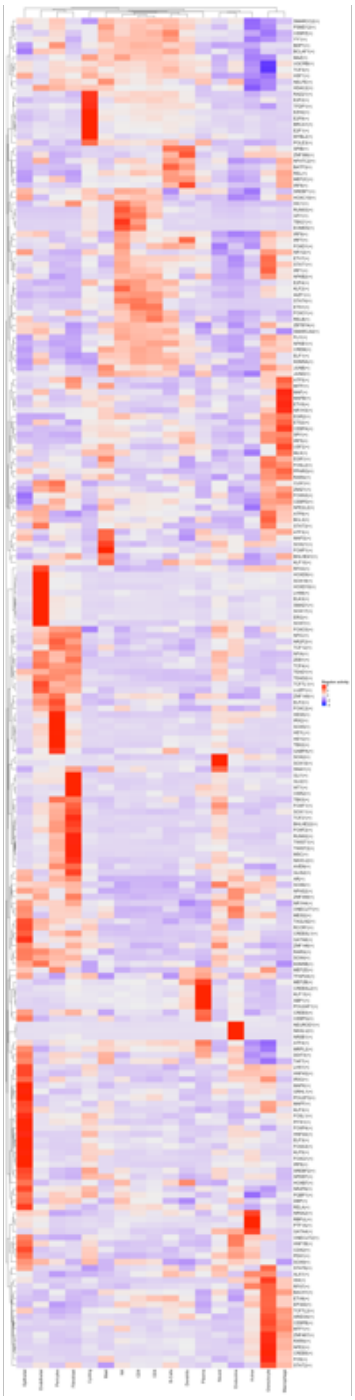

Table 2 Transcription Factor Inference Analysis for Tumor Derived Tissue

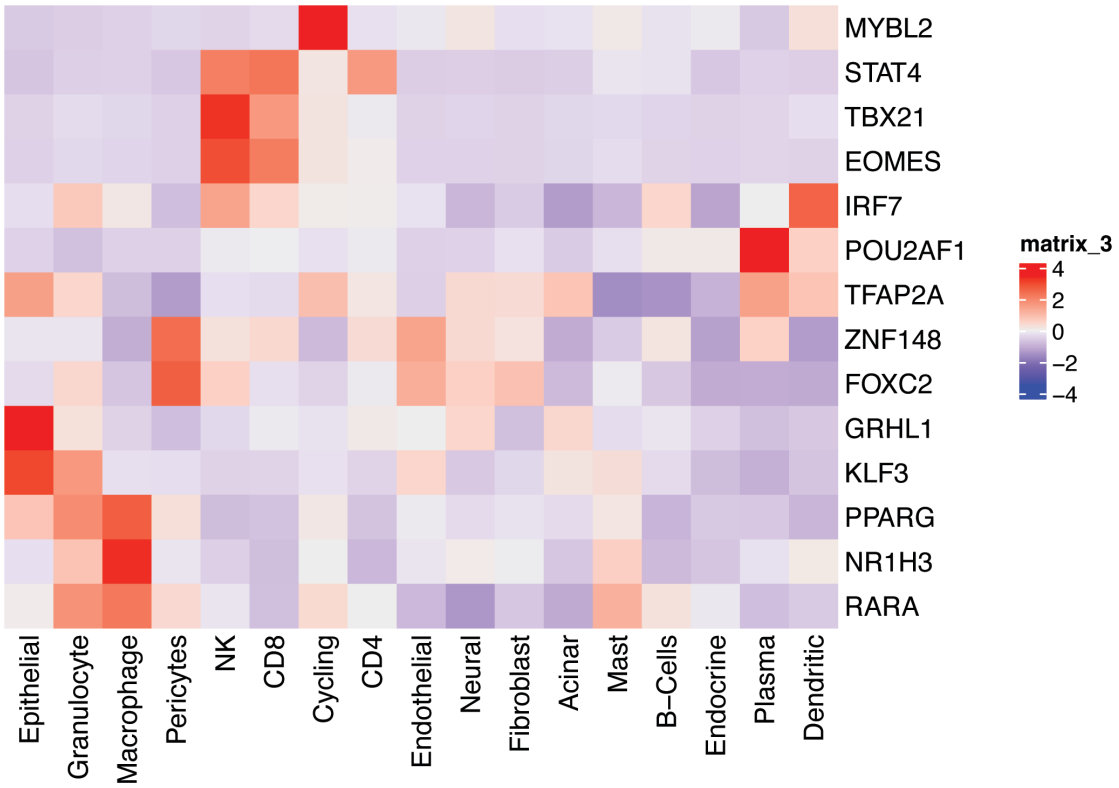

Table 3 Transcription factors with highest log fold change in PDA compared to healthy tissue

2.3.2 Pancreatic cancer cells engage vitamin A metabolism and downregulate amino acid catabolism.

We started our investigation into metabolic rewiring with cancer epithelial cells relative to normal epithelial cells (Figure 2.3A). Cancer cells co-opt a wide array of metabolic adaptations to manage deregulated nutrient and oxygen availability and to disrupt access to anti-tumor immune cells (45). Similar to prior reports, we observed that pentose conversions were increased in cancer cells, as described previously (6,46), as were lipid and vitamin metabolism pathways (Figure 3.1A and Figure 3.1B). Specifically, epithelial cells derived from tumor tissue decreased oxidative phosphorylation and fatty acid oxidation, as well as several amino acid catabolic pathways (Figure 2.3A, Figure 2.3C-E and Figure 2.4A) (47,48).

Next, we examined differential expression of genes that contributed most to the enrichment score, denoted as leading edge genes (Figure 2.3F-I). Retinol metabolism was the only significantly increased pathway in tumor derived epithelial cells compared to healthy epithelial cells (Figure 2.3B). Within in this pathway, we observed that tumor cells differentially increased the expression of genes encoding enzymes related to the production of retinol aldehydes, retinyl esters, and retinoic acid (Figure 2.3F). Retinoic acid signaling is involved in development, proliferation, and mediation of mechanosensing in the stroma through its interaction with myosin light chain 2 (MLC-2) (49,50). More specifically, the vitamin A metabolite all-trans retinoic acid has been implicated in reprogramming the PDA stroma via downregulation of MLC-2, leading to pancreatic stellate cell quiescence (51). For this reason, targeting vitamin A metabolism has been proposed as a potential therapeutic strategy for stromal reprogramming (52). Our data demonstrate a significant increase in RETSTAT expression (Figure 2.3F), which Bi et al. identified as a crucial mediator of ferroptosis (53). Collectively,

our data add to the growing body of research pointing towards retinoic acid signaling as a critical mediator of tumor progression and maintenance.

Amino acid degradation pathways were the most downregulated in epithelial cells from pancreatic tumors, relative to normal epithelial cells (Figure 2.3C-E). These included branched chain amino acid (BCAA) metabolism; glycine/serine/threonine metabolism; and cysteine/methionine metabolism. In general, the broad downregulation of amino acid catabolism may suggest increased utilization/prioritization of amino acids for protein biosynthesis. However, each of these pathways serve other functions and their downregulation may reflect other altered purposes. For example, BCAA catabolism can fuel tricarboxylic acid (TCA) cycle anaplerosis, a process that also provides nitrogen for other functions (54) (Figure 3.1G). In either case, our observation is consistent with a recent study that illustrated decreased BCAA degradation in PDA models (23). In a related study, it was also shown that stromal cell reprogramming in PDA can lead to the production and release of BCAAs from stromal cells and their provision to PDA cells (11). These studies and others (54) have focused on the branched chain amino acid transaminase (BCAT); our data showed significantly decreased BCAT1/2 gene expression in tumor derived epithelial cells, thereby adding to a growing body of work demonstrating that PDA cells seemingly prioritize BCAAs for purposes other than degradation.

Similarly, glycine/serine/threonine have non-proteinogenic functions. In humans, threonine is not catabolized (55), and the inclusion of this GSEA term was captured based on the functions of glycine and serine. Unlike BCAAs, glycine and serine are non-essential amino acids. They can be obtained through diet or made de novo in most cell types in the body (56). We observed that both serine synthesis (based on PHGDH expression) and catabolism (based on SHMT1 expression) were downregulated in cancerous epithelial cells (Figure 2.3H), indicating

that serine is likely derived from diet or other cell types in pancreatic cancer. Further, glycine and serine are substrates for 1-carbon metabolism, and glycine (which can be derived from serine) is one of three amino acids in the glutathione tripeptide. Our data also suggest a decreased reliance on serine and glycine for these pathways.

GSEA also revealed a significant decrease in cysteine and methionine metabolism in tumor derived epithelial cells compared to healthy epithelial cells (Figure 2.3E). Based on the genes involved, this centered around methionine metabolism, and its role in providing one carbon units (Figure 2.3I). The decrease in 1-carbon units from serine/glycine and methionine metabolism indicates that either there is a decrease in histone methylation or that another source of one carbon units stand in for these amino acids. Collectively, these observations suggest decreased amino acid catabolism in the cancer cells may support protein biosynthesis.

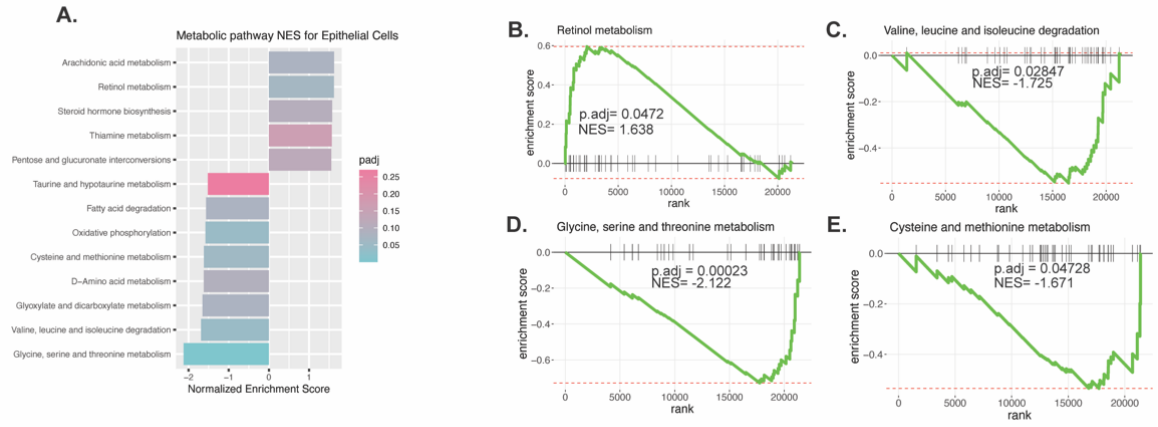
A.
Metabolic pathway NES for Epithelial Cells
Arachidonic acid metabolism
Retinol metabolism
Steroid hormone biosynthesis
Thiamine metabolism
Pentose and glucuronate interconversions
Taurine and hypotaurine metabolism
Fatty acid degradation
Oxidative phosphorylation
Cysteine and methionine metabolism
D-Amino acid metabolism
Glyoxylate and dicarboxylate metabolism
Valine, leucine and isoleucine degradation
Glycine, serine and threonine metabolism
padj
0.25
0.20
0.15
0.10
0.05
Normalized Enrichment Score
B.
Retinol metabolism
p.adj= 0.0472
NES= 1.638
enrichment score
rank
C.
Valine, leucine and isoleucine degradation
p.adj= 0.02847
NES= -1.725
D.
Glycine, serine and threonine metabolism
p.adj = 0.00023
NES= -2.122
E.
Cysteine and methionine metabolism
p.adj = 0.04728
NES= -1.671

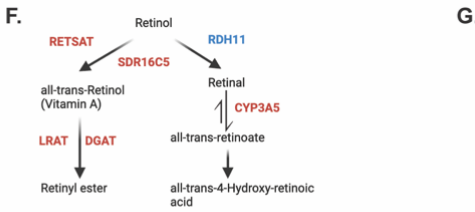
F.
Retinol
RETSAT
RDH11
SDR16C5
all-trans-Retinol
(Vitamin A)
Retinal
CYP3A5
LRAT
DGAT
all-trans-retinoate
Retinyl ester
all-trans-4-Hydroxy-retinoic
acid

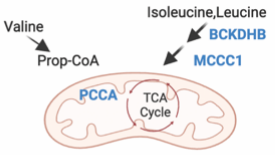
G.
Valine
Isoleucine,Leucine
BCKDHB
Prop-CoA
MCCC1
PCCA
TCA
Cycle

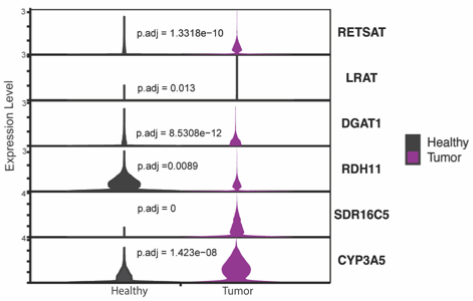
Expression Level
p.adj = 1.3318e−10
RETSAT
p.adj = 0.013
LRAT
p.adj = 8.5308e−12
DGAT1
p.adj =0.0089
RDH11
p.adj = 0
SDR16C5
p.adj = 1.423e−08
CYP3A5
Healthy
Tumor
Healthy
Tumor

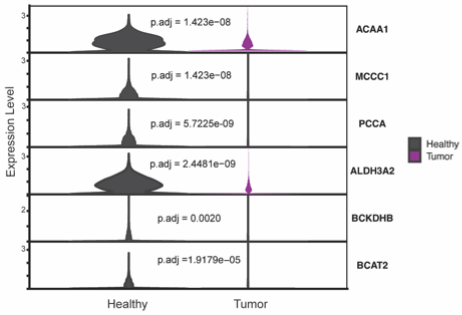
Expression Level
p.adj = 1.423e−08
ACAA1
p.adj = 1.423e−08
MCCC1
p.adj = 5.7225e−09
PCCA
p.adj = 2.4481e−09
ALDH3A2
p.adj = 0.0020
BCKDHB
p.adj =1.9179e−05
BCAT2
Healthy
Tumor
Healthy
Tumor

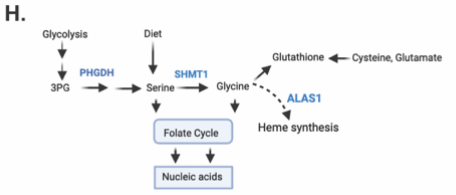
H.
Glycolysis
Diet
PHGDH
SHMT1
3PG
Serine
Glycine
Glutathione
Cysteine, Glutamate
ALAS1
Heme synthesis
Folate Cycle
Nucleic acids

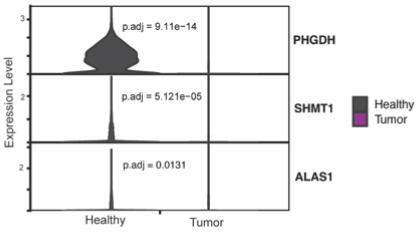
Expression Level
p.adj = 9.11e−14
PHGDH
p.adj = 5.121e−05
SHMT1
p.adj = 0.0131
ALAS1
Healthy
Tumor
Healthy
Tumor

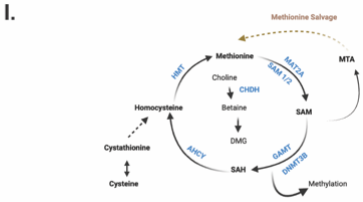
I.
Methionine Salvage
Methionine
MTA
Choline
CHDH
Betaine
SAM
Homocysteine
DMG
Cystathionine
Cysteine
SAH
Methylation

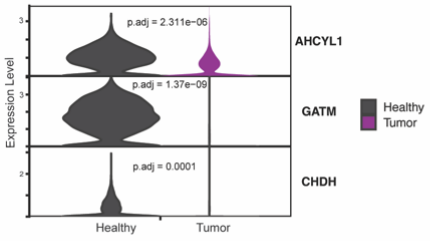
Expression Level
p.adj = 2.311e−06
AHCYL1
p.adj = 1.37e−09
GATM
p.adj = 0.0001
CHDH
Healthy
Tumor
Healthy
Tumor

Figure 2.3 Metabolic co-adaptations in pancreatic cancer cells.

(**A)** Significantly altered metabolic pathways in epithelial cells derived from pancreatic cancer samples compared to healthy pancreas samples, with corresponding normalized enrichment scores (NES) and adjusted p-values from GSEA analysis.

(**B-E**) GSEA Enrichment plots of significantly up or down regulated metabolic pathways in cancer cells with corresponding NES and adjusted p-values.

(**F)** Schematic of retinol metabolism, blue corresponding to differentially decreased genes, and red to differentially increased in tumor derived epithelial cells. Violin plots of selected retinol metabolism genes comparing healthy to tumor, with adjusted p-values for significantly differentially expressed genes.

(**G)** Schematic of valine, leucine, and isoleucine degradation. Violin plots of selected valine, leucine, and isoleucine metabolism genes comparing healthy to tumor, with adjusted p-values for significantly differentially expressed genes.

(**H)** Schematic of glycine, serine , and threonine metabolism . Violin plots of selected glycine, serine , and threonine metabolism genes comparing healthy to tumor, with adjusted p-values for significantly differentially expressed genes.

(**I)** Schematic of cysteine and methionine metabolism . Violin plots of cysteine and methionine metabolism genes comparing healthy to tumor, with adjusted p-values for significantly differentially expressed genes.

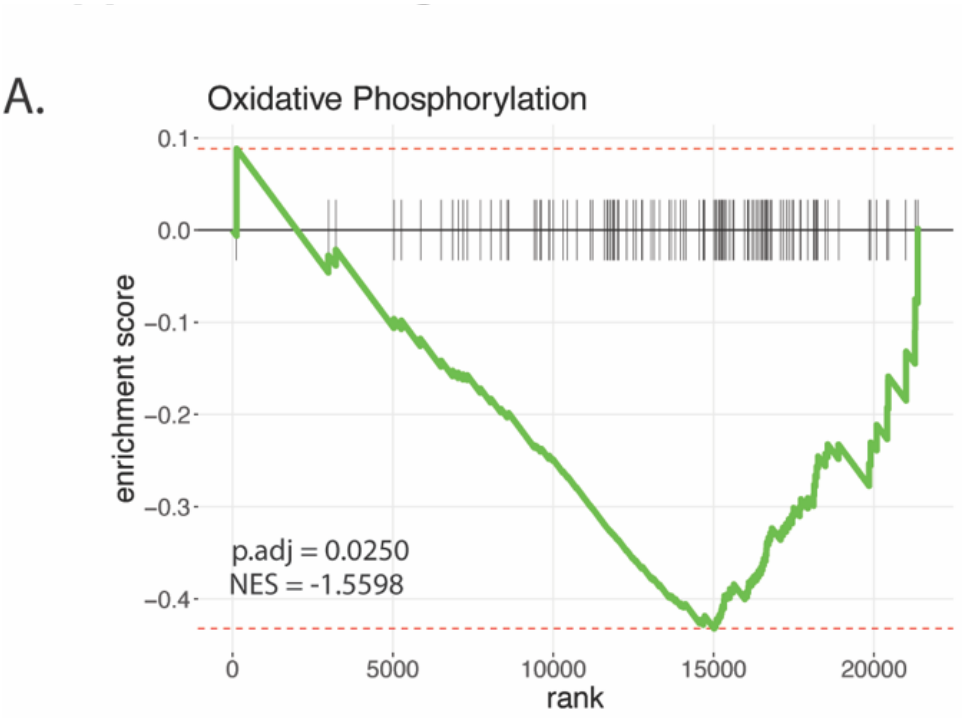

Figure 2.4 GSEA Analysis.

(A) Enrichment plot of oxidative phosphorylation signature significantly increased in cancer cells, with corresponding NES and adjusted p-value.

2.3.3 Differential repression of oxidative phosphorylation machinery across immune populations in pancreatic tumors.

Next, we sought to determine how innate and adaptive immunity is metabolically shaped by the tumor microenvironment**.** We observed that multiple immune compartments in pancreatic cancer samples significantly decreased their oxidative phosphorylation signature compared to healthy human pancreas tissue (Figure 2.5A). Most prominent among these were $CD8^+$ T cells, B cells, and granulocytes (Figure 2.5B-D). Next, we assessed the leading edge genes per cell type and per ETC complex (Figure 2.5E-K). As shown in Figure 2.5E, we performed principal component analysis (PCA) based on gene expression of the 44 subunits in Complex I. Remarkably, we found that expression levels of genes encoding for subunits of Complex I distinguished immune compartments from each other in the tumor condition, without lineage markers (Figure 2.5E)**.** In other words, the metabolic signature of each immune cell population in the tumor is as distinct as the canonical cell surface markers used to define immune cells.

Next, we segregated immune compartments in the tumor condition based on average expression and percentage of cells expressing genes that encode for the subunits of complexes (Figure 2.5F-I). Complex I-encoding gene expression components were downregulated to varying degrees across all immune compartments, compared to their counterparts in healthy pancreata (Figure 2.5F). Most notably, B cells in the tumor decreased expression of multiple genes encoding proteins that drive complex I. Meanwhile, complex I genes were not highly expressed in granulocytes, nor did they differ significantly based on sample condition. Lastly, tumor CD8+ T cells exhibited decreased expression of a few genes in complex I. In complex II, the second entry into the electron transport chain, tumor associated granulocytes decreased expression of succinate dehydrogenase isoforms SDHC and SDHB (Figure 2.5G). To our

knowledge, dysregulation of complex II in tumor associated granulocytes has not been shown in pancreatic cancer. In contrast, B cells did not display a shift in expression of complex II genes in the tumor compared to healthy tissue (Figure 2.5G). CD8+ T cells showed a slight increase in the expression of SDHA and SDHD in tumors (Figure 2.5G).

Differences in expression based on cell type in the tumor compared to healthy pancreas were also seen in complexes III and IV (Figure 2.5H and Figure 2.5I). Notably, B cells had the greatest decrease in expression of genes encoding Complexes III and IV. Segregation based on expression and percentage of cells expressing complex IV and III genes, respectively, did not display a pattern in the tumor condition, unlike our findings in complex I (Figure 2.6A and Figure 2.6B). However, expression of leading-edge genes related to ATP synthase, i.e., complex V, led to segregation of the immune compartments in the tumor condition (Figure 2.5J). As previous trends demonstrated, the degree of downregulation and the leading edge genes that decreased in expression were cell type dependent for complex V (Figure 2.5K). Each immune compartment followed a different pattern of expression in tumor compared to healthy tissue. Importantly, we assessed read coverage of glycolytic genes across immune compartments and found adequate coverage, and yet tumor associated B cells and granulocytes did not significantly alter glycolysis in relative to the normal pancreas **(**Figure 2.6C-E**)**. In contrast, there is a marked upregulation of glycolytic gene expression in CD8+ T cells, as is discussed below. The increase in glycolytic gene expression beginning at GAPDH is reflective only of CD8+ T cells, not granulocytes and B cells (Figure 2.6F-G). Collectively**,** this may suggest that tumor associated B cells and granulocytes don't shift towards glycolytic dependence in the same manner as $CD8^+$ T cells.

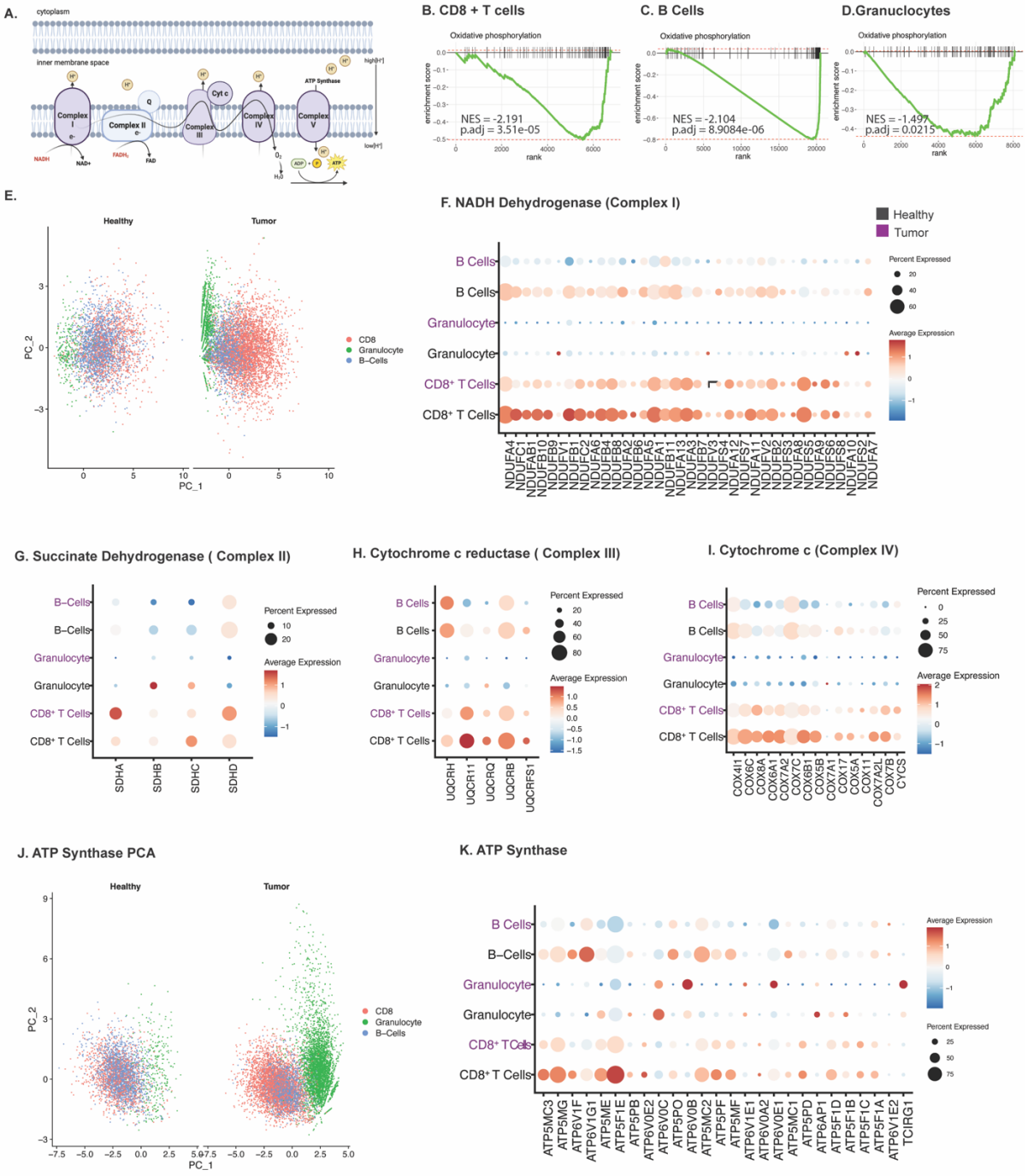
A.
cytoplasm
inner membrane space
Complex I
Complex II
Complex III
Complex IV
Complex V
Cyt c
Q
ATP Synthase
NADH
NAD+
FADH2
FAD
B. CD8 + T cells
C. B Cells
D.Granuclocytes
Oxidative phosphorylation
enrichment score
rank
NES = -2.191
p.adj = 3.51e-05
NES = -2.104
p.adj = 8.9084e-06
NES = -1.497
p.adj = 0.0215
E.
Healthy
Tumor
PC_1
PC_2
CD8
Granulocyte
B–Cells
F. NADH Dehydrogenase (Complex I)
B Cells
Granulocyte
CD8⁺ T Cells
Percent Expressed
Average Expression
G. Succinate Dehydrogenase (Complex II)
B–Cells
SDHA
SDHB
SDHC
SDHD
H. Cytochrome c reductase (Complex III)
UQCRH
UQCR11
UQCRQ
UQCRB
UQCRFS1
I. Cytochrome c (Complex IV)
COX4I1
COX6C
COX8A
COX6A1
COX7A2
COX7C
COX6B1
COX5B
COX7A1
COX17
COX5A
COX11
COX7A2L
COX7B
CYCS
J. ATP Synthase PCA
K. ATP Synthase
ATP5MC3
ATP5MG
ATP6V1F
ATP6V1G1
ATP5ME
ATP5F1E
ATP5PB
ATP6V0E2
ATP6V0C
ATP5PO
ATP6V0B
ATP5MC2
ATP5PF
ATP5MF
ATP6V1E1
ATP6V0A2
ATP6V0E1
ATP5MC1
ATP5PD
ATP6AP1
ATP5F1D
ATP5F1B
ATP5F1C
ATP5F1A
ATP6V1E2
TCIRG1

Figure 2.5 Down regulation of oxidative phosphorylation in immune cells.

(**A**)Schematic of electron transport chain.

(**B-D)**GSEA Enrichment plots demonstrating oxidative phosphorylation is significantly downregulated in CD8+ T cells, B cells, and granulocytes derived from PDA samples, compared to healthy human pancreas tissue, with corresponding NES and adjusted p-values.

(**E)** PCA visualization based on the expression of genes driving complex I in B cells, granulocytes, and CD8+ T cells in healthy human and PDA samples.

(**F-I**) Dot plot visualization based on the average expression and percent of cells expressing genes driving complex I, II, II and IV, respectively, in B cells, granulocytes, and CD8+ T cells in healthy human (black) and PDA samples (purple).

(**J)** Principal component analysis (PCA) visualization based on the expression of genes driving ATP synthase in B cells, granulocytes, and CD8+ T cells in healthy human and PDA samples.

(**K**) Dot plot visualization cells expressing ATP synthase related genes and percent expressing these genes in immune cells from tumor tissue (purple) and healthy tissue(black).

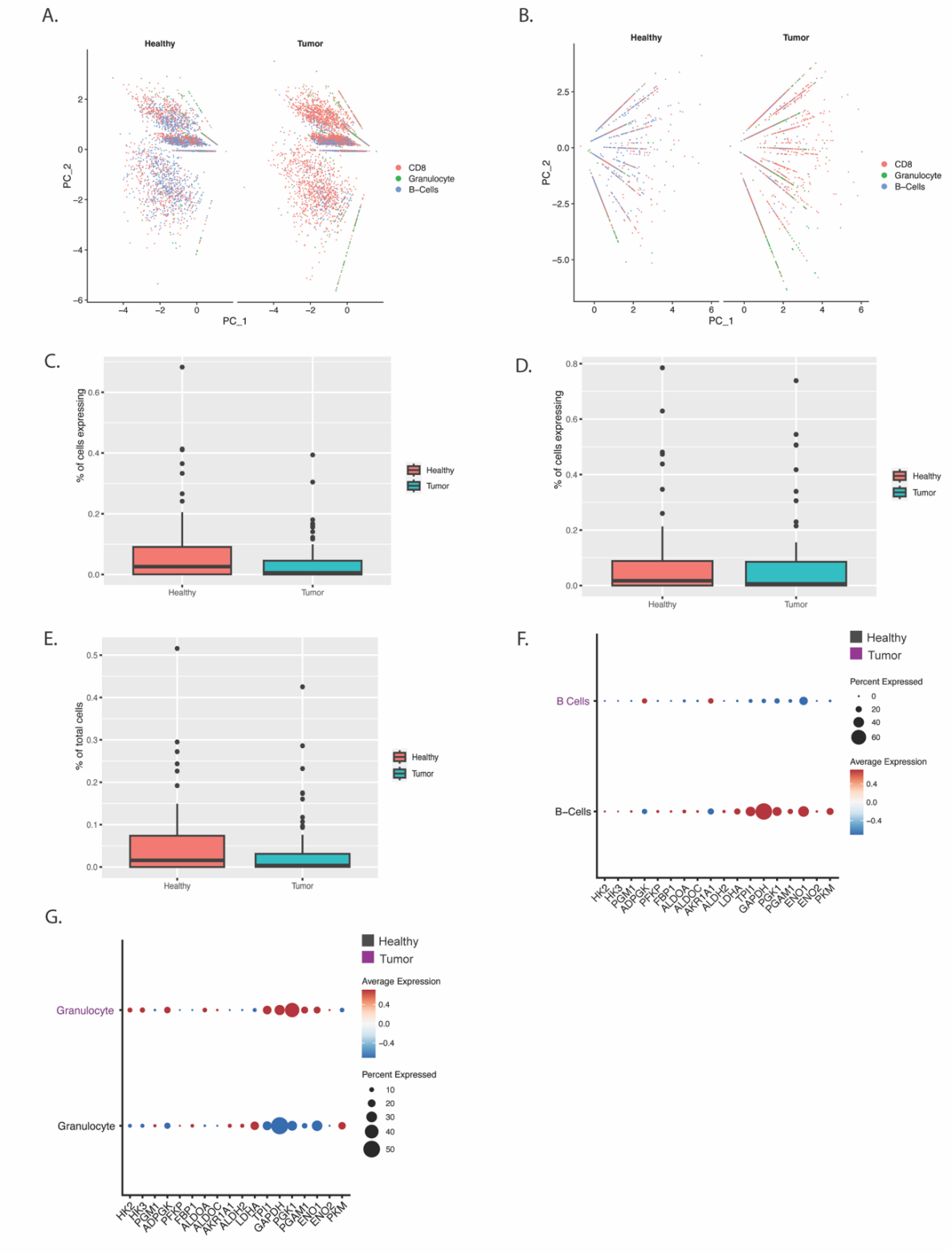
A.
Healthy
Tumor
PC_2
PC_1
CD8
Granulocyte
B–Cells
B.
Healthy
Tumor
PC_2
PC_1
CD8
Granulocyte
B–Cells
C.
% of cells expressing
Healthy
Tumor
D.
% of cells expressing
Healthy
Tumor
E.
% of total cells
Healthy
Tumor
F.
Healthy
Tumor
Percent Expressed
Average Expression
B Cells
B–Cells
HK2
HK3
PGM1
ADPGK
PFKP
FBP1
ALDOA
ALDOC
AKR1A1
ALDH2
LDHA
TPI1
GAPDH
PGK1
PGAM1
ENO1
ENO2
PKM
G.
Healthy
Tumor
Average Expression
Percent Expressed
Granulocyte
Granulocyte

Figure 2.6 Tumor associated immune compartments have adequate coverage of glycolytic genes

(**A)** Principal Component Analysis (PCA) visualization based on the average expression and percent of cells expressing genes related to complex IV in B cells, granulocytes, and CD8+ T cells in healthy human and PDA samples.

(**B)** PCA visualization based on the average expression and percent of cells expressing SDH/A/B/C/D in B cells, granulocytes, and CD8+ T cells in healthy human and PDA samples.

(**C-E)** Box plots of reads corresponding to glycolytic genes in healthy and tumor conditions for B cells, CD8+ T cells, and granulocytes.

(**F-G)** Dot Plot visualization of glycolytic genes, displaying average expression and percent expressed in B cells and granulocytes, respectively, in tumor (purple) and healthy pancreas tissue (black).

2.3.4 Metabolic rewiring of T cells.

Intrigued by the marked decrease in ETC complex expression, we next assessed more globally the metabolic differences between tumor derived $CD8^+$ T cells and $CD8^+$ T cells from the healthy pancreas by performing GSEA (Figure 2.7A). In agreement with previous studies of T cells in solid tumors, tumor derived $CD8^+$ T cells showed significant upregulation of glycolysis (57,58) (Figure 2.7A). However, unlike classical descriptions of $CD8^+$ T cell differentiation and expansion, the increase in glycolytic gene expression was accompanied by a decrease in oxidative phosphorylation (Figure 2.7A and Figure 2.7B). We put forth that this dichotomous activation of bioenergetic pathways is the likely result of low oxygen availability in the pancreatic TME, based on the observed hypoxia signature in $CD8^+$ T cells (Figure 2.8 A and Figure 2.8B). Further, analysis of expression of individual glycolytic enzymes demonstrated an increase in expression of genes downstream of GAPDH (Figure 2.7B and Figure 2.7C). We hypothesize that this occurs to assist in clearance of reductive stress to facilitate continued glycolysis in low oxygen conditions. When $CD8^+$ T cells were subsetted into exhausted, cytotoxic, and naive populations, no significant metabolic alterations were seen between conditions (Figure 2.8D-F). It is important to note that since sample sizes decreased when subsetting $CD8^+$ T cell populations, these comparisons are less robust. At the population level, $CD4^+$ T cells did not exhibit significant differences in gene expression between the tumor condition and healthy pancreas. Thus, we subclustered the $CD4^+$ T populations to gain a more granular view (Figure 2.7D). We used previously published markers to delineate the various subtypes of T cells (Figure 2.8C). Subclustering $CD8^+$ and $CD4^+$ T cells revealed additional insights(Figure 2.7E); for example, naive $CD4^+$ T cells exhibited metabolic changes in the tumor microenvironment that largely mirror those in bulk $CD8^+$ T cell populations (Figure 2.7F).

To interrogate master regulators of transcriptional programs in T cells, transcription factor analysis was performed using the scenic package in R. The activity of transcription factor target genes corresponds to regulon activity, where a higher score indicates a higher inferred activity level of target genes. The strongest scoring transcription factor for this analysis was FOXO1. We observed that $CD8^+$ T cells and $CD4^+$ T cells derived from tumors showed increased FOXO1 regulon activity scores in comparison to $CD4^+$ and $CD8^+$ cells derived from healthy pancreas tissue (Figure 2.7G and Figure 2.7H). FOXO1 is critical for the activation of memory T cells capable of re-expansion in response to antigen presentation (36,37,59). In this capacity FOXO1 mediates glycosylation (38), pathways that we observed to be highly differentially regulated in the GSEA (Figure 2.7A).

Second to FOXO1 was EOMES, a transcription factor involved in the regulation of memory and regulatory T cell function and homeostasis. Increased expression of EOMES has been observed in a terminally exhausted subset of infiltrating CD8+ T cells (60). Interestingly, TBX21 regulon activity was increased in tumor derived T cells (Table 3). TBX21 is a critical transcription factor in chronic infection and has been shown to promote a terminally exhausted phenotype in T cells (33,61). Collectively, our data suggest that a population of tumor associated T cells may be on a trajectory towards progenitor or terminal exhaustion, unable to execute tumor clearance. This is consistent with previous observations, including by our group, that T cells in pancreatic cancer are dysfunctional (22,62,63).Overall, the metabolic profiles of T cell subsets derived from PDA samples suggest a dysfunctional phenotype, marked by hypoxia, decreased oxidative phosphorylation, and a compensatory increase in glycolysis. These results provide a more detailed understanding of how the pancreatic tumor microenvironment

deregulates CD8+ T cell metabolism and thus function, as well as insight into how T cells compensate.

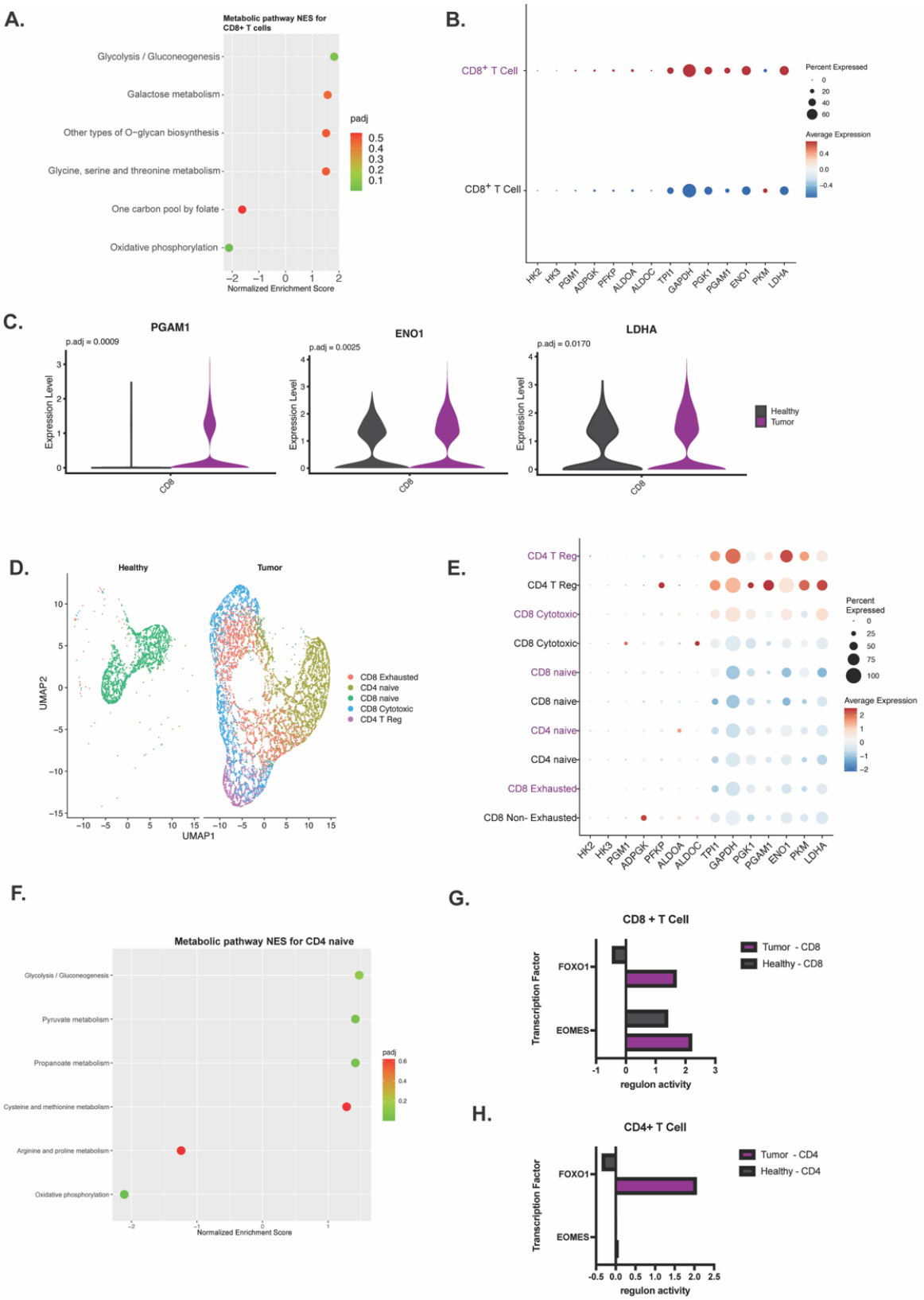
A.
Metabolic pathway NES for CD8+ T cells
Glycolysis / Gluconeogenesis
Galactose metabolism
Other types of O−glycan biosynthesis
Glycine, serine and threonine metabolism
One carbon pool by folate
Oxidative phosphorylation
padj
0.5
0.4
0.3
0.2
0.1
−2 −1 0 1 2
Normalized Enrichment Score
B.
CD8+ T Cell
CD8+ T Cell
Percent Expressed
0
20
40
60
Average Expression
0.4
0.0
−0.4
HK2 HK3 PGM1 ADPGK PFKP ALDOA ALDOC TPI1 GAPDH PGK1 PGAM1 ENO1 PKM LDHA
C.
PGAM1
p.adj = 0.0009
ENO1
p.adj = 0.0025
LDHA
p.adj = 0.0170
Expression Level
CD8
Healthy
Tumor
D.
Healthy
Tumor
UMAP2
UMAP1
CD8 Exhausted
CD4 naive
CD8 naive
CD8 Cytotoxic
CD4 T Reg
E.
CD4 T Reg
CD4 T Reg
CD8 Cytotoxic
CD8 Cytotoxic
CD8 naive
CD8 naive
CD4 naive
CD4 naive
CD8 Exhausted
CD8 Non- Exhausted
Percent Expressed
0
25
50
75
100
Average Expression
2
1
0
−1
−2
HK2 HK3 PGM1 ADPGK PFKP ALDOA ALDOC TPI1 GAPDH PGK1 PGAM1 ENO1 PKM LDHA
F.
Metabolic pathway NES for CD4 naive
Glycolysis / Gluconeogenesis
Pyruvate metabolism
Propanoate metabolism
Cysteine and methionine metabolism
Arginine and proline metabolism
Oxidative phosphorylation
padj
0.6
0.4
0.2
Normalized Enrichment Score
G.
CD8 + T Cell
Transcription Factor
FOXO1
EOMES
Tumor - CD8
Healthy - CD8
regulon activity
H.
CD4+ T Cell
Transcription Factor
FOXO1
EOMES
Tumor - CD4
Healthy - CD4
regulon activity

Figure 2.7 Metabolic rewiring of T cells in the pancreatic cancer microenvironment.

(**A)** Significantly altered pathways in CD8+ T cells from PDA samples compared to CD8 + T cells derived from the healthy.

(**B)** Dot plot visualization of the average expression and percent of cells expressing genes driving glycolysis in CD8+ T cells from tumor tissue (purple) and healthy tissue (black).

(C) Violin plots of the expression of selected differentially expressed glycolysis metabolism genes comparing CD8+ T cells from tumor samples to those from healthy samples.

(**D)** Uniform manifold approximation and projection (UMAP) visualization of CD4 and CD8 T cells populations in the tumor and healthy tissue**.**

(E) Dot plot visualization of the average expression and percent of cells expressing genes driving glycolysis in CD4 and CD8 T cells populations from tumor tissue (purple) and healthy tissue (black).

(**F)** Significantly altered pathways in CD4 naïve cells from PDA samples compared to healthy naïve CD4+ cells.

(**G-H)** Transcription Factor Analysis showing regulon activity of FOXO1 and EOMES in CD8+ T cells in tumor and healthy samples.

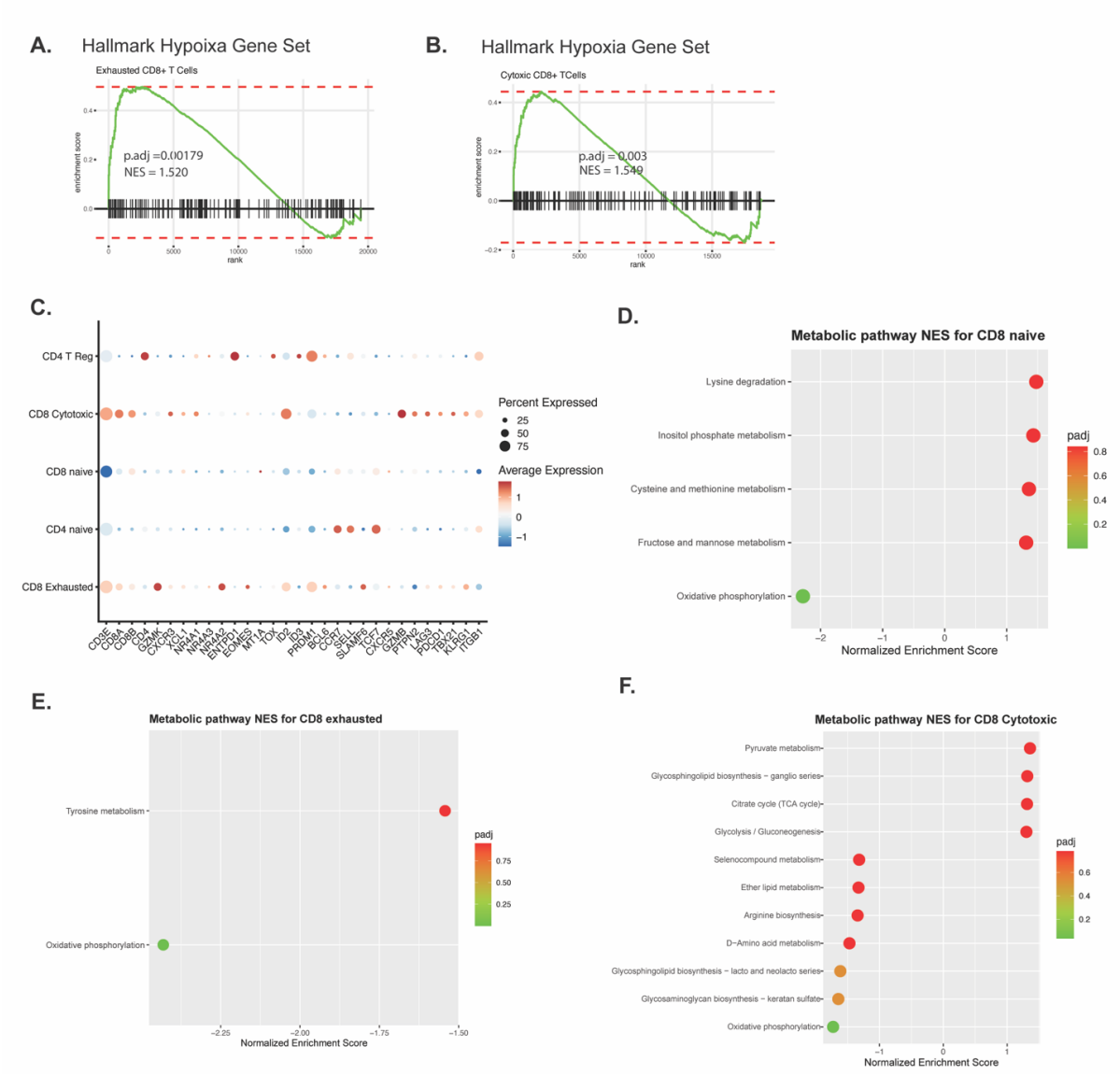
A.
Hallmark Hypoixa Gene Set
Exhausted CD8+ T Cells
p.adj =0.00179
NES = 1.520
enrichment score
rank
B.
Hallmark Hypoxia Gene Set
Cytoxic CD8+ TCells
p.adj = 0.003
NES = 1.549
enrichment score
rank
C.
CD4 T Reg
CD8 Cytotoxic
CD8 naive
CD4 naive
CD8 Exhausted
Percent Expressed
25
50
75
Average Expression
1
0
−1
CD3E
CD8A
CD8B
CD4
GZMK
CXCR3
XCL1
NR4A1
NR4A3
NR4A2
ENTPD1
EOMES
MT1A
TOX
ID2
ID3
PRDM1
BCL6
CCR7
SELL
SLAMF6
IL7R
CXCR5
GZMB
PTPN13
ACD
PDCD1
FOXP3
KLRG1
ITGB1
D.
Metabolic pathway NES for CD8 naive
Lysine degradation
Inositol phosphate metabolism
Cysteine and methionine metabolism
Fructose and mannose metabolism
Oxidative phosphorylation
padj
0.8
0.6
0.4
0.2
Normalized Enrichment Score
E.
Metabolic pathway NES for CD8 exhausted
Tyrosine metabolism
Oxidative phosphorylation
padj
0.75
0.50
0.25
Normalized Enrichment Score
F.
Metabolic pathway NES for CD8 Cytotoxic
Pyruvate metabolism
Glycosphingolipid biosynthesis − ganglio series
Citrate cycle (TCA cycle)
Glycolysis / Gluconeogenesis
Selenocompound metabolism
Ether lipid metabolism
Arginine biosynthesis
D−Amino acid metabolism
Glycosphingolipid biosynthesis − lacto and neolacto series
Glycosaminoglycan biosynthesis − keratan sulfate
Oxidative phosphorylation
padj
0.6
0.4
0.2
Normalized Enrichment Score

Figure 2.8 Tumor derived cytotoxic and exhausted CD8+ T Cell subsets significantly increase hypoxic signature

(**A-B)** GSEA Enrichment plots demonstrating hypoxia is significantly downregulated in exhausted and cytotoxic CD8+ T cells in pancreatic cancer tissue compared to healthy counterpart. (**C)**Dot plot visualization of marker expression utilized to subset T cell populations.

(**D-F**) GSEA results for CD8 naïve, exhausted, and cytotoxic T cells from PDA samples compared to healthy samples, with corresponding normalized enrichment scores (NES) and adjusted p-values.

2.3.5 Metabolic alterations in TAMs.

Macrophages, play important roles in healthy tissues, and many metabolic crosstalk features have been documented in the tumor microenvironment. In PDA, TAMs dictate milieu composition, immunosuppressive programs, and efficacy of therapeutic agents (14,20, 64, 65). To begin our interrogation into macrophages, we first investigated significantly increased or decreased metabolic pathways in TAMs compared to macrophages in the healthy pancreas (Figure 2.9A). In TAMs, we observed that glycolysis, the pentose phosphate pathway (PPP), unsaturated fatty acid synthesis, and fructose and mannose metabolism were significantly increased. This is consistent with previous studies pointing to altered carbohydrate, lipid, and amino acid metabolism in TAMs (20,64, 66).

We then observed that TAMs upregulated the expression of several enzymes that drive unsaturated fatty acid synthesis, including ACOT2/4/7, HACD4, and SCD (Figure 2.9B and Figure 2.10A). In addition, we found PPARG regulon activity to be increased in TAMs compared to healthy macrophages based on PPARG regulon activity (Figure 2.9C). As upregulation of unsaturated fatty acid synthesis enzymes in pancreatic TAMs has not been previously reported, we employed a murine model of pancreatic TAM polarization to assess whether SCD, a key enzyme in this pathway, was expressed at the protein level. In brief, we isolated bone marrow derived monocytes and polarized them with tumor conditioned media; this approach activates expression of hallmark genes of tumor associated macrophages (15). Polarization with tumor conditioned media promoted increased SCD expression in TAMs at the protein level (Figure 2.9D). These results indicate that TAMs upregulate components of the unsaturated fatty acid synthesis pathway in response to cancer cell signals. TAMs can display considerable cellular plasticity, dependent on exogenous signaling factors in their environment.

To explore this, we next subclustered macrophage populations for higher resolution analysis using markers reflecting current classification paradigms (67,68) (Figure 2.10B and Figure 2.10C). To better visualize the changes between macrophage subsets in tumor compared to normal tissue, we assessed the following pathways: glycolysis, PPP, and tryptophan catabolism based on the percentage of cells expressing genes related to each significantly altered pathway, alongside average expression (Figure 2.9E-H).

TAMs exhibited the greatest increase in glycolysis in tumor samples compared to healthy counterparts (69) (Figure 2.9E and Figure 2.9F). Monocyte derived cells also trended towards an increase in glycolysis. Consistent with precedent, pro-inflammatory macrophages derived from both tumor and healthy pancreas expressed genes driving the PPP to a greater degree than the other macrophage subtypes (Figure 2.9G). Next, we looked at tryptophan metabolism in macrophage subtypes, as it was borderline significant in our analysis and a well-known metabolic pathway in macrophages (70–72). The shift towards tryptophan metabolism in tissue resident macrophages derived from tumor compared to healthy pancreas exhibited several notable features (Figure 2.9D and Figure 2.10D). Indeed, we observed a combination of increased tryptophan catabolism, based on IL4I1 expression, and a marked increase in AFMID, which yields kynurenine, a well-known metabolic suppressor of T cell function and activation (12,69,73). Lastly, we performed GSEA on each subpopulation of macrophages and found significantly increased glycolysis and oxidative phosphorylation metabolic signatures in alternatively activated macrophages (Figure 2.10E). In contrast, the remaining macrophage subsets in pancreatic cancer samples did not have significantly altered metabolic programs compared to healthy pancreas (Figure 2.10F-H), demonstrating that TAMs engage in

heterogeneous metabolic activities in the tumor microenvironment that are not restricted to either pro- or anti-tumor programs.

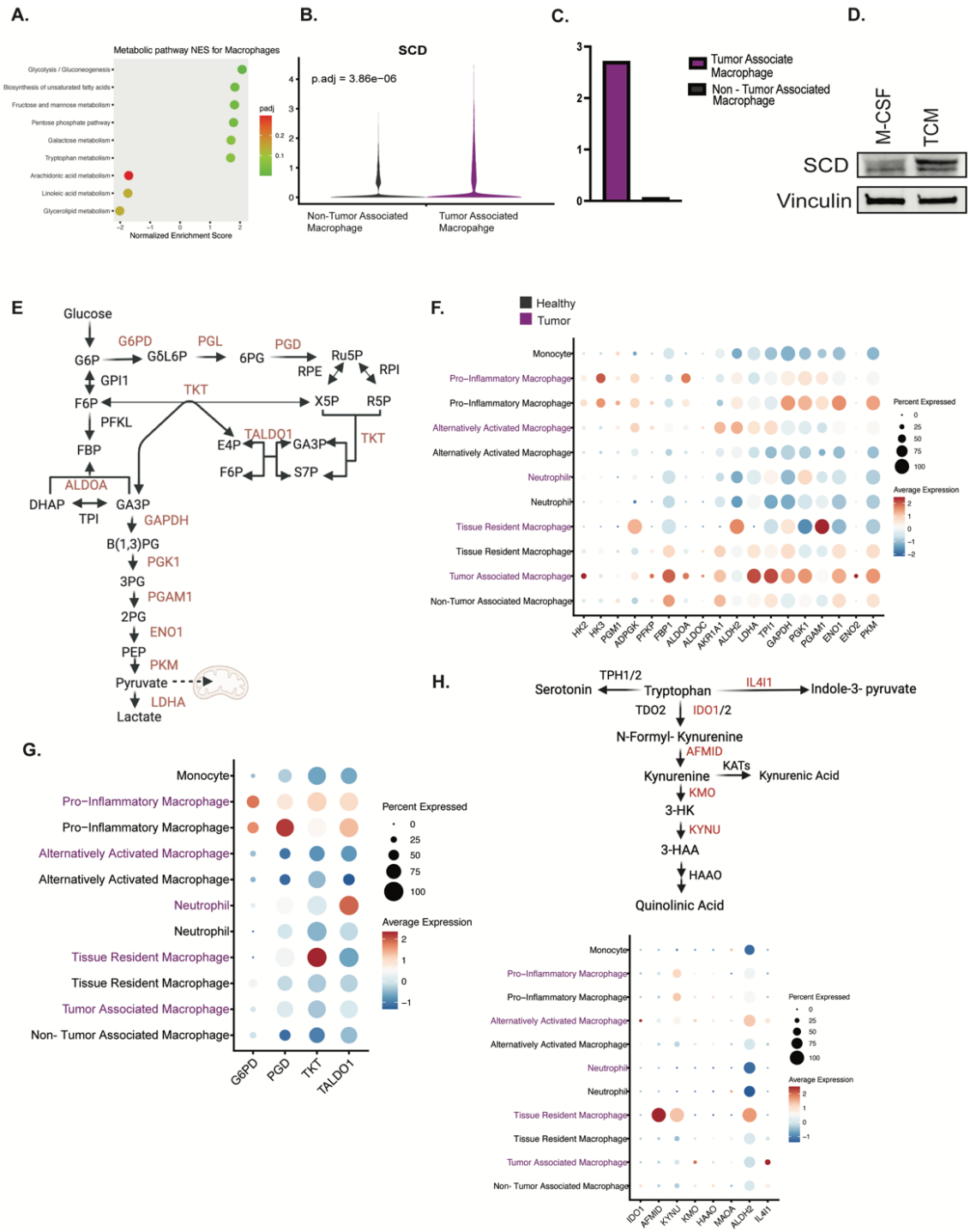
A.
Metabolic pathway NES for Macrophages
Glycolysis / Gluconeogenesis
Biosynthesis of unsaturated fatty acids
Fructose and mannose metabolism
Pentose phosphate pathway
Galactose metabolism
Tryptophan metabolism
Arachidonic acid metabolism
Linoleic acid metabolism
Glycerolipid metabolism
padj
Normalized Enrichment Score
B.
SCD
p.adj = 3.86e−06
Non-Tumor Associated Macrophage
Tumor Associated Macropahge
C.
Tumor Associate Macrophage
Non - Tumor Associated Macrophage
D.
M-CSF
TCM
SCD
Vinculin
E
Glucose
G6P
G6PD
G6L6P
PGL
6PG
PGD
Ru5P
RPE
RPI
GPI1
F6P
TKT
X5P
R5P
PFKL
TALDO1
E4P
GA3P
TKT
FBP
F6P
S7P
ALDOA
DHAP
TPI
GA3P
GAPDH
B(1,3)PG
PGK1
3PG
PGAM1
2PG
ENO1
PEP
PKM
Pyruvate
LDHA
Lactate
F.
Healthy
Tumor
Monocyte
Pro−Inflammatory Macrophage
Pro−Inflammatory Macrophage
Alternatively Activated Macrophage
Alternatively Activated Macrophage
Neutrophil
Neutrophil
Tissue Resident Macrophage
Tissue Resident Macrophage
Tumor Associated Macrophage
Non-Tumor Associated Macrophage
HK2
HK3
PGM1
ADPGK
PFKP
FBP1
ALDOA
ALDOC
AKR1A1
ALDH2
LDHA
TPI1
GAPDH
PGK1
PGAM1
ENO1
ENO2
PKM
Percent Expressed
Average Expression
G.
Monocyte
Pro−Inflammatory Macrophage
Pro−Inflammatory Macrophage
Alternatively Activated Macrophage
Alternatively Activated Macrophage
Neutrophil
Neutrophil
Tissue Resident Macrophage
Tissue Resident Macrophage
Tumor Associated Macrophage
Non- Tumor Associated Macrophage
G6PD
PGD
TKT
TALDO1
Percent Expressed
Average Expression
H.
Serotonin
TPH1/2
Tryptophan
IL4I1
Indole-3- pyruvate
TDO2
IDO1/2
N-Formyl- Kynurenine
AFMID
Kynurenine
KATs
Kynurenic Acid
KMO
3-HK
KYNU
3-HAA
HAAO
Quinolinic Acid
Monocyte
Pro−Inflammatory Macrophage
Pro−Inflammatory Macrophage
Alternatively Activated Macrophage
Alternatively Activated Macrophage
Neutrophil
Neutrophil
Tissue Resident Macrophage
Tissue Resident Macrophage
Tumor Associated Macrophage
Non- Tumor Associated Macrophage
IDO1
AFMID
KYNU
KMO
HAAO
MAOA
ALDH2
IL4I1
Percent Expressed
Average Expression

Figure 2.9 Metabolic alterations in tumor associated macrophages.

(**A)** Significantly altered metabolic pathways in macrophages derived from pancreatic cancer samples compared to healthy pancreas samples, with corresponding normalized enrichment scores (NES) and adjusted p-values.

(**B)** Violin plot of the expression of stearoyl-CoA Desaturase (SCD) in macrophages in tumor and healthy samples, showing differential expression.

(**C)** Transcription Factor Analysis showing regulon activity of PPARG in macrophages in tumor and healthy samples. (**D)** Western blot, protein expression of SCD is higher in murine BMDMs treated with tumor condition media compared to control condition with M-CSF.

(**E)** Glucose and PPP pathway schematic.

(**F)** Dot Plot visualization of genes driving glycolysis displaying average expression and percent expressed in macrophages in tumor (purple) and healthy pancreas tissue (black).

(**G)** Dot Plot visualization of genes driving PPP that don't overlap with glycolysis, displaying average expression and percent expressed macrophages in tumor (purple) and healthy pancreas tissue (black).

(**H)** Tryptophan metabolism schematic, Dot Plot visualization of genes driving tryptophan metabolism, displaying average expression and percent expressed in macrophages in tumor (purple) and healthy pancreas tissue (black).

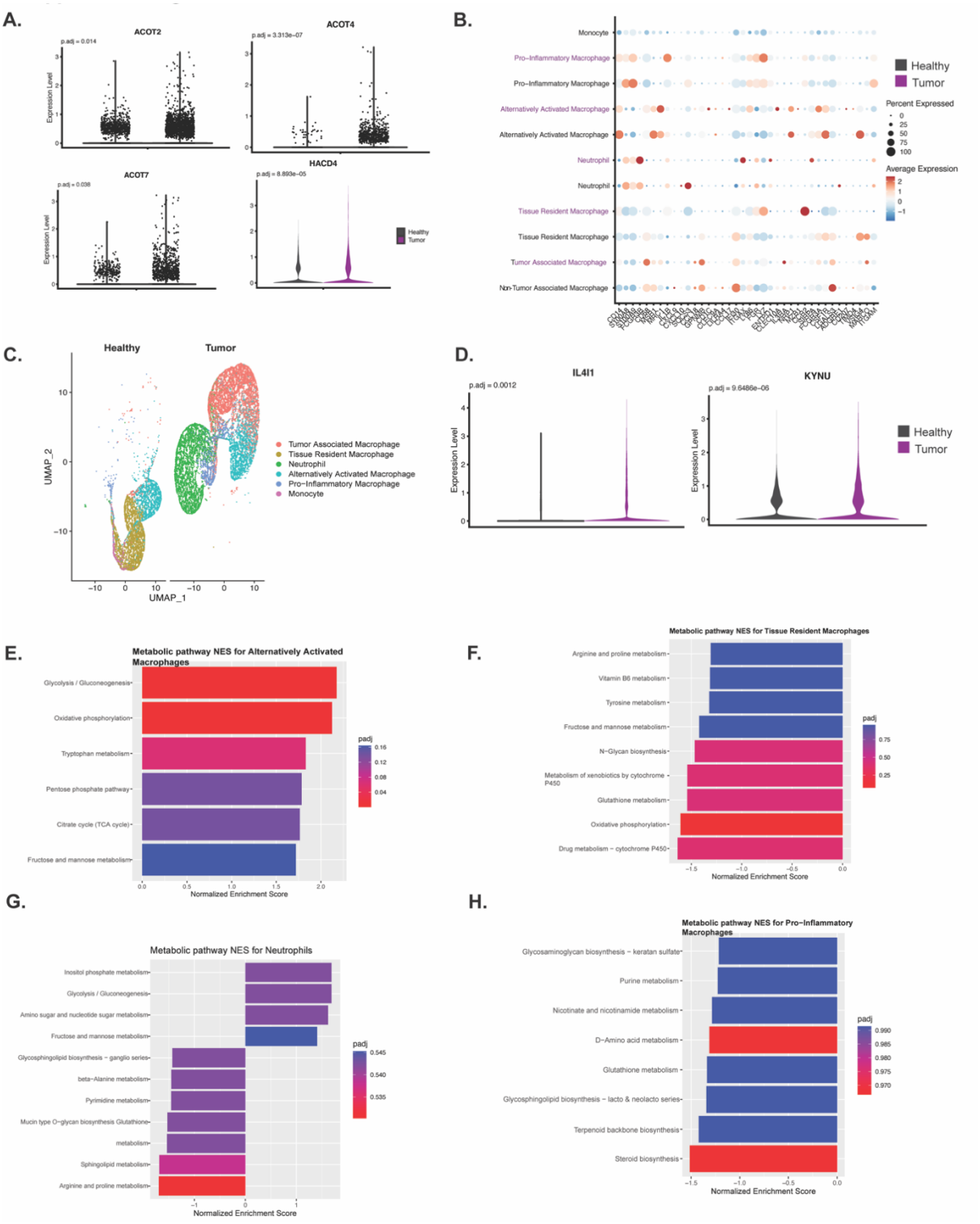
A.
ACOT2
p.adj = 0.014
ACOT4
p.adj = 3.313e−07
ACOT7
p.adj = 0.038
HACD4
p.adj = 8.893e−05
Expression Level
Healthy
Tumor
B.
Monocyte
Pro−Inflammatory Macrophage
Pro−Inflammatory Macrophage
Alternatively Activated Macrophage
Alternatively Activated Macrophage
Neutrophil
Neutrophil
Tissue Resident Macrophage
Tissue Resident Macrophage
Tumor Associated Macrophage
Non-Tumor Associated Macrophage
Healthy
Tumor
Percent Expressed
Average Expression
C.
Healthy
Tumor
UMAP_2
UMAP_1
Tumor Associated Macrophage
Tissue Resident Macrophage
Neutrophil
Alternatively Activated Macrophage
Pro−Inflammatory Macrophage
Monocyte
D.
IL4I1
p.adj = 0.0012
KYNU
p.adj = 9.6486e−06
Expression Level
Healthy
Tumor
E.
Metabolic pathway NES for Alternatively Activated Macrophages
Glycolysis / Gluconeogenesis
Oxidative phosphorylation
Tryptophan metabolism
Pentose phosphate pathway
Citrate cycle (TCA cycle)
Fructose and mannose metabolism
padj
Normalized Enrichment Score
F.
Metabolic pathway NES for Tissue Resident Macrophages
Arginine and proline metabolism
Vitamin B6 metabolism
Tyrosine metabolism
Fructose and mannose metabolism
N−Glycan biosynthesis
Metabolism of xenobiotics by cytochrome P450
Glutathione metabolism
Oxidative phosphorylation
Drug metabolism − cytochrome P450
padj
Normalized Enrichment Score
G.
Metabolic pathway NES for Neutrophils
Inositol phosphate metabolism
Glycolysis / Gluconeogenesis
Amino sugar and nucleotide sugar metabolism
Fructose and mannose metabolism
Glycosphingolipid biosynthesis − ganglio series
beta−Alanine metabolism
Pyrimidine metabolism
Mucin type O−glycan biosynthesis Glutathione
metabolism
Sphingolipid metabolism
Arginine and proline metabolism
padj
Normalized Enrichment Score
H.
Metabolic pathway NES for Pro−Inflammatory Macrophages
Glycosaminoglycan biosynthesis − keratan sulfate
Purine metabolism
Nicotinate and nicotinamide metabolism
D−Amino acid metabolism
Glutathione metabolism
Glycosphingolipid biosynthesis − lacto & neolacto series
Terpenoid backbone biosynthesis
Steroid biosynthesis
padj
Normalized Enrichment Score

Figure 2.10 Subsetting myeloid subsets

(**A)**Violin plots of genes involved in unsaturated fatty acid synthesis, with adjusted p-values for significantly differentially expressed genes.

(**B)** Dot Pot of markers used to identify sub populations of myeloid cells.

(**C**) Uniform Manifold Approximation and Projection (UMAP) of myeloid populations in the healthy and tumor conditions.

(**D)** Violin plots of differentially genes involved in tryptophan metabolism.

(**E)** GSEA results for alternatively activated macrophages.

(**F)** GSEA results for tissue resident macrophages. (**G)** GSEA analysis for neutrophils.

(**H)** GSEA results for pro-inflammatory macrophages. All GSEA results contain corresponding normalized enrichment scores (NES) and adjusted p-values.

2.3.6 Cellular crosstalk between epithelial cells and TAMs.

Pancreatic tumors have limited functional vasculature. Thus, cells in the tumor have varied and constrained access to serum-derived nutrients and oxygen. To compensate, numerous reports have detailed cooperative metabolic cross-feeding pathways where cancer cells capture nutrients from other non-cancer cell types present in the tumor microenvironment to sustain cellular proliferation and tumor growth (12). We sought to investigate if we could identify putative cross-feeding pathways from our datasets based on differential pathway activity or importer/exporter expression between cellular compartments that could result in a symbiotic relationship when considered together. Application of this approach led us to identify increased expression of the cholesterol exporter ABCG1 in TAMs relative to macrophages derived from healthy pancreatic tissue (Figure 2.11A). This observation suggests that TAMs release more cholesterol. Next, we found that the low density lipoprotein receptor (LDLR) was differentially increased in cancer cells (Figure 2.11A), suggesting that cancer cells may selectively import cholesterol (Figure 7.1B).

The transcription factor SREBP2 activates genes involved in cholesterol synthesis, efflux, and expression of the LDL receptor (31). We assessed the regulon activity score associated with SREBF2, the transcript encoding for SREBP2, and found it to be higher in epithelial cells derived from PDA compared to healthy tissue (Figure 2.11C). To assess if cancer cell derived factors play a functional role in TAM ABCG1 expression, we utilized the in vitro mouse model of pancreatic TAM polarization described above. Treatment of unpolarized macrophages with cancer cell conditioned media boosted ABCG1 expression in TAMs by western blot, relative to that in unpolarized macrophages (Figure 2.11D). Next, we set out to corroborate these findings at the protein level in human samples. We stained normal pancreas and pancreatic tumor tissue for

macrophage specific (CD163+) expression of ABCG1. Indeed, ABCG1 expression was higher in TAMs compared to non-tumor associated macrophages present in healthy human pancreatic tissue (Figure 2.11E). In parallel, human pancreatic cancer tissue and healthy human pancreata were probed for LDLR expression in epithelial cells (panCK+). LDLR expression was elevated in human pancreatic cancer tissue compared to healthy human pancreatic tissue (Figure 2.11F). Collectively, these data suggest that pancreatic TAMs may provide cholesterol to cancer cells, as has been previously described in prostate and breast cancer (65,74).

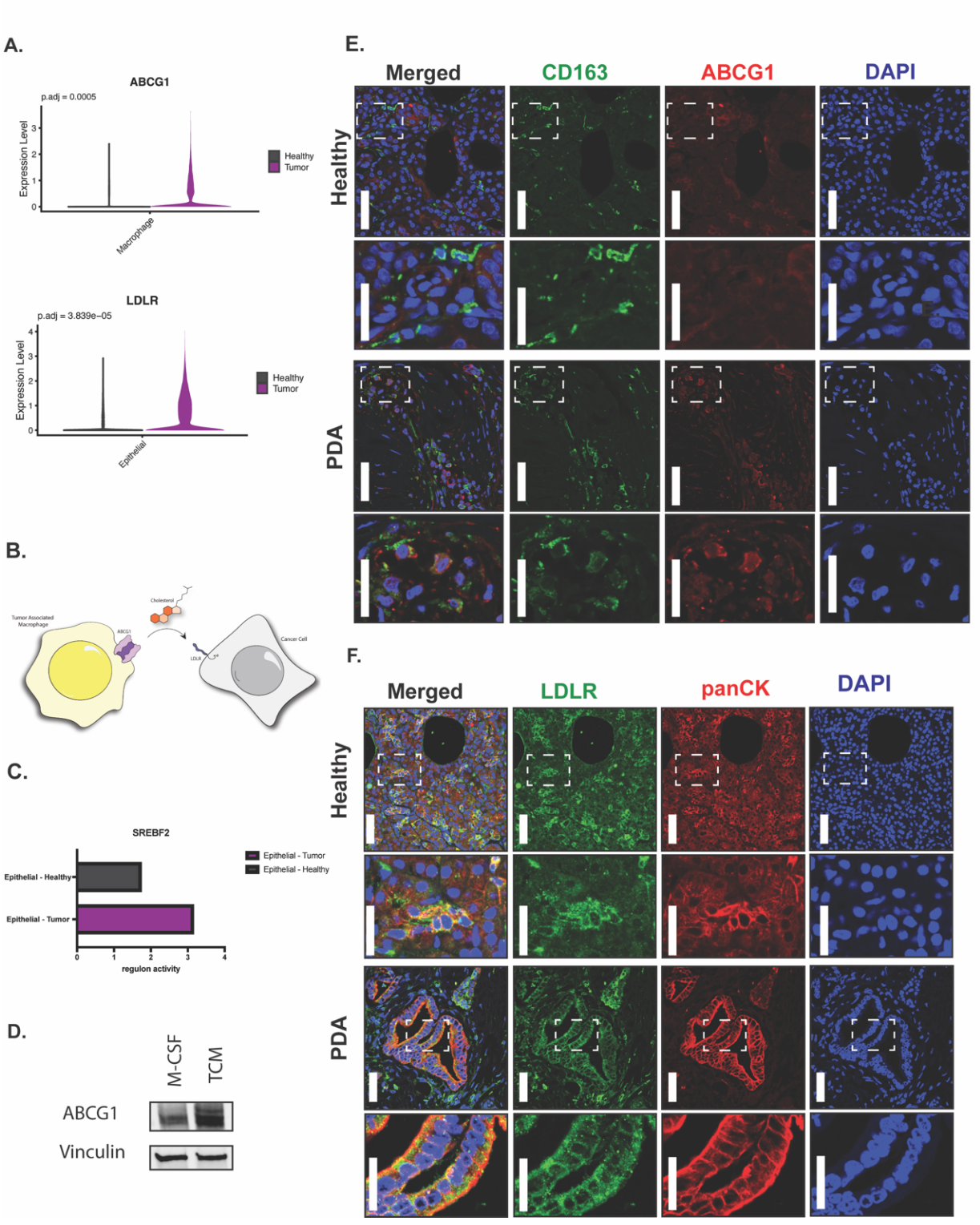
A.
ABCG1
p.adj = 0.0005
Expression Level
Healthy
Tumor
Macrophage
LDLR
p.adj = 3.839e−05
Epithelial
B.
Tumor Associated Macrophage
Cholesterol
ABCG1
LDLR
Cancer Cell
C.
SREBF2
Epithelial - Tumor
Epithelial - Healthy
regulon activity
D.
M-CSF
TCM
ABCG1
Vinculin
E.
Merged
CD163
ABCG1
DAPI
Healthy
PDA
F.
Merged
LDLR
panCK
DAPI
Healthy
PDA

Figure 2.11 Metabolic cellular crosstalk between epithelial cells and TAMs.

(**A)** Violin plots showing ABCG1 is significantly upregulated in TAMs, and LDLR is significantly upregulated in tumor derived epithelial cells.

(**B)** Schematic of TAMs significantly increasing ABCG1 (cholesterol exporter) expression, and cancer cells significantly increase expression of a corresponding lipid/cholesterol receptor LDLR.

(C) Transcription Factor Analysis showing SREBF2 regulon activity is increased in tumor derived epithelial cells.

(**D)**Western blot, protein expression of ABCG1 is higher in murine BMDMs treated with tumor condition media compared to control condition with M-CSF.

(**E)** Immunofluorescent staining. Healthy human tissue and pancreatic cancer tissue probed for CD163, ABCG1, and DAPI.

(**F)** Immunofluorescent staining. Healthy human tissue and pancreatic cancer tissue probed for LDLR, panCK, and DAPI.

2.4 Discussion

Cancer and immune cells acquire a wide array of metabolic adaptations, including autonomous and symbiotic adaptations, to circumvent the nutrient deregulated conditions in the tumor microenvironment, sustain increased bio-energetic demands, and engage in competition for scarce fuel sources (13,45,73,80). Since cancer cells participate in immune-metabolic crosstalk in the TME, oncogenic signaling can both directly and indirectly affect immune cells. This leads to metabolic alterations also engendered in several immune compartments (43,73,81). Previous studies have shown immune cell dysfunction in PDA attributed to exhausted T cells unable to execute effector functions, regulatory T cell activity hindered by interactions with TAMs excreting kynurenine, and other signaling pathways co-opted by cancer cells (30,55,82,83). Metabolism directly informs the functional phenotypes of every cell present in the microenvironment.

The advent of next generation single cell sequencing technology has enabled the mapping of gene expression, metabolic pathways, and potential cellular interactions in the tumor microenvironment at high resolution (75,76,77). Single cell RNA-seq has been employed to query metabolic heterogeneity in TAMs from other tumor models, where a correlation between metabolic phenotype and function in murine models was observed (77). Nevertheless, access to patient tumor tissue for investigation using single cell techniques remains difficult; especially from organs not routinely sampled for medical procedures (78,79). Adjacent normal pancreatic tissue, often used as control, is not “normal”, as it is affected by inflammation and desmoplasia in the pancreas. The availability of “true normal” allowed us to map out gene expression changes linked to malignancy, and specifically query metabolic alterations across all cellular compartments. Thereby, building a metabolic atlas from healthy and pancreatic tumor tissue.

Here, we characterize metabolic rewiring of malignant, non-malignant, and immune cells in the healthy human pancreas compared to human PDA cancer samples. Our findings serve as a resource atlas for understanding the various pathways co-opted by pancreatic cancer cells to maintain survival, while detailing immune cell rewiring and crosstalk in response to oncogenic signaling. Many metabolic studies have leveraged in vitro systems, which enable manipulation of media, metabolite levels, and can include select stromal and immune cells (5,8,9,20,66,84,85–89). These conditions do not fully recapitulate physiological circumstances in which the tumor microenvironment milieu contributes to metabolic dysregulation and competition for bio-energetic substrates, nor do they account for the complexities of immunosuppression. Accordingly, this unique resource could also be of value to compare/contrast metabolic rewiring of the TME in other cancers, immunometabolism in other healthy and diseased states, including but not limited to those interested in the truly healthy pancreas. Our work suggests that mitochondrial respiration is downregulated across multiple immune compartments; CD8+ T cells, B cells, and granulocytes. This significant decrease in oxidative phosphorylation dependency may be attributed to hypoxic regions in the tumor, a hallmark feature of PDA (90,91). Limited oxygen availability may pressure immune cells to downregulate ETC dependency (92,93). Interestingly, the manner in which immune cells shift dependency is not homogenous – rather, it is ETC complex and cell-type specific. Remarkably, our work shows CI subunit expression is reduced in B cells, CII is down in granulocytes, and ETC complex expression is more uniformly decreased in CD8+ T cells. Recent work demonstrated that the oxidative flow of electrons through the ETC plays a critical role in cancer cell immune evasion in melanoma. In melanoma cells, loss of CII augmented succinate levels, leading to epigenetic activation of genes related to antigen presentation and processing (94). Or stated reciprocally,

enhanced CI activity promotes anti-tumor immune cell recognition. Our data reveals for the first time that CI subunit expression is decreased B cells in pancreatic cancer. This sets precedence for the investigation of electron flow manipulation employed by immune cells in PDA, and how this may contribute to immunosuppression. In addition, nutrient scarcity, as well as the secreted products of altered metabolism in cancer cells, shifts phenotypes of innate immune cells, which are supported by metabolic processes (57).

Overall, our data shows a comprehensive analysis across immune compartments that points to mitochondrial immune dysfunction in PDA. TAMs are a metabolically heterogeneous group of cells that engage in cellular exchange of nutrients and metabolites with cancer cells present in the TME. Our work agrees with previous findings, and sheds light on more novel metabolic changes and interactions. We found that TAMs significantly increase expression of the unsaturated fatty acid synthesis protein SCD1 in vitro, and that this was regulated by factors secreted from tumor cells. Thus, we became interested in investigating metabolic exchanges advantageous to cancer cells. For example, a recent study illustrated that TAMs transfer cholesterol to cancer cells, conferring therapeutic resistance in castration resistant prostate cancer by modulating cholesterol/androgen signaling. This phenomenon was demonstrated in a breast cancer model, although in an IL-4 mediated fashion as well (74). These findings, together with altered lipid metabolism in TAMs in our data, prompted us to investigate the reciprocal relationship between the increased expression of the ABC cholesterol exporter on TAMs and the cognate lipid/cholesterol receptor on pancreatic cancer cells. Through co-immunofluorescent staining in healthy human tissue and pancreatic cancer samples we found increased ABCG1 expression in macrophages and increased LDLR in pancreatic cancer samples. To our knowledge this is the first report suggesting pancreatic cancer cells engage in cholesterol exchange with TAMs. How

this crosstalk may mediate an immunosuppressive signaling axis in pancreatic cancer remains to be further investigated.

2.5 Methods

2.5.1 Donor Sample Procurement and Tissue Processing

Donor pancreata were collected at the Gift of Life Michigan Donor Care Center and preserved as previously published in Carpenter et al., 2023 (21).The research project and protocol for sample acquisition was approved by the Gift of Life research review group. The protocol was previously described and approved by the University of Michigan Institutional Review Board (HUM00025339). Briefly, portions of the dissected pancreas (head, body, and tail) were each placed into DMEM with 1% BSA/10 μmol/L Y27632 or 10% formalin for single cell sequencing or paraffin embedding, respectively. Further processing was done to prepare the samples for single-cell processing: mince tissue into 1-mm^3 pieces, digest with 1 mg/mL collagenase P for 20 to 30 minutes at 37°C with gentle agitation, rinse three times with DMEM/1% BSA/10 μmol/L Y27632 and then filter through a 40-μm mesh. Resulting cells were submitted to the University of Michigan Advanced Genomics Core for single cell sequencing using the 10x Genomics Platform.

2.5.2 PDA patient samples

Resected PDA from patients seen at the University of Michigan Healthy system from 2021 to 2022 were included in this study, described previously (Steele et al., 2020)(22). Tissues were fixed in 10% neutral buffered formalin and paraffin embedded using standard protocols before sectioning and staining. All hematoxylin and eosin-stained slides were reviewed, diagnoses confirmed, and corresponding areas were carefully selected and marked. The collection of

patient-derived tissues for histological analyses was approved by the Institutional Review Board at the University of Michigan (IRB number: HUM00098128).

2.5.3 Single- cell RNA Sequencing

The samples were run on the 10x Genomics platform and subsequent analysis was previously described and published by Carpenter et al., 2023 (21). To subset the T cell population, as well as the myeloid population for higher resolution of cell types, markers from previously published studies were utilized to annotate sub populations.

2.5.4 Pseudobulk RNA Differential Gene Expression

As previously published in Carpenter et al., 2023, counts were aggregated from all of the different samples, or for a subset of cells (21). Counts were corrected by removing background contamination signal and transformed to integer. To aggregate to the sample level, the mean function was utilized. For normalization and differential gene expression (DGE) analysis of the samples the DESeq2 package was used. Dimensionality reduction was employed better visualization of differences between groups was performed using the PCAtools package.

2.5.5 Metabolic pathways and gene set enrichment analysis

Selected metabolic pathways were retrieved from the Kyoto Encyclopedia of Genes and Genomes database: https://www.genome.jp/kegg/pathway.html#metabolism.
The list of pathways was downloaded using a bash script and the pathway to gene mapping was downloaded from the KEGG database at: https://rest.kegg.jp/link/pathway/hsa. Gene set enrichment was performed using the GSEABase (https://bioconductor.org/packages/release/bioc/html/GSEABase.html) R package. For gene set enrichment analysis, the fgsea package in R was used together with the metabolic gene sets

downloaded from KEGG. This analysis was performed to identify significantly enriched metabolic pathways.

2.5.6 Transcription factor inference analysis

Transcription factor inference analysis was performed using SCENIC (v1.3.1) per cell type with raw count matrices corresponding to tumor and healthy tissue respectively. The regulons and TF activity (AUC) per cell was calculated with the pySCENIC program (v 0.12.1) with motif collection version mc9nr.

2.5.7 Data Availability

Human sc-RNA-seq data were previously published in Steele et al., 2020 (NIH dbGaP database accession #phs002071.v1.p1). Human sc-RNA-seq data were previously published in Carpenter et al., 2023, Raw single-cell sequencing data from donor pancreata are available at the NIH dbGaP database under the accession phs003229. Feature matrices of single-cell RNA data are available at accession number GSE229413.

2.5.8 Cell Culture (BMDM isolation + cell culture (TCM))

Conditioned media:

To make fibroblast or tumor conditioned media (CM), L929 fibroblast or 7940b tumor cells were cultured in Dulbecco's Modified Eagle Medium (DMEM, 11965-092) with 10% fetal bovine serum (FBS) and media were collected after 48 hours of growth. CM were centrifuged at 200 g for 5 min and passed through a 0.22 um filter to remove cells.

BMDM isolation/ polarization:

To make macrophage growth media, fibroblast CM were added at 30% volume to DMEM. Bone marrow cells were then harvested from WT C57BL/6 mice femurs and tibias and cultured in

macrophage growth media for 7 days. Fresh media were added on days 2 and 5 and cells were re-seeded in 6-well plates on day 6 to prepare for polarization.

On day 7, media were replaced with polarization media, which consisted of DMEM with either M-CSF (10 ug/ml, PeproTech), LPS (10 ug/ml, Fisher Scientific), IL-4 (PeproTech) or 50% tumor CM. Polarized macrophages were harvested after 48 hours for analysis by western blot.

2.5.9 Western blot analysis

Western Blotting. Protein was isolated from cells with RIPA Lysis and Extraction Buffer(Thermo Fisher Scientific). Isolated protein was quantified and normalized via Pierce BCA assay (Thermo Fisher Scientific). 60 μg protein was run on 4-15% SDS- polyacrylamide gel electrophoresis gel and transferred onto nitrocellulose membranes(Invitrogen, Life Technologies). Membrane was blocked with 5% BSA(Fisher Scientific) in Tris-buffered saline-Tween buffer. The membranes were probed with the antibodies mentioned above.

2.5.10 Immunofluorescence

FFPE normal pancreas and pancreatic cancer tissue sections were mounted onto glass slides, deparaffinized, dehydrated in graded ethanol, and rinsed in deionized water. Slides were quenched with hydrogen peroxide solution for 15 minutes and washed with PBS. Antigen retrieval was performed with 10 mM sodium citrate buffer at pH 6.0 with 0.05% Tween 20 for 30 min in 96°C. Slides were cooled to room temperature and washed three times with PBS.

For co-immunofluorescence with primary antibodies made in the same animal (ABCG1 and F4/80) the Tyramide SuperBoost™ Kit with Alexa Fluor™ Tyramide (Invitrogen) was used per manufacturer's protocol. Briefly, tissues were blocked with kit blocking buffer (Component A) for one hour at room temperature and the first primary antibody was added and incubated

overnight at 4C in PBS with 2.5% BSA and 0.2% Triton-X. Slides were rinsed with PBS, and kit HRP-conjugated streptavidin (Component B) was added for one hour at room temperature. Tyramide working solution was added for 10 minutes followed by Reaction Stop Reagent working solution for 5 minutes. After rinsing in PBS, slides were boiled in 10 mM sodium citrate buffer at pH 6.0 with 0.05% Tween 20 for 20 minutes. Slides were cooled and blocked in kit blocking buffer (Component A) for one hour at room temperature. Additional primary antibodies were incubated overnight at 4C in PBS with 2.5% BSA and 0.2% Triton-X. Slides were rinsed with PBS and secondary antibodies were added for one hour at room temperature. DAPI was added to slide for 10 minutes at room temperature, slides were rinsed in PBS, and mounted in ProLong Gold Antifade Mountant (Invitrogen).

For co-immunofluorescence with primary antibodies made in different animals, slides were blocked for one hour at room temperature in PBS with 2.5% BSA and 0.2% Triton-X. Primary antibodies were incubated overnight at 4C. The next day, slides were rinsed and incubated with secondary antibodies for one hour at room temperature. DAPI was added for 10 minutes at room temperature, slides were rinsed in PBS, and mounted in ProLong Gold Antifade Mountant (Invitrogen).High-magnification images were obtained on a Leica Stellaris confocal microscope at the University of Michigan Biomedical Research Core Facilities Microscope Core.

Table 4 Immunofluorescence and western blot antibodies and dilutions used in Chapter 2

Reagent Type (species) or resource	Designation	Source or reference	Identifiers	Additional Information
Antibody	ABCG1(rabbit)	Proteintech	13578-1-AP	IF: 1:100
Antibody	F4/80 (rabbit)	Cell Signaling	70776S	IF: 1:250
Antibody	LDLR	Invitrogen	MA5-32075	IF: 1:100
Antibody	Pan-cytokeratin(mouse)	Biolegend	628602	IF: 1:200
Antibody	Alexa 488 (goat anti-rabbit secondary)	Invitrogen	A32731	IF: 1:500
Antibody	Alexa 594 (goat anti- rabbit secondary)	Fisher	A11012	IF:1:500
Antibody	Alexa 555(goat anti-mouse secondary)	Invitrogen	A32727	IF: 1:500
Antibody	Vinculin (rabbit)	Cell Signaling	13901S	WB:1:1000
cell line (M. musculus)	7940B	Long et al., 2016		KPC cell line
Commercial Assay Kit	Alexa fluor 488 Tyramide SuperBoost Kit	Invitrogen	B40922	

2.6 Authors and Affiliations

Monica E. Bonilla[1,4], Megan D. Radyk[2], Matthew D.Perricone[3], Ahmed M. Elhossiny[4], Alexis C. Harold[1], Paola I. Medina-Cabrera[1], Padma Kadiyala[3], Jiaqi Shi[5,6], Timothy L. Frankel[5,7], Eileen S. Carpenter[5,8], Michael D. Green[1,5,10,11,12] , Cristina Mitrea[4,†], Costas A. Lyssiotis[2,5,8,†], Marina Pasca di Magliano[5,7,9,†]

[1]Program in Cancer Biology; [2]Department of Molecular and Integrative Physiology ; [3]Program in Immunology; [4]Department of Computational Medicine and Bioinformatics; [5]Rogel Cancer Center; [6]Department of Pathology; [7]Department of Surgery; [8]Department of Internal Medicine, Division of Gastroenterology and Hepatology;[9]Department of Cell and Developmental Biology, University of Michigan, Ann Arbor, Michigan, 48109 USA. [10]Department of Radiation Oncology, University of Michigan, Ann Arbor, Michigan, [11]Department of Microbiology and Immunology, University of Michigan, Ann Arbor, Michigan. [12] Department of Radiation Oncology, Veterans Affairs Ann Arbor Healthcare System, Ann Arbor, MI.

2.7 Funding

Dr. Jiaqi Shi is supported in part by the National Cancer Institute
of the National Institutes of Health under award number R37CA262209. Dr. Michael Green is supported in part by the National Cancer Institute of the National Institutes of Health under award number R01CA252010. CAL was supported by the NCI (R37CA237421, R01CA248160, R01CA244931). M. Pasca di Magliano is supported by NIH/NCI grants U54CA274371 and R01-CA27150. Pasca di Magliano and T.L. Frankel were supported by NIH/NCI R01-CA268426. M.E. Bonilla is supported by NIH/NCI T32 CA140044.

2.8 Author Contributions

M.E. Bonilla: Conceptualization, formal analysis, supervision, validation, investigation, visualization, methodology, writing–original draft, writing–review and editing. **M.D. Radyk**: Validation, methodology, writing–review. **M.D. Perricone:** Validation, methodology, writing–review**. A.M. Elhossiny**: Methodology. **A.C Harold:** Validation, methodology. **P.I. Medina-Cabrera:** Visualizations. **P. Kadiyala:** Data curation. **J. Shi:** Resources. **T.L Frankel:** Resources. **E.S. Carpenter:** Data curation. **M.D. Green:** Resources, writing–review. **C. Mitrea:** Conceptualization, supervision, methodology, writing–review and editing. **M. Pasca di Magliano**: Conceptualization, resources, supervision, funding acquisition, investigation, methodology, project administration, writing–review and editing. **C.A. Lyssiotis:** Conceptualization, resources, supervision, funding acquisition, investigation, methodology, project administration, writing–review and editing.

References

1. Siegel RL, Giaquinto AN, Jemal A. Cancer statistics, 2024. CA Cancer J Clin. 2024;74(1):12-49. doi:10.3322/caac.21820
2. Sarantis P, Koustas E, Papadimitropoulou A, Papavassiliou AG, Karamouzis MV. Pancreatic ductal adenocarcinoma: Treatment hurdles, tumor microenvironment and immunotherapy. World J Gastrointest Oncol. 2020;12(2):173. doi:10.4251/wjgo.v12.i2.173
3. Ying H, Dey P, Yao W, et al. Genetics and biology of pancreatic ductal adenocarcinoma. Genes Dev. 2016;30(4):355-385. doi:10.1101/gad.275776.115
4. Tsujikawa T, Kumar S, Borkar RN, et al. Quantitative Multiplex Immunohistochemistry Reveals Myeloid-Inflamed Tumor-Immune Complexity Associated with Poor Prognosis. Cell Rep. 2017;19(1):203-217. doi:10.1016/j.celrep.2017.03.037
5. Halbrook CJ, Thurston G, Boyer S, et al. Differential integrated stress response and asparagine production drive symbiosis and therapy resistance of pancreatic adenocarcinoma cells. Nat Cancer. 2022;3(11):1386-1403. doi:10.1038/s43018-022-00463-1
6. Ying H, Kimmelman AC, Lyssiotis CA, et al. Oncogenic Kras maintains pancreatic tumors through regulation of anabolic glucose metabolism. Cell. 2012;149(3):656-670. doi:10.1016/j.cell.2012.01.058
7. Kamphorst JJ, Nofal M, Commisso C, et al. Human pancreatic cancer tumors are nutrient poor and tumor cells actively scavenge extracellular protein. Cancer Res. 2015;75(3):544-553. doi:10.1158/0008-5472.CAN-14-2211
8. Sousa CM, Biancur DE, Wang X, et al. Pancreatic stellate cells support tumour metabolism through autophagic alanine secretion. Nature. 2016;536(7617):479-483. doi:10.1038/nature19084
9. Nwosu ZC, Ward MH, Sajjakulnukit P, et al. Uridine-derived ribose fuels glucose-restricted pancreatic cancer. Nature. 2023;618(7963):151-158. doi:10.1038/s41586-023-06073-w
10. Banh RS, Biancur DE, Yamamoto K, et al. Neurons Release Serine to Support mRNA Translation in Pancreatic Cancer. Cell. 2020;183(5):1202-1218.e25. doi:10.1016/j.cell.2020.10.016
11. Zhu Z, Achreja A, Meurs N, et al. Tumour-reprogrammed stromal BCAT1 fuels branched-chain ketoacid dependency in stromal-rich PDAC tumours. Nat Metab. 2020;2(8):775-792. doi:10.1038/s42255-020-0226-5
12. Lyssiotis CA, Kimmelman AC. Metabolic Interactions in the Tumor Microenvironment. Trends Cell Biol. 2017;27(11):863-875. doi:10.1016/j.tcb.2017.06.003
13. Chang CH, Qiu J, O'Sullivan D, et al. Metabolic Competition in the Tumor Microenvironment Is a Driver of Cancer Progression. Cell. 2015;162(6):1229-1241. doi:10.1016/j.cell.2015.08.016
14. Zuo C, Baer JM, Knolhoff BL, et al. Stromal and therapy-induced macrophage proliferation promotes PDAC progression and susceptibility to innate immunotherapy. J Exp Med. 2023;220(6):e20212062. doi:10.1084/jem.20212062
15. Menjivar RE, Nwosu ZC, Du W, et al. Arginase 1 is a key driver of immune suppression in pancreatic cancer. eLife. 2023;12:e80721. doi:10.7554/eLife.80721

16. Arlauckas SP, Garren SB, Garris CS, et al. Arg1 expression defines immunosuppressive subsets of tumor-associated macrophages. Theranostics. 2018;8(21):5842-5854. doi:10.7150/thno.26888
17. Rodriguez PC, Quiceno DG, Zabaleta J, et al. Arginase I Production in the Tumor Microenvironment by Mature Myeloid Cells Inhibits T-Cell Receptor Expression and Antigen-Specific T-Cell Responses. Cancer Res. 2004;64(16):5839-5849. doi:10.1158/0008-5472.CAN-04-0465
18. Sullivan MR, Danai LV, Lewis CA, et al. Quantification of microenvironmental metabolites in murine cancers reveals determinants of tumor nutrient availability. eLife. 2019;8:e44235. doi:10.7554/eLife.44235
19. Apiz Saab JJ, Dzierozynski LN, Jonker PB, et al. Pancreatic tumors exhibit myeloid-driven amino acid stress and upregulate arginine biosynthesis. DeNicola GM, El-Deiry WS, DeNicola GM, Gomes A, eds. eLife. 2023;12:e81289. doi:10.7554/eLife.81289
20. Halbrook CJ, Pontious C, Kovalenko I, et al. Macrophage-Released Pyrimidines Inhibit Gemcitabine Therapy in Pancreatic Cancer. Cell Metab. 2019;29(6):1390-1399.e6. doi:10.1016/j.cmet.2019.02.001
21. Carpenter ES, Elhossiny AM, Kadiyala P, et al. Analysis of Donor Pancreata Defines the Transcriptomic Signature and Microenvironment of Early Neoplastic Lesions. Cancer Discov. 2023;13(6):1324-1345. doi:10.1158/2159-8290.CD-23-0013
22. Steele NG, Carpenter ES, Kemp SB, et al. Multimodal Mapping of the Tumor and Peripheral Blood Immune Landscape in Human Pancreatic Cancer. Nat Cancer. 2020;1(11):1097-1112. doi:10.1038/s43018-020-00121-4
23. Mayers JR, Wu C, Clish CB, et al. Elevation of circulating branched-chain amino acids is an early event in human pancreatic adenocarcinoma development. Nat Med. 2014;20(10):1193-1198. doi:10.1038/nm.3686
24. Lien EC, Vander Heiden MG. A framework for examining how diet impacts tumour metabolism. Nat Rev Cancer. 2019;19(11):651-661. doi:10.1038/s41568-019-0198-5
25. Hosein AN, Huang H, Wang Z, et al. Cellular heterogeneity during mouse pancreatic ductal adenocarcinoma progression at single-cell resolution. JCI Insight. 2019;4(16). doi:10.1172/jci.insight.129212
26. Halbrook CJ, Lyssiotis CA, Pasca di Magliano M, Maitra A. Pancreatic cancer: Advances and challenges. Cell. 2023;186(8):1729-1754. doi:10.1016/j.cell.2023.02.014
27. Aibar S, González-Blas CB, Moerman T, et al. SCENIC: single-cell regulatory network inference and clustering. Nat Methods. 2017;14(11):1083-1086. doi:10.1038/nmeth.4463
28. He Y, Gan M, Wang Y, et al. EGFR-ERK induced activation of GRHL1 promotes cell cycle progression by up-regulating cell cycle related genes in lung cancer. Cell Death Dis. 2021;12(5):1-13. doi:10.1038/s41419-021-03721-9
29. Kim H, Feng Y, Murad R, et al. Melanoma-intrinsic NR2F6 activity regulates antitumor immunity. Sci Adv. 2023;9(27):eadf6621. doi:10.1126/sciadv.adf6621
30. Zhang L, He Y, Tu X, et al. FOXC2 as a prognostic marker and a potential molecular target in patients with human solid tumors. Front Surg. 2022;9:960698. doi:10.3389/fsurg.2022.960698
31. Guo C, Chi Z, Jiang D, et al. Cholesterol Homeostatic Regulator SCAP-SREBP2 Integrates NLRP3 Inflammasome Activation and Cholesterol Biosynthetic Signaling in Macrophages. Immunity. 2018;49(5):842-856.e7. doi:10.1016/j.immuni.2018.08.021

32. Botti E, Spallone G, Moretti F, et al. Developmental factor IRF6 exhibits tumor suppressor activity in squamous cell carcinomas. Proc Natl Acad Sci. 2011;108(33):13710-13715. doi:10.1073/pnas.1110931108
33. McLane LM, Ngiow SF, Chen Z, et al. Role of nuclear localization in the regulation and function of T-bet and Eomes in exhausted CD8 T cells. Cell Rep. 2021;35(6):109120. doi:10.1016/j.celrep.2021.109120
34. Guo H, Ci X, Ahmed M, et al. ONECUT2 is a driver of neuroendocrine prostate cancer. Nat Commun. 2019;10(1):1-13. doi:10.1038/s41467-018-08133-6
35. Qian C, Yang Q, Rotinen M, et al. ONECUT2 Activates Diverse Resistance Drivers of Androgen Receptor-Independent Heterogeneity in Prostate Cancer. Published online October 1, 2023:2023.09.28.560025. doi:10.1101/2023.09.28.560025
36. Zhang W, Patil S, Chauhan B, et al. FoxO1 Regulates Multiple Metabolic Pathways in the Liver: EFFECTS ON GLUCONEOGENIC, GLYCOLYTIC, AND LIPOGENIC GENE EXPRESSION*. J Biol Chem. 2006;281(15):10105-10117. doi:10.1074/jbc.M600272200
37. Delpoux A, Marcel N, Hess Michelini R, et al. FOXO1 constrains activation and regulates senescence in CD8 T cells. Cell Rep. 2021;34(4):108674. doi:10.1016/j.celrep.2020.108674
38. Cabrera-Ortega AA, Feinberg D, Liang Y, Rossa C, Graves DT. The Role of Forkhead Box 1 (FOXO1) in the Immune System: Dendritic Cells, T Cells, B Cells, and Hematopoietic Stem Cells. Crit Rev Immunol. 2017;37(1):1-13. doi:10.1615/CritRevImmunol.2017019636
39. Vahedi G, Takahashi H, Nakayamada S, et al. STATs Shape the Active Enhancer Landscape of T Cell Populations. Cell. 2012;151(5):981-993. doi:10.1016/j.cell.2012.09.044
40. Daniels MA, Luera D, Teixeiro E. NFκB signaling in T cell memory. Front Immunol. 2023;14. Accessed December 5, 2023. https://www.frontiersin.org/articles/10.3389/fimmu.2023.1129191
41. Toobian D, Ghosh P, Katkar GD. Parsing the Role of PPARs in Macrophage Processes. Front Immunol. 2021;12:783780. doi:10.3389/fimmu.2021.783780
42. Niu Z, Shi Q, Zhang W, et al. Caspase-1 cleaves PPARγ for potentiating the pro-tumor action of TAMs. Nat Commun. 2017;8(1):766. doi:10.1038/s41467-017-00523-6
43. Hernandez-Quiles M, Broekema MF, Kalkhoven E. PPARgamma in Metabolism, Immunity, and Cancer: Unified and Diverse Mechanisms of Action. Front Endocrinol. 2021;12. Accessed May 2, 2023. https://www.frontiersin.org/articles/10.3389/fendo.2021.624112
44. Kanehisa M, Goto S. KEGG: Kyoto Encyclopedia of Genes and Genomes. Nucleic Acids Res. 2000;28(1):27-30. doi:10.1093/nar/28.1.27
45. Kerk SA, Papagiannakopoulos T, Shah YM, Lyssiotis CA. Metabolic networks in mutant KRAS-driven tumours: tissue specificities and the microenvironment. Nat Rev Cancer. 2021;21(8):510-525. doi:10.1038/s41568-021-00375-9
46. Bechard ME, Word AE, Tran AV, Liu X, Locasale JW, McDonald OG. Pentose conversions support the tumorigenesis of pancreatic cancer distant metastases. Oncogene. 2018;37(38):5248-5256. doi:10.1038/s41388-018-0346-5
47. Viale A, Pettazzoni P, Lyssiotis CA, et al. Oncogene ablation-resistant pancreatic cancer cells depend on mitochondrial function. Nature. 2014;514(7524):628-632. doi:10.1038/nature13611

48. Netea-Maier RT, Smit JWA, Netea MG. Metabolic changes in tumor cells and tumor-associated macrophages: A mutual relationship. Cancer Lett. 2018;413:102-109. doi:10.1016/j.canlet.2017.10.037
49. Matellan C, Lachowski D, Cortes E, et al. Retinoic acid receptor β modulates mechanosensing and invasion in pancreatic cancer cells via myosin light chain 2. Oncogenesis. 2023;12(1):1-11. doi:10.1038/s41389-023-00467-1
50. Mere Del Aguila E, Tang XH, Gudas LJ. Pancreatic Ductal Adenocarcinoma: New Insights into the Actions of Vitamin A. Oncol Res Treat. 2022;45(5):291-298. doi:10.1159/000522425
51. Chronopoulos A, Robinson B, Sarper M, et al. ATRA mechanically reprograms pancreatic stellate cells to suppress matrix remodelling and inhibit cancer cell invasion. Nat Commun. 2016;7(1):12630. doi:10.1038/ncomms12630
52. Lavudi K, Nuguri SM, Olverson Z, Dhanabalan AK, Patnaik S, Kokkanti RR. Targeting the retinoic acid signaling pathway as a modern precision therapy against cancers. Front Cell Dev Biol. 2023;11. Accessed November 30, 2023. https://www.frontiersin.org/articles/10.3389/fcell.2023.1254612
53. Bi G, Liang J, Shan G, et al. Retinol Saturase Mediates Retinoid Metabolism to Impair a Ferroptosis Defense System in Cancer Cells. Cancer Res. 2023;83(14):2387-2404. doi:10.1158/0008-5472.CAN-22-3977
54. Li JT, Yin M, Wang D, et al. BCAT2-mediated BCAA catabolism is critical for development of pancreatic ductal adenocarcinoma. Nat Cell Biol. 2020;22(2):167-174. doi:10.1038/s41556-019-0455-6
55. Shyh-Chang N, Locasale JW, Lyssiotis CA, et al. Influence of Threonine Metabolism on S-adenosyl-methionine and Histone Methylation. Science. 2013;339(6116):222-226. doi:10.1126/science.1226603
56. Geeraerts SL, Heylen E, De Keersmaecker K, Kampen KR. The ins and outs of serine and glycine metabolism in cancer. Nat Metab. 2021;3(2):131-141. doi:10.1038/s42255-020-00329-9
57. Klein Geltink RI, Kyle RL, Pearce EL. Unraveling the Complex Interplay Between T Cell Metabolism and Function. Annu Rev Immunol. 2018;36(1):461-488. doi:10.1146/annurev-immunol-042617-053019
58. van der Windt GJW, Everts B, Chang CH, et al. Mitochondrial respiratory capacity is a critical regulator of CD8+ T cell memory development. Immunity. 2012;36(1):68-78. doi:10.1016/j.immuni.2011.12.007
59. Man K, Kallies A. Synchronizing transcriptional control of T cell metabolism and function. Nat Rev Immunol. 2015;15(9):574-584. doi:10.1038/nri3874
60. Llaó-Cid L, Roessner PM, Chapaprieta V, et al. EOMES is essential for antitumor activity of CD8+ T cells in chronic lymphocytic leukemia. Leukemia. 2021;35(11):3152-3162. doi:10.1038/s41375-021-01198-1
61. Marcel N, Hedrick SM. A key control point in the T cell response to chronic infection and neoplasia: FOXO1. Curr Opin Immunol. 2020;63:51-60. doi:10.1016/j.coi.2020.02.001
62. Jiang Y, Li Y, Zhu B. T-cell exhaustion in the tumor microenvironment. Cell Death Dis. 2015;6(6):e1792-e1792. doi:10.1038/cddis.2015.162
63. Heiduk M, Klimova A, Reiche C, et al. TIGIT Expression Delineates T-cell Populations with Distinct Functional and Prognostic Impact in Pancreatic Cancer. Clin Cancer Res. 2023;29(14):2638-2650. doi:10.1158/1078-0432.CCR-23-0258

64. Mantovani A, Allavena P, Marchesi F, Garlanda C. Macrophages as tools and targets in cancer therapy. Nat Rev Drug Discov. 2022;21(11):799-820. doi:10.1038/s41573-022-00520-5
65. El-Kenawi A, Dominguez-Viqueira W, Liu M, et al. Macrophage-Derived Cholesterol Contributes to Therapeutic Resistance in Prostate Cancer. Cancer Res. 2021;81(21):5477-5490. doi:10.1158/0008-5472.CAN-20-4028
66. Boyer S, Lee HJ, Steele N, et al. Multiomic characterization of pancreatic cancer-associated macrophage polarization reveals deregulated metabolic programs driven by the GM-CSF–PI3K pathway. Fertig EJ, Zaidi M, DeNardo D, eds. eLife. 2022;11:e73796. doi:10.7554/eLife.73796
67. Loke P, Lin JD. Redefining inflammatory macrophage phenotypes across stages and tissues by single-cell transcriptomics. Sci Immunol. 2022;7(70):eabo4652. doi:10.1126/sciimmunol.abo4652
68. Qian J, Olbrecht S, Boeckx B, et al. A pan-cancer blueprint of the heterogeneous tumor microenvironment revealed by single-cell profiling. Cell Res. 2020;30(9):745-762. doi:10.1038/s41422-020-0355-0
69. Puthenveetil A, Dubey S. Metabolic reprograming of tumor-associated macrophages. Ann Transl Med. 2020;8(16):1030. doi:10.21037/atm-20-2037
70. Seo SK, Kwon B. Immune regulation through tryptophan metabolism. Exp Mol Med. 2023;55(7):1371-1379. doi:10.1038/s12276-023-01028-7
71. Stone TW, Williams RO. Modulation of T cells by tryptophan metabolites in the kynurenine pathway. Trends Pharmacol Sci. 2023;44(7):442-456. doi:10.1016/j.tips.2023.04.006
72. Fallarino F, Grohmann U, Vacca C, et al. T cell apoptosis by tryptophan catabolism. Cell Death Differ. 2002;9(10):1069-1077. doi:10.1038/sj.cdd.4401073
73. Elia I, Haigis MC. Metabolites and the tumor microenvironment: from cellular mechanisms to systemic metabolism. Nat Metab. 2021;3(1):21-32. doi:10.1038/s42255-020-00317-z
74. Goossens P, Rodriguez-Vita J, Etzerodt A, et al. Membrane Cholesterol Efflux Drives Tumor-Associated Macrophage Reprogramming and Tumor Progression. Cell Metab. 2019;29(6):1376-1389.e4. doi:10.1016/j.cmet.2019.02.016
75. Burclaff J, Bliton RJ, Breau KA, et al. A Proximal-to-Distal Survey of Healthy Adult Human Small Intestine and Colon Epithelium by Single-Cell Transcriptomics. Cell Mol Gastroenterol Hepatol. 2022;13(5):1554-1589. doi:10.1016/j.jcmgh.2022.02.007
76. Huang Y, Mohanty V, Dede M, et al. Characterizing cancer metabolism from bulk and single-cell RNA-seq data using METAFlux. Nat Commun. 2023;14(1):4883. doi:10.1038/s41467-023-40457-w
77. Li S, Yu J, Huber A, et al. Metabolism drives macrophage heterogeneity in the tumor microenvironment. Cell Rep. 2022;39(1):110609. doi:10.1016/j.celrep.2022.110609
78. Morioka F, Tani N, Ikeda T, et al. Morphological and biochemical changes in the pancreas associated with acute systemic hypoxia. Hum Cell. 2021;34(2):400-418. doi:10.1007/s13577-020-00481-0
79. Cocariu EA, Mageriu V, Stăniceanu F, Bastian A, Socoliuc C, Zurac S. Correlations Between the Autolytic Changes and Postmortem Interval in Refrigerated Cadavers. Romanian J Intern Med Rev Roum Med Interne. 2016;54(2):105-112. doi:10.1515/rjim-2016-0012

80. Purohit V, Simeone DM, Lyssiotis CA. Metabolic Regulation of Redox Balance in Cancer. Cancers. 2019;11(7):955. doi:10.3390/cancers11070955
81. Rosa Neto JC, Calder PC, Curi R, Newsholme P, Sethi JK, Silveira LS. The Immunometabolic Roles of Various Fatty Acids in Macrophages and Lymphocytes. Int J Mol Sci. 2021;22(16):8460. doi:10.3390/ijms22168460
82. Reina-Campos M, Scharping NE, Goldrath AW. CD8+ T cell metabolism in infection and cancer. Nat Rev Immunol. 2021;21(11):718-738. doi:10.1038/s41577-021-00537-8
83. Buck MD, O'Sullivan D, Klein Geltink RI, et al. Mitochondrial Dynamics Controls T Cell Fate through Metabolic Programming. Cell. 2016;166(1):63-76. doi:10.1016/j.cell.2016.05.035
84. Steele NG, Biffi G, Kemp SB, et al. Inhibition of Hedgehog Signaling Alters Fibroblast Composition in Pancreatic Cancer. Clin Cancer Res Off J Am Assoc Cancer Res. 2021;27(7):2023-2037. doi:10.1158/1078-0432.CCR-20-3715
85. Kerk SA, Lin L, Myers AL, et al. Metabolic requirement for GOT2 in pancreatic cancer depends on environmental context. Finley LW, White RM, eds. eLife. 2022;11:e73245. doi:10.7554/eLife.73245
86. Raghavan KS, Francescone R, Franco-Barraza J, et al. NetrinG1+ Cancer-Associated Fibroblasts Generate Unique Extracellular Vesicles that Support the Survival of Pancreatic Cancer Cells Under Nutritional Stress. Cancer Res Commun. 2022;2(9):1017-1036. doi:10.1158/2767-9764.CRC-21-0147
87. Van de Velde LA, Subramanian C, Smith AM, et al. T Cells Encountering Myeloid Cells Programmed for Amino Acid-dependent Immunosuppression Use Rictor/mTORC2 Protein for Proliferative Checkpoint Decisions. J Biol Chem. 2017;292(1):15-30. doi:10.1074/jbc.M116.766238
88. Auciello FR, Bulusu V, Oon C, et al. A Stromal Lysolipid–Autotaxin Signaling Axis Promotes Pancreatic Tumor Progression. Cancer Discov. 2019;9(5):617-627. doi:10.1158/2159-8290.CD-18-1212
89. Zhang Y, Yan W, Mathew E, et al. Epithelial-Myeloid cell crosstalk regulates acinar cell plasticity and pancreatic remodeling in mice. Rath S, ed. eLife. 2017;6:e27388. doi:10.7554/eLife.27388
90. Chen Z, Han F, Du Y, Shi H, Zhou W. Hypoxic microenvironment in cancer: molecular mechanisms and therapeutic interventions. Signal Transduct Target Ther. 2023;8(1):1-23. doi:10.1038/s41392-023-01332-8
91. Mello AM, Ngodup T, Lee Y, et al. Hypoxia promotes an inflammatory phenotype of fibroblasts in pancreatic cancer. Oncogenesis. 2022;11(1):1-9. doi:10.1038/s41389-022-00434-2
92. Hao X, Ren Y, Feng M, Wang Q, Wang Y. Metabolic reprogramming due to hypoxia in pancreatic cancer: Implications for tumor formation, immunity, and more. Biomed Pharmacother. 2021;141:111798. doi:10.1016/j.biopha.2021.111798
93. Pietrobon V, Marincola FM. Hypoxia and the phenomenon of immune exclusion. J Transl Med. 2021;19(1):9. doi:10.1186/s12967-020-02667-4
94. Mangalhara KC, Varanasi SK, Johnson MA, et al. Manipulating mitochondrial electron flow enhances tumor immunogenicity. Science. 2023;381(6664):1316-1323. doi:10.1126/science.abq1053

Chapter 3 The Role of Oncogenic KRAS in Late Stage PDA

3.1 Abstract

Oncogenic KRAS is a hallmark mutation and drives progression and maintenance of pancreatic adenocarcinoma (PDA). Preliminary data shows that oncogenic Kras, expressed by pancreatic cancer cells, promotes a T cell-poor, immunosuppressive microenvironment. Here, I used a genetically engineered murine model of PDA, single cell RNA-Seq data, and a combination of in vitro and in vivo approaches to dissect the pathways driving immune suppression in pancreatic cancer. Overall, I aimed to characterize the role of mutant KRAS on the immune landscape in late stage pancreatic cancer by leveraging wet lab techniques and bioinformatics approaches.

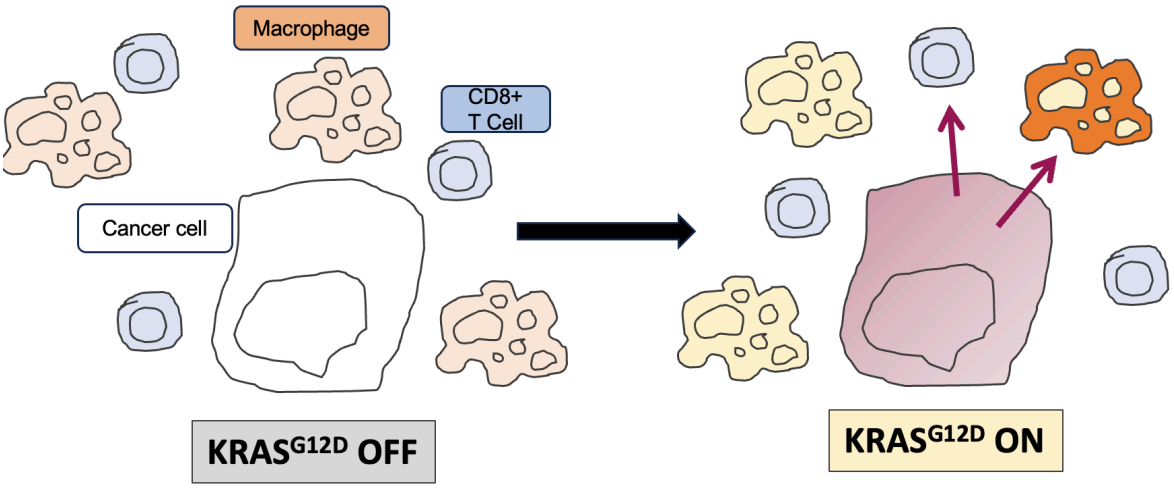

Figure 3.1Schematic for oncogenic KRAS driven alterations in TME.

Oncogenic KRAS drives immunosuppressive signaling in the tumor microenvironment that results in cytotoxic T cell dysfunction/exhaustion and phenotypic changes in tumor associated macrophages.

3.2 Introduction

Oncogenic KRAS is a driving mutation in PDA; 95% of tumors carry the mutant form with a single amino acid substitution, most frequently $KRAS^{G12D}$ (4–6). Oncogenic signaling reprograms immune cells in proximity of the cancer cells, creating an immunosuppressive microenvironment adept at suppressing anti-tumor immune responses (8–15). Thus, there is a need to understand drivers of late stage PDA to develop more effective therapeutic strategies that target both cancer cells and stromal cells in the tumor microenvironment (TME). The Pasca lab and others have shown that oncogenic Kras regulates the surrounding microenvironment in a cell extrinsic manner and is necessary for tumor maintenance (10,12,13,15–17).

To investigate the role of $KRAS^{G12D}$ inhibition in late stage PDA, the iKras murine model was employed and single cell data from orthoptic tumors was analyzed. In addition, bulk transcriptomic data derived from patients with pancreatic cancer was mined to assess expression of genes reported to play a critical role in PDA progression. To ascertain immune landscape alterations following inhibition of oncogenic KRAS multiplex immunofluorescent staining and flow cytometry were performed. Dissecting changes in immune profiles as consequence of mutant Kras signaling may aid in targeting stromal and cancer cells for increased therapeutic efficacy.

3.3 Results

3.3.1 Investigating the role of oncogenic Kras in the regulation of CD8+ T cell status in PDA

The stroma is composed of pro and anti-inflammatory fibroblasts and immune cells which play a role in creating an immunosuppressive immune environment in PDA. More specifically, tumor-associated macrophages (TAMs), regulatory T cells (Tregs) and inflammatory cancer-associated fibroblasts (iCAFs) make up a signaling axis that dampens the activation of CD8+ T cells (13,17–20). The inability of CD8+ T cells to recognize and execute tumor clearance allows for immune evasion. Further, CD8+ T cells display an exhausted phenotype in human pancreatic cancer (3). How mutant Kras regulates functional CD8+ T cell status remains to be fully determined in advanced PDA. I sought to determine whether the dysfunctional status of CD8+ T cells is directly mediated by oncogenic Kras expression in cancer cells using genetically engineered mouse models that recapitulate the human disease.

To investigate if mouse models recapitulate the dysfunctional status of CD8+ T cells seen in human tumor tissue I orthotopically implanted murine PDA cells with doxycycline inducible mutant $Kras^{G12D}$ cells derived from genetically engineered mice into syngeneic mice (5). These cells, referred to as iKRAS, express oncogenic KRAS in presence of Doxycycline (DOX); withdrawal of DOX inactivates oncogenic KRAS expression (Figure 3.2A).The iKRAS cells are derived in FVBN pure strain mice and can be implanted in syngeneic FVBN host mice, thus retaining a functional immune system. We harvested tumors from mice kept on DOX for the

whole experiment, or following 3 days DOX withdrawal, dissociated them, and performed single-cell RNA sequencing (scRNA-seq). I visualized the results, and projected them using uniform manifold approximation and projection (UMAP) (Figure 3.2A). Interestingly, there were few lymphocytes in the Kras ON state, consistent with the immunosuppressive nature of pancreatic cancer (Figure 3.2B). Genetic inhibition of Kras globally reshaped the tumor immune microenvironment composition, with a notable increase in CD8+ T cells. CD8+ T cells are responsible for mounting anti-tumor responses; their increase upon Kras inactivation is consistent with lessened immune suppression. However, CD8+ T cells still expressed Tox, a transcription factor known to promote T cell exhaustion, following Kras inactivation, showing that even as T cell infiltration increased these cells are not likely to mount an anti-tumor immune response (Figure 3.2C). Additionally, I also observed changes in fibroblast abundance and type upon KRAS inactivation, similar to recent findings from our lab in early-stage disease (13). These preliminary data suggests that CD8+ T cell dysfunction is regulated by oncogenic Kras in epithelial cells.

Next, to assess alterations in tumor associated macrophages (TAMs) as a result of acute Kras inhibition, macrophages were isolated and profiled using flow cytometry with the following panel:anti-Cd11b, anti-F4/80, anti-Ly6C, anti-Ly6G (Figure 3.2D). This analysis revealed that the population number of macrophages (F480+) did not change due to Kras inhibition, but a greater proportion became Ly6C+ . The data suggests that macrophage density is not changed due to genetic inhibition of Kras, but that the polarization status is altered and should be further investigated.

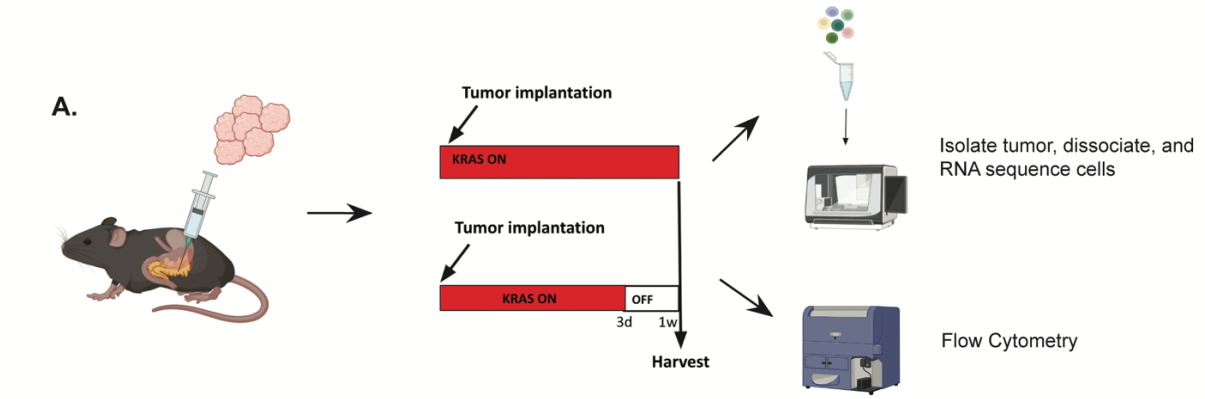
A.
Tumor implantation
KRAS ON
Tumor implantation
KRAS ON
OFF
3d
1w
Harvest
Isolate tumor, dissociate, and RNA sequence cells
Flow Cytometry

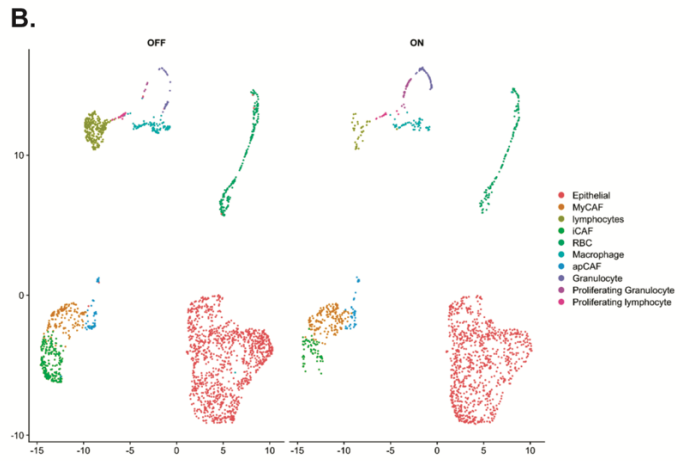
B.
OFF
ON
Epithelial
MyCAF
lymphocytes
iCAF
RBC
Macrophage
apCAF
Granulocyte
Proliferating Granulocyte
Proliferating lymphocyte

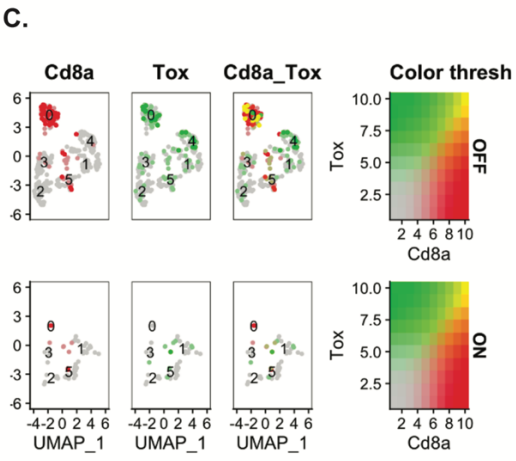
C.
Cd8a
Tox
Cd8a_Tox
Color thresh
OFF
ON
Tox
Cd8a
UMAP_1

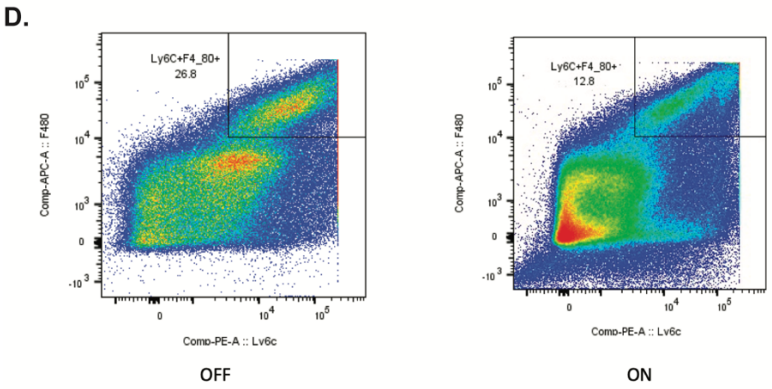
D.
Ly6C+F4_80+
26.8
12.8
Comp-APC-A :: F480
Comp-PE-A :: Lv6c
OFF
ON

Figure 3.2 Genetic Kras inhibition remodels the tumor microenvironment.

(A) Three weeks after tumor implantation a subset of mice continued receiving doxycycline(Kras on) and a subset of mice did not receive doxycycline (Kras off) for three days or one week. Tumors were then harvested and dissociated to perform scRNA-Seq.

(B) Results demonstrate remodeling of the immune microenvironment, with fewer lymphocytes (immune cells) and a more inflammatory fibroblasts (iCAFs) when Kras is expressed .

(C)Acute inhibition of Kras restores CD8+T cell infiltration but exhaustion marker (Tox) was still expressed by T cells demonstrating ongoing dysfunction.

(D) Representative flow plots for the analysis of F4/80+ cells following acute genetic Kras inhibition.

3.3.2 Interrogation of T cell infiltration following acute genetic Kras inactivation in vivo

To assess infiltration of CD8 and CD4 T cells in the tumor, the above mentioned murine model was orthotopically implanted with iKras* cells, after tumor formation Kras was inactivated for three days, then tumors were harvested (Figure 3.3A) . Multiplex immunofluorescent staining for CD8+ and CD4+ T cells revealed an increase in immune cell infiltration following acute inhibition (Figure 3.3B). To ascertain if T cells colocalized with tumor cells, staining for CK19 was performed. Both CD4 and CD8 T cells significantly increased levels following inhibition regardless of whether in CK19 high or low regions (Figure 3.3C-D).

3.4 Discussion

Pharmacological inhibition and genetic inactivation of Kras altered the immune landscape of TAMs and infiltrating lymphocytes in a murine model of PDA (Figure 3.1 and Figure 3.2) .The question remains whether this is a direct effect of the interaction between cancer cells and T cells, or whether it is mediated by other cell types (e.g., fibroblasts, macrophages, or other

myeloid cells, with known immunosuppressive role). To address this question, I will utilize a 3D co-culture system of pancreatic tumor cells and CD8+ T cells sorted from the tumor; I will determine whether the exhaustion phenotype is induced in vitro. I will then repeat these experiments adding cancer associated fibroblasts (CAFs) and/or tumor associated macrophages (TAMs) to determine whether they are required/contribute to T cell exhaustion.

In vivo, I will orthotopically implant pancreatic cancer cells into a GEMM of PDA previously described with inducible Kras expression and inactivation. Two weeks after tumor implantation I will pharmacologically inhibit mutant KRASG12D with MRTX1133 at 10 mg/kg twice daily for three weeks or remove doxycycline (genetic inhibition) for 3 weeks to achieve tumor regression. Once tumors are established, I will leave half the mice in each group untreated, while I will administer anti-TIGIT based on work by us and others a key checkpoint in pancreatic cancer (15,17,25) or CD40 agonist (21–23). I will then harvest tumors and isolate CD8+ T cells for immune profiling to determine if an "exhausted" phenotype is displayed amongst any of the treatment strategies. To do so I will perform flowcytometry with the following panel: anti-PD1, anti-TIGIT, anti-LAG3, anti-TIM3. I will also perform multiplex immunofluorescent staining to examine immune tone (functional status) in the tissue samples from all conditions. I will stain for CD8+T cell, CD4+ T cells , F480(macrophages), and Arginase 1(Arg1) as well to assess TAM polarization as well. Next, I will perform scRNA-seq on the tumor tissue to investigate differences in differentially expressed genes in each cellular compartment based on treatment condition, followed by gene set enrichment analysis to examine different pathways upregulated and downregulated. This analysis will reveal extrinsic changes

and intrinsic changes in the tumor. I will also analyze the interactome, to characterize ligand-ligand interactions that drive signaling and co-adaptations. Lastly, to identify potential metabolic co-adaptations utilized by pancreatic cancer cells to overcome ICI therapy following mutant Kras inhibition mass spectrometry will be employed to identify metabolic proteins that are up/downregulated due to experimental treatment conditions.

.

A.

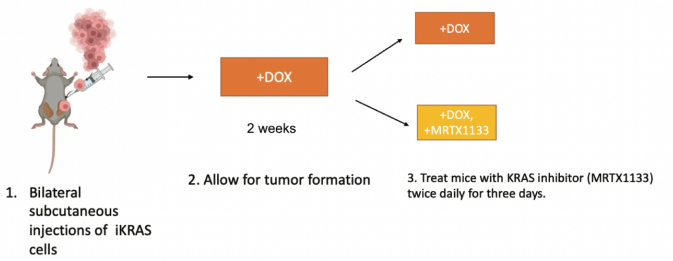
+DOX
+DOX
2 weeks
+DOX, +MRTX1133
1. Bilateral subcutaneous injections of iKRAS cells
2. Allow for tumor formation
3. Treat mice with KRAS inhibitor (MRTX1133) twice daily for three days.

B.

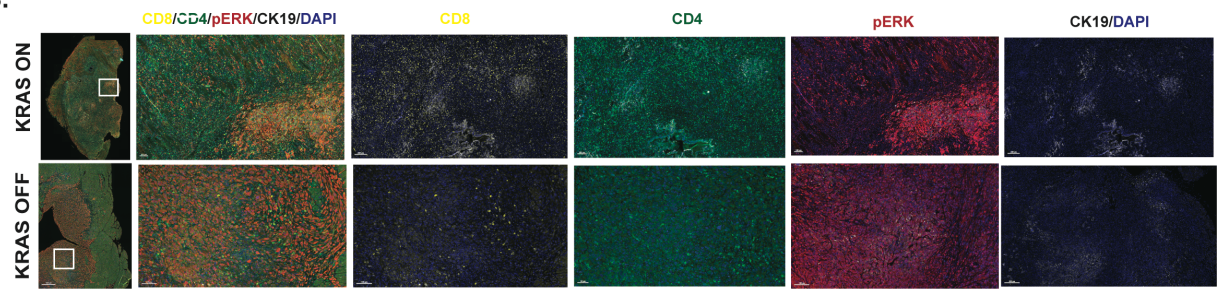
CD8/CD4/pERK/CK19/DAPI
CD8
CD4
pERK
CK19/DAPI
KRAS ON
KRAS OFF

C.

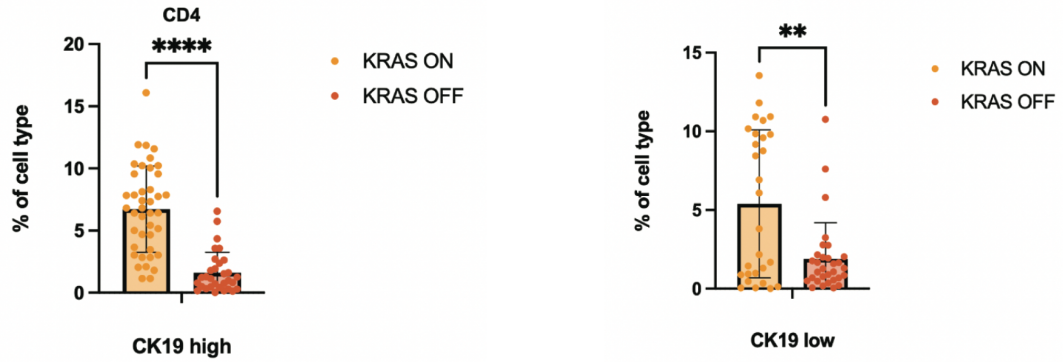
CD4
****
% of cell type
CK19 high
KRAS ON
KRAS OFF
CD4
**
% of cell type
CK19 low
KRAS ON
KRAS OFF

D


CD8
**
% of cell type
CK19 high
KRAS ON
KRAS OFF
CD8
**
% of cell type
CK19 low
KRAS ON
KRAS OFF

Figure 3.3 Inactivation of Kras augments T cell infiltration in orthoptic murine model.

(A)Schematic of orthoptic tumor implementation into syngeneic mice. After two weeks Kras was pharmacologically inhibited for 3 days and tumors were harvested.

(B)Multiplex immunofluorescent staining to probe for CD8+ Tcells, CD4+ T cells, CK19,and pERK.

(C)Percentage of CD4+ T cells in CK19 high and low regions of tissue, in KRAS on and off conditions.

(D)Percentage of CD8+ T cells in CK19 high and low regions of tissue, in KRAS on and off conditions.

3.5 Methods

3.5.1 Orthoptic Surgeries

50 µl of 50,000 A9805 cells (derived from iKras^{G12D}P53^{R172H}(ptf1a-Cre; TetO-Kras^{G12D};Rosa26$^{rtTa/+;}$p53$^{R172H/+}$) were resuspended in a 1:1 ratio of RPMI medium (Gibco, 11875093) and Matrigel matrix basement membrane (Corning, 354234) and injected into the pancreas of FVBN mice. Activation of KRAS^{G12D} was induced in mice by providing doxycycline chow in place of regular chow. Cells used for orthoptic surgery were tested for mycoplasma with the MycoAlertTM Plus Mycoplasma Detection Kit(Lonza). After two weeks post implantation mice had formed established tumors and were randomly divided into two treatment groups (Kras activation) with MRTX1133 treatment or Kras activation without pharmacologically inhibition.

3.5.2 Multiplex Immunofluorescent Staining

Multiplex immunofluorescent staining was performed on paraffin embedded murine pancreatic tissue sections. First, slides were baked in a hybridization oven for 1 hour at 60^0C, cooled for 10

minutes at room temperature, then submerged in Xylene for paraffin removal. Slides were then rehydrated in alcohol, followed by washes in deionized water for 2 minutes, then placed in formalin neutralizing buffer for 30 minutes. Again, slides were washed for 2 minutes with deionized water. The rest of the procedure has been previously described (13). Primary antibodies were diluted in blocking buffer and incubated on slides overnight at 4^{o}C, followed by secondary antibody (Alexa Flour secondaries, 1:300) for 45 min at RT. Slides were then mounted with Prolong Diamond Antifade Mountant with DAPI(Invitrogen). In addition, TSA Plus Fluorescein was used during co-immunofluorescent staining of primary antibodies.

3.5.3 Flow Cytometry

Murine pancreatic tumors were harvested and dissociated into single cells by finely mincing tissue with scissors and collagenase IV (1 mg/mL; Sigma) digestion for 35 minutes at 37^{o}C while shaking. To separate tumors into single cells, 40-um mesh strainers was utilized, and all red blood cells were lysed with lysis buffer. Live cells were stained for anti-F4/80, anti-CD11b, anti-Ly6C, anti-Ly6G, then cells were stained for primary antibodies and fixed. Flow-cytometric analysis was done on a BD LSRFortessa (BD Bioscience) using BD FACS Diva software, and data analysis was performed using FlowJo v10 software.

3.5.4 Statistics

GraphPad Prism version 10.0.2 software was used for analysis, either a t-test or Man- Whitney test was performed for statistical analysis. The statistically significant threshold was set at $P<0.05$.

3.5.5 Single cell RNA-Sequencing

Orthoptic tumors were established in the pancreas of murine PDA model by injecting 50 µl of 50,000 iKras* cells into (FVB/N strain) mice. Tumor were established as previously described (Velez), and then harvested for single cell RNA-Seq. Single-cell cDNA library was prepared and sequenced at the University of Michigan Sequencing Core using the 10x Genomics Platform.

References

1. Siegel RL, Giaquinto AN, Jemal A. Cancer statistics, 2024. CA Cancer J Clin. 2024;74(1):12-49. doi:10.3322/caac.21820
2. Sarantis P, Koustas E, Papadimitropoulou A, Papavassiliou AG, Karamouzis MV. Pancreatic ductal adenocarcinoma: Treatment hurdles, tumor microenvironment and immunotherapy. World J Gastrointest Oncol. 2020;12(2):173. doi:10.4251/wjgo.v12.i2.173
3. Steele NG, Carpenter ES, Kemp SB, et al. Multimodal Mapping of the Tumor and Peripheral Blood Immune Landscape in Human Pancreatic Cancer. Nat Cancer. 2020;1(11):1097-1112. doi:10.1038/s43018-020-00121-4
4. Kemp SB, Cheng N, Markosyan N, et al. Efficacy of a Small-Molecule Inhibitor of KrasG12D in Immunocompetent Models of Pancreatic Cancer. Cancer Discov. 2023;13(2):298-311. doi:10.1158/2159-8290.CD-22-1066
5. Collins MA, Bednar F, Zhang Y, et al. Oncogenic Kras is required for both the initiation and maintenance of pancreatic cancer in mice. J Clin Invest. 2012;122(2):639-653. doi:10.1172/JCI59227
6. Cowzer D, Zameer M, Conroy M, Kolch W, Duffy AG. Targeting KRAS in Pancreatic Cancer. J Pers Med. 2022;12(11):1870. doi:10.3390/jpm12111870

7. Ying H, Dey P, Yao W, et al. Genetics and biology of pancreatic ductal adenocarcinoma. Genes Dev. 2016;30(4):355-385. doi:10.1101/gad.275776.115
8. Low V, Li Z, Blenis J. Metabolite activation of tumorigenic signaling pathways in the tumor microenvironment. Sci Signal. 2022;15(759):eabj4220. doi:10.1126/scisignal.abj4220
9. Huang L, Guo Z, Wang F, Fu L. KRAS mutation: from undruggable to druggable in cancer. Signal Transduct Target Ther. 2021;6(1):1-20. doi:10.1038/s41392-021-00780-4
10. Boyer S, Lee HJ, Steele N, et al. Multiomic characterization of pancreatic cancer-associated macrophage polarization reveals deregulated metabolic programs driven by the GM-CSF–PI3K pathway. Fertig EJ, Zaidi M, DeNardo D, eds. eLife. 2022;11:e73796. doi:10.7554/eLife.73796
11. Halbrook CJ, Thurston G, Boyer S, et al. Differential integrated stress response and asparagine production drive symbiosis and therapy resistance of pancreatic adenocarcinoma cells. Nat Cancer. 2022;3(11):1386-1403. doi:10.1038/s43018-022-00463-1
12. Kerk SA, Lin L, Myers AL, et al. Metabolic requirement for GOT2 in pancreatic cancer depends on environmental context. Finley LW, White RM, eds. eLife. 2022;11:e73245. doi:10.7554/eLife.73245
13. Velez-Delgado A, Donahue KL, Brown KL, et al. Extrinsic KRAS Signaling Shapes the Pancreatic Microenvironment Through Fibroblast Reprogramming. Cell Mol Gastroenterol Hepatol. 2022;13(6):1673-1699. doi:10.1016/j.jcmgh.2022.02.016
14. Son J, Lyssiotis CA, Ying H, et al. Glutamine supports pancreatic cancer growth through a KRAS-regulated metabolic pathway. Nature. 2013;496(7443):101-105. doi:10.1038/nature12040
15. Menjivar RE, Nwosu ZC, Du W, et al. Arginase 1 is a key driver of immune suppression in pancreatic cancer. eLife. 2023;12:e80721. doi:10.7554/eLife.80721
16. Carpenter ES, Elhossiny AM, Kadiyala P, et al. Analysis of Donor Pancreata Defines the Transcriptomic Signature and Microenvironment of Early Neoplastic Lesions. Cancer Discov. 2023;13(6):1324-1345. doi:10.1158/2159-8290.CD-23-0013
17. Zhang Y, Velez-Delgado A, Mathew E, et al. Myeloid cells are required for PD-1/PD-L1 checkpoint activation and the establishment of an immunosuppressive environment in pancreatic cancer. Gut. 2017;66(1):124-136. doi:10.1136/gutjnl-2016-312078
18. Van de Velde LA, Subramanian C, Smith AM, et al. T Cells Encountering Myeloid Cells Programmed for Amino Acid-dependent Immunosuppression Use Rictor/mTORC2 Protein for Proliferative Checkpoint Decisions. J Biol Chem. 2017;292(1):15-30. doi:10.1074/jbc.M116.766238
19. Kemp SB, Pasca di Magliano M, Crawford HC. Myeloid Cell Mediated Ilmmune Suppression in Pancreatic Cancer. Cell Mol Gastroenterol Hepatol. 2021;12(5):1531-1542. doi:10.1016/j.jcmgh.2021.07.006

20. Steele NG, Biffi G, Kemp SB, et al. Inhibition of Hedgehog Signaling Alters Fibroblast Composition in Pancreatic Cancer. Clin Cancer Res Off J Am Assoc Cancer Res. 2021;27(7):2023-2037. doi:10.1158/1078-0432.CCR-20-3715
21. Vonderheide RH. CD40 Agonist Antibodies in Cancer Immunotherapy. Annu Rev Med. 2020;71:47-58. doi:10.1146/annurev-med-062518-045435
22. Wattenberg MM, Herrera VM, Giannone MA, Gladney WL, Carpenter EL, Beatty GL. Systemic inflammation is a determinant of outcomes of CD40 agonist-based therapy in pancreatic cancer patients. JCI Insight. 2021;6(5):e145389, 145389. doi:10.1172/jci.insight.145389
23. Panni RZ, Herndon JM, Zuo C, et al. Agonism of CD11b reprograms innate immunity to sensitize pancreatic cancer to immunotherapies. Sci Transl Med. 2019;11(499):eaau9240. doi:10.1126/scitranslmed.aau9240

Chapter 4 Summary and Future Directions

PDA is characterized by a fibroinflammatory stroma, high infiltration rate of tumor associated macrophages (TAMs), and T cells with exhausted/dysfunctional profiles (2–12). Extracellular matrix components also contribute to disease progression and metastasis through mediation of ECM stiffness, and contribution of tumor milieu components that may be up taken by cancer cells (13,14). PDA is marked by a high infiltration of myeloid derived suppressor cells; of which TAMs are the most abundant and metabolically diverse with a myriad of functional phenotypes and altered metabolic processes (15–21). Further, TAMs engage in cooperative metabolic crosstalk with cancer cells that enables sustained growth and survival of cancer cells (22,23). TAMs also secrete cytokines which can promote immunosuppressive signaling, and reports have found that interactions between TAMs and cytotoxic T cells dampens T cell's ability to mount an effective anti-tumor response (4,24–26). TAMs have been shown to secrete pyrimidine analogs which inhibit efficacy of gemcitabine, a chemotherapeutic agent used to treat PDA (27). Cancer cells also been shown to co-opt bio energetic derivatives from fibroblasts in the tumor milieu, for example intaking branch chain keto acid derivatives to fuel protein synthesis, TCA cycle precursors, and lipid biosynthesis (28). To investigate metabolic alterations in cell type specific manner, I leveraged a unique single cell RNA-Seq dataset comprised of healthy pancreata procured through a collaboration with Gift of Life Michigan (29). This dataset was compared to human pancreatic cancer samples utilizing robust computational approaches;

pseudo bulking, DGE analysis, metabolic GSEA, and transcription factor inference analysis. Further, computational findings were validated with in vitro and histology approaches.

Overall, this study resulted in a metabolic atlas of metabolic alterations engendered as a result of malignancy across cell types, providing a resource for understanding metabolic vulnerabilities in PDA. This work may also be a reference for metabolic rewiring induced by malignancy in other cancers and disease settings. In this section I will summarize the main findings from this body of work and present future directions.

4.1 Immune cells significantly decrease dependence on oxidative phosphorylation in the TME

A main finding in chapter 2 corresponded to CD8+ T cells, B cells, and granulocytes significantly decreasing the oxidative phosphorylation signature in the tumor compared to healthy counterparts (Figure 2.5 B-D). During T cell development, CD8+ T cells upregulate dependence on glycolysis and oxidative phosphorylation to facilitate effector function demands. In our data, glycolysis was significantly increased in tumor derived CD8 T cells, but oxidative phosphorylation was not, we speculate this might be due hypoxic regions in the tumor. Hypoxia is common amongst solid tumors and is a hallmark of PDA, to adapt to oxygen deprivation cancer and immune cells undergo metabolic reprogramming (30–32). This is mediated by hypoxia inducible transcription factors (HIFs) activation which regulate processes related to angiogenesis, metabolism, invasion, etc. (30). Interestingly, principal component analysis (PCA) revealed that immune populations could be segregated by expression of genes driving the

electron transport chain complexes (Figure 2.5F). B cells in specific displayed decreased expression of genes driving CII (Figure 2.5F). In a previous report electron flow was found to be decreased in CII of the ETC which enabled tumorgenicity and immune evasion in a melanoma model (33). Augmenting electron flow led to increased levels of succinate production in CII via an epigenetic mediated signaling axis, ultimately leading to activation of genes involved in antigen presentation and processing(33).This study performed a knockout of mitochondrial respiration genes in CI (sgNdufa) and CII (sgSdha or sgSdhc) in melanoma cells and found that loss of CII did not change NADH activity related to CI but did result in succinate dehydrogenase activity diminishing.

As a future direction I propose implementing a similar experimental design in pancreatic cancer cells to assess tumor growth and metastatic potential upon CII loss. To do this, I will generate 7904B KPC pancreatic cancer cells with either succinate dehydrogenase a (Sdha) or succinate dehydrogenase C (Sdhc) knocked out via CRISPR. Then these cells will be orthotopically implanted into a syngeneic mouse model, and tumor growth volume and weight will be tracked. Flow cytometry analysis will be performed on the tumors to profile immune markers, specifically assessing CD45+, CD8+, and CD4+ expression. To assess activation status of cytotoxic T cells expression of the following markers will be measured; GZMA, GZMB, and IFNG. In addition to genetic inhibition, pancreatic cancer cells will be treated with the mitochondrial inhibitor 3-nitropropionic acid (3-NPA) and proliferative capacity will be assessed (34). Lastly, if there is no change in tumor proliferation capacity and antigen processing and presentation in cancer cells it could be that other immune or stromal cells in the TME are

dictating the immune response. To test if CII loss in other cell types might be the culprit of immune evasion, I will utilize a 3D co-culture system of pancreatic tumor cells and CAFs with Sdhc or Sdha knocked out. These experiments will then be repeated with co-cultures between T cells with CII loss and pancreatic cancer cells Ultimately, the aim of the above experiments will be to investigate if CII loss in malignant or non-malignant cells plays a role in immune evasion and tumorgenicity in PDA.

4.2 TAMs upregulate a myriad of metabolic processes

TAMs drive a myriad of metabolic processes, in Chapter 2 we showed that TAMs upregulate glycolysis, PPP, fructose and mannose metabolism, and unsaturated fatty acid synthesis (Figure 2.9A). This prompted us to investigate unsaturated fatty acid biosynthesis in greater detail, we found stearoyl-CoA desaturase 1 (SCD1) to be differentially upregulated in TAMs compared to healthy macrophages (Figure 2.9B). To see if this held true in vitro we isolated bone marrow derived macrophages and polarized the macrophages as previously described and found SCD1 to be increased in TAMs at the protein level as well (Figure 2.9D). Myeloid derived suppressor cells, specifically TAMs make up a significant portion of the pancreatic tumor and can engage in pro and anti-tumor responses. As a future direction I propose that SCD1 be pharmacologically inhibited to see if the polarization profile of TAMS is altered. The in vitro BMDM isolation and polarization methodology will be implemented, and TAM polarization markers associated with M1-like and M2-like signatures will be assessed with qPCR. The goal of this experiment would

be to investigate if unsaturated fatty acid synthesis promotes an immunosuppressive phenotype in TAMs, and if this process is plastic and can be reversed.

4.3 TAMs engage in metabolic crosstalk with cancer cells

In Chapter 2, we found that TAMs engage in cooperative metabolic crosstalk with cancer cells (Figure 2.11 A and Figure 2.11B). TAMs differentially increase expression of the gene ABCG1 which encodes a cholesterol exporter, and tumor derived epithelial cells significantly increase expression of the gene encoding the cognate receptor for lipid/cholesterol uptake LDLR. TAMs were also found to increase production of ABCG1 at the protein level. As a future direction, it would be imperative to perform a cholesterol assay to ascertain cholesterol efflux from TAMs polarized with conditioned media. To do so, I would utilize a the Amplex Red Cholesterol Assay kit on media collected post isolation and polarization of BMDM to assess if there are differences in levels of free cholesterol in control condition with MCSF vs. tumor conditioned media. Next, to investigate if pancreatic cancer cells promote cholesterol efflux from TAMs for subsequent uptake, I would co culture pancreatic cancer cells and BMDMs in vitro and perform the a cholera toxin B (CBT) staining (35). A CBT staining is commonly used when studying cholesterol rich lipid rafts, since it binds to ganglioside GM1 which is linked to cholesterol levels (35). If indeed, pancreatic cancer are intaking free cholesterol derived from TAMs there should be a change in CBT staining of TAMs as cholesterol would be depleted. Overall, these initial future directions would serve to clarify if cholesterol is expelled from cholesterol rich lipid rafts to then serve as a fuel source for pancreatic cancer cells.

As a computational future direction an algorithm could be developed to infer putative transporter and exporter relationships based on gene expression from single cell data. This concept has been demonstrated in algorithms aimed at inferring ligand-receptor interactions from single cell data, in this case a curated list of known exporters and transporters with interactions would be constructed from querying public databases. This would provide potential leads for exporter/importer processes increased/decreased in cancer settings compared to basal physiology. In conclusion, the work described here serves as a resource for understanding the immune landscape of the pancreatic tumor microenvironment, metabolic alterations engendered by malignancy across multiple cellular compartments, and provides potential therapeutic targets to be further investigated.

References

1. Siegel RL, Giaquinto AN, Jemal A. Cancer statistics, 2024. CA Cancer J Clin. 2024;74(1):12-49. doi:10.3322/caac.21820
2. Ying H, Dey P, Yao W, et al. Genetics and biology of pancreatic ductal adenocarcinoma. Genes Dev. 2016;30(4):355-385. doi:10.1101/gad.275776.115
3. Puthenveetil A, Dubey S. Metabolic reprograming of tumor-associated macrophages. Ann Transl Med. 2020;8(16):1030. doi:10.21037/atm-20-2037
4. Tsujikawa T, Kumar S, Borkar RN, et al. Quantitative Multiplex Immunohistochemistry Reveals Myeloid-Inflamed Tumor-Immune Complexity Associated with Poor Prognosis. Cell Rep. 2017;19(1):203-217. doi:10.1016/j.celrep.2017.03.037
5. Huang Y, Si X, Shao M, Teng X, Xiao G, Huang H. Rewiring mitochondrial metabolism to counteract exhaustion of CAR-T cells. J Hematol OncolJ Hematol Oncol. 2022;15(1):38. doi:10.1186/s13045-022-01255-x
6. Jiang Y, Li Y, Zhu B. T-cell exhaustion in the tumor microenvironment. Cell Death Dis. 2015;6(6):e1792-e1792. doi:10.1038/cddis.2015.162

7. Li J, He Y, Hao J, Ni L, Dong C. High Levels of Eomes Promote Exhaustion of Anti-tumor CD8+ T Cells. Front Immunol. 2018;9. Accessed October 2, 2023. https://www.frontiersin.org/articles/10.3389/fimmu.2018.02981
8. T-cell exhaustion in the tumor microenvironment | Cell Death & Disease. Accessed January 31, 2024. https://www.nature.com/articles/cddis2015162
9. Steele NG, Carpenter ES, Kemp SB, et al. Multimodal Mapping of the Tumor and Peripheral Blood Immune Landscape in Human Pancreatic Cancer. Nat Cancer. 2020;1(11):1097-1112. doi:10.1038/s43018-020-00121-4
10. Velez-Delgado A, Donahue KL, Brown KL, et al. Extrinsic KRAS Signaling Shapes the Pancreatic Microenvironment Through Fibroblast Reprogramming. Cell Mol Gastroenterol Hepatol. 2022;13(6):1673-1699. doi:10.1016/j.jcmgh.2022.02.016
11. Menjivar RE, Nwosu ZC, Du W, et al. Arginase 1 is a key driver of immune suppression in pancreatic cancer. eLife. 2023;12:e80721. doi:10.7554/eLife.80721
12. Nywening TM, Wang-Gillam A, Sanford DE, et al. Targeting tumour-associated macrophages with CCR2 inhibition in combination with FOLFIRINOX in patients with borderline resectable and locally advanced pancreatic cancer: a single-centre, open-label, dose-finding, non-randomised, phase 1b trial. Lancet Oncol. 2016;17(5):651-662. doi:10.1016/S1470-2045(16)00078-4
13. Kamphorst JJ, Nofal M, Commisso C, et al. Human pancreatic cancer tumors are nutrient poor and tumor cells actively scavenge extracellular protein. Cancer Res. 2015;75(3):544-553. doi:10.1158/0008-5472.CAN-14-2211
14. Raghavan KS, Francescone R, Franco-Barraza J, et al. NetrinG1+ Cancer-Associated Fibroblasts Generate Unique Extracellular Vesicles that Support the Survival of Pancreatic Cancer Cells Under Nutritional Stress. Cancer Res Commun. 2022;2(9):1017-1036. doi:10.1158/2767-9764.CRC-21-0147
15. Wculek SK, Dunphy G, Heras-Murillo I, Mastrangelo A, Sancho D. Metabolism of tissue macrophages in homeostasis and pathology. Cell Mol Immunol. 2022;19(3):384-408. doi:10.1038/s41423-021-00791-9
16. Boyer S, Lee HJ, Steele N, et al. Multiomic characterization of pancreatic cancer-associated macrophage polarization reveals deregulated metabolic programs driven by the GM-CSF–PI3K pathway. Fertig EJ, Zaidi M, DeNardo D, eds. eLife. 2022;11:e73796. doi:10.7554/eLife.73796
17. Wu H, Han Y, Rodriguez Sillke Y, et al. Lipid droplet-dependent fatty acid metabolism controls the immune suppressive phenotype of tumor-associated macrophages. EMBO Mol Med. 2019;11(11):e10698. doi:10.15252/emmm.201910698
18. Eisinger S, Sarhan D, Boura VF, et al. Targeting a scavenger receptor on tumor-associated macrophages activates tumor cell killing by natural killer cells. Proc Natl Acad Sci U S A. 2020;117(50):32005-32016. doi:10.1073/pnas.2015343117
19. DeNardo DG, Ruffell B. Macrophages as regulators of tumour immunity and immunotherapy. Nat Rev Immunol. 2019;19(6):369-382. doi:10.1038/s41577-019-0127-6

20. Li S, Yu J, Huber A, et al. Metabolism drives macrophage heterogeneity in the tumor microenvironment. Cell Rep. 2022;39(1):110609. doi:10.1016/j.celrep.2022.110609
21. Rosa Neto JC, Calder PC, Curi R, Newsholme P, Sethi JK, Silveira LS. The Immunometabolic Roles of Various Fatty Acids in Macrophages and Lymphocytes. Int J Mol Sci. 2021;22(16):8460. doi:10.3390/ijms22168460
22. El-Kenawi A, Dominguez-Viqueira W, Liu M, et al. Macrophage-Derived Cholesterol Contributes to Therapeutic Resistance in Prostate Cancer. Cancer Res. 2021;81(21):5477-5490. doi:10.1158/0008-5472.CAN-20-4028
23. Goossens P, Rodriguez-Vita J, Etzerodt A, et al. Membrane Cholesterol Efflux Drives Tumor-Associated Macrophage Reprogramming and Tumor Progression. Cell Metab. 2019;29(6):1376-1389.e4. doi:10.1016/j.cmet.2019.02.016
24. Miret JJ, Kirschmeier P, Koyama S, et al. Suppression of Myeloid Cell Arginase Activity leads to Therapeutic Response in a NSCLC Mouse Model by Activating Anti-Tumor Immunity. J Immunother Cancer. 2019;7(1):32. doi:10.1186/s40425-019-0504-5
25. Van de Velde LA, Subramanian C, Smith AM, et al. T Cells Encountering Myeloid Cells Programmed for Amino Acid-dependent Immunosuppression Use Rictor/mTORC2 Protein for Proliferative Checkpoint Decisions. J Biol Chem. 2017;292(1):15-30. doi:10.1074/jbc.M116.766238
26. Zhang Y, Velez-Delgado A, Mathew E, et al. Myeloid cells are required for PD-1/PD-L1 checkpoint activation and the establishment of an immunosuppressive environment in pancreatic cancer. Gut. 2017;66(1):124-136. doi:10.1136/gutjnl-2016-312078
27. Halbrook CJ, Pontious C, Kovalenko I, et al. Macrophage-Released Pyrimidines Inhibit Gemcitabine Therapy in Pancreatic Cancer. Cell Metab. 2019;29(6):1390-1399.e6. doi:10.1016/j.cmet.2019.02.001
28. Zhu Z, Achreja A, Meurs N, et al. Tumour-reprogrammed stromal BCAT1 fuels branched-chain ketoacid dependency in stromal-rich PDAC tumours. Nat Metab. 2020;2(8):775-792. doi:10.1038/s42255-020-0226-5
29. Carpenter ES, Elhossiny AM, Kadiyala P, et al. Analysis of Donor Pancreata Defines the Transcriptomic Signature and Microenvironment of Early Neoplastic Lesions. Cancer Discov. 2023;13(6):1324-1345. doi:10.1158/2159-8290.CD-23-0013
30. Hao X, Ren Y, Feng M, Wang Q, Wang Y. Metabolic reprogramming due to hypoxia in pancreatic cancer: Implications for tumor formation, immunity, and more. Biomed Pharmacother. 2021;141:111798. doi:10.1016/j.biopha.2021.111798
31. Mello AM, Ngodup T, Lee Y, et al. Hypoxia promotes an inflammatory phenotype of fibroblasts in pancreatic cancer. Oncogenesis. 2022;11(1):1-9. doi:10.1038/s41389-022-00434-2
32. Pietrobon V, Marincola FM. Hypoxia and the phenomenon of immune exclusion. J Transl Med. 2021;19(1):9. doi:10.1186/s12967-020-02667-4
33. Mangalhara KC, Varanasi SK, Johnson MA, et al. Manipulating mitochondrial electron flow enhances tumor immunogenicity. Science. 2023;381(6664):1316-1323. doi:10.1126/science.abq1053

34. Scallet AC, Haley RL, Scallet DM, Duhart HM, Binienda ZK. 3-nitropropionic acid inhibition of succinate dehydrogenase (complex II) activity in cultured Chinese hamster ovary cells: antagonism by L-carnitine. Ann N Y Acad Sci. 2003;993:305-312; discussion 345-349. doi:10.1111/j.1749-6632.2003.tb07538.x
35. Petr T, Šmíd V, Šmídová J, et al. Histochemical detection of GM1 ganglioside using cholera toxin-B subunit. Evaluation of critical factors optimal for in situ detection with special emphasis to acetone pre-extraction. Eur J Histochem EJH. 2010;54(2):e23. doi:10.4081/ejh.2010.e23